1521-009X/49/3/188–201$35.00
DRUG METABOLISM AND DISPOSITION

https://doi.org/10.1124/dmd.120.000294
Drug Metab Dispos 49:188–201, March 2021

Impact of Plasma Protein Binding in Drug Clearance Prediction: A Database Analysis of Published Studies and Implications for In Vitro-In Vivo Extrapolation

L. J. Francis, J. B. Houston, and D. Hallifax

Centre for Applied Pharmacokinetic Research, Division of Pharmacy and Optometry, School of Health Sciences, Faculty of Biology, Medicine and Health, University of Manchester, Manchester Academic Health Science Centre, Manchester, United Kingdom

Received October 23, 2020; accepted December 7, 2020

ABSTRACT

Plasma protein–mediated uptake (PMU) and its effect on clearance (CL) prediction have been studied in various formats; however, a comprehensive analysis of the overall impact of PMU on CL parameters from hepatocyte assays (routinely used for IVIVE) has not previously been performed. The following work collated data reflecting the effect of PMU for 26 compounds with a wide variety of physicochemical, drug, and in vivo CL properties. PMU enhanced the unbound intrinsic clearance in vitro ($CL_{int,u\ in\ vitro}$) beyond that conventionally calculated using fraction unbound and was correlated with the unbound fraction of drug in vitro and in plasma (fu_p) and absolute unbound intrinsic clearance in vivo ($CL_{int,u\ in\ vivo}$) in both rat and human hepatocytes. PMU appeared to be more important for highly bound (fu_p < 0.1) and high $CL_{int,u\ in\ vivo}$ drugs. These trends were independent of species, assay conditions, ionization, and extended clearance classification system group, although the type of plasma protein used in in vitro assays may require further investigation. Such generalized trends (spanning fu_p 0.0008–0.99) may suggest a generic mechanism behind PMU; however, multiple drug-dependent mechanisms are also possible. Using the identified relationship between the impact of PMU on $CL_{int,u\ in\ vitro}$ and fu_p, PMU-enhanced predictions of $CL_{int,u\ in\ vivo}$ were calculated for both transporter substrates and metabolically cleared drugs. PMU was accurately predicted, and incorporation of predicted PMU improved the IVIVE of hepatic CL, with an average fold error of 1.17 and >50% of compounds predicted within a 2-fold error for both rat and human data sets ($n \geq 100$).

SIGNIFICANCE STATEMENT

Current strategies for prediction of hepatic clearance from in vitro data are recognized to be inaccurate, but they do not account for PMU. The impact of PMU on $CL_{int,u\ in\ vitro}$ is wide ranging and can be predicted based on fraction unbound in plasma and applied to $CL_{int,u\ in\ vitro}$ values obtained by standard procedures in the absence of plasma protein. Such PMU-enhanced predictions improved IVIVE, and future studies may easily incorporate this PMU relationship to provide more accurate IVIVE.

Introduction

The quantitative prediction of hepatic clearance (CL) of drugs from in vitro systems remains challenging and is currently inadequate for reliable estimation of first-in-human dosing (Bowman and Benet, 2016; Wood et al., 2017). The characteristic underprediction of high-CL compounds when using physiologically mechanistic scaling is deemed to be multifactorial in origin (Wood et al., 2017). Confounding in vitro phenomena such as the unstirred water layer (UWL) barrier, cofactor depletion, and loss of enzyme activity in vitro have been explored (Wood et al., 2018), but a consistent improvement in methodological accuracy and precision has yet to be achieved across a wide range of drugs. Conventionally, plasma protein binding has only been a consideration when extrapolating in vitro intrinsic clearance ($CL_{int\ in\ vitro}$) to in vivo CL (and vice versa) using liver models [e.g., the well stirred liver model (WSLM)]. This methodology follows the free drug hypothesis (FDH), in which drug association to, and dissociation from, plasma protein is rapid (not rate limiting), only unbound drug penetrates hepatocytes (reversibly), and unbound drug (at equilibrium with plasma concentration) provides the driving concentration for metabolism.

However, numerous cases over several decades of both endogenous and exogenous compounds have shown hepatic uptake kinetics that appeared to be driven by bound rather than unbound compound—apparently challenging the FDH. Use of isolated perfused livers (IPL) during the 1980s provided evidence of "albumin-mediated uptake" for taurocholate, oleate, and warfarin (Forker and Luxon, 1981, 1983; Weisiger and Ma, 1987; Tsao et al., 1988). This plasma protein–mediated uptake (PMU) was initially hypothesized to involve either a specific albumin receptor or rate-limiting albumin-ligand dissociation (Weisiger

This work was supported by the Centre for Applied Pharmacokinetic Research consortium membership, which included Certara, Genentech, Johnson & Johnson, Lilly, Merck, and Takeda.

The authors declare no conflict of interest.

https://doi.org/10.1124/dmd.120.000294.

This article has supplemental material available at dmd.aspetjournals.org.

ABBREVIATIONS: AAG, α1-acid-glycoporotein 1; AFE, average fold error; ANS, 1-anilino-8-naphthalene sulfonate; BSA, bovine serum albumin; CL, clearance; CL_H, hepatic clearance; $CL_{int\ in\ vitro}$, intrinsic clearance in vitro; $CL_{int,u\ in\ vitro}$, unbound intrinsic clearance in vitro; $CL_{int,u\ in\ vivo}$, unbound intrinsic clearance in vivo; ECCS, extended clearance classification system; FDH, free drug hypothesis; fu, fraction unbound; fu_b, fraction unbound in blood; fu_p, fraction unbound in plasma; HSA, human serum albumin; IPL, isolated perfused liver; IVIVE, in vitro-in vivo extrapolation; OATP, organic anion transporting polypeptide; PMU, plasma protein–mediated uptake; PP, plasma protein; RMSE, root-mean square error; UWL, unstirred water layer; WSLM, well stirred liver model.

et al., 1981), but alternative mechanistic explanations followed. IPL studies with warfarin led Tsao et al. (1988) to suggest a facilitated dissociation model involving a less specific interaction with the plasma membrane. Ichikawa et al. (1992) suggested that albumin may enhance drug diffusion through the UWL in hepatic sinusoids, as rate-limited diffusion was observed in the absence, but not presence, of albumin. More recently, Bowman et al. (2019) observed a reduction in unbound uptake affinity ($K_{m,u}$) for several organic anion transporting polypeptide (OATP) substrates, suggesting PMU is driven by high-affinity drug transporters, which may be able to "strip" the drug directly from the albumin. Miyauchi et al. (2018) have recently applied the facilitated dissociation model to kinetics from hepatocyte assays, giving a mechanistic solution for in vitro observations of PMU. Although this type of analysis provides useful insight, it is retrospective and requires detailed uptake kinetic measurements from hepatocyte assays.

Although the mechanistic details behind PMU remain inconclusive, and potentially multiple, the importance of considering PMU in in vivo CL predictions has become compelling. In addition to the cases above, the use of plasma/isolated plasma protein in assay medium for the in vitro prediction of CL has been explored (prompted by raised unbound $CL_{int\ in\ vitro}$ relative to the conventional, protein-free approach), and improvements in in vitro-in vivo extrapolations (IVIVE) have been reported (Shibata et al., 2000; Blanchard et al., 2004, 2005, 2006; Li et al., 2020). Considering the overall number of cases that challenge conventional prediction strategies (and appear to challenge the FDH), progression of PMU to a mainstream component of the prediction of CL might now be appropriate. As such, there is a need for an integrated assessment of the experimental evidence from various sources, focusing on hepatocyte-based in vitro systems, as relied upon for CL prediction. Therefore, the main aim of the current study was to collate published data in which PMU has been quantified and assess trends common across all studies. A total of 74 individual observations (from 26 drugs in 11 studies) were identified involving rat and human hepatocytes. Correlations between the extent of protein binding and the impact on CL parameters were examined in relation to species, protein type, or other experimental approaches, as well as fundamental drug properties. Subsequently, a generic relationship was identified and incorporated into prediction methodology to assess the utility of this approach and its ability to improve IVIVE of CL.

Methods

Database Construction

The literature was searched to obtain studies that measured the impact of plasma protein (PP) on $CL_{int\ in\ vitro}$. The $CL_{int\ in\ vitro}$ was obtained only from hepatocyte experiments, measured in both the presence and absence of PP, allowing for the assessment of the impact of PP (and thus PMU) under identical experimental conditions. Although other studies investigating the impact of PP using microsomes have been performed, these data sets were excluded from the current work. Microsomal studies only account for the impact of PP on cytochrome P450 metabolism (and not total clearance) and are likely to reflect a different mechanism [albumin has an anti-inhibitory effect on microsomes as a result of albumin binding avidly to long-chain unsaturated fatty acids, which inhibit many cytochrome P450 enzymes (Rowland et al., 2008; Fujino et al., 2018)] and thus is not representative of the PMU phenomenon under investigation here.

Data from all cellular species, sources of PP (isolated albumin, plasma, and serum), and compounds (drugs, in-house and nontherapeutic compounds) were considered. Only in vitro clearance parameters were included in the database (and back-calculated from scaled in vivo values when appropriate) to avoid potential bias of different scaling factors used across different studies. The in vitro fraction unbound (fu, under the exact same experimental conditions as the $CL_{int\ in\ vitro}$ studies were performed), was also recorded when possible. This includes nonspecific binding of the experimental conditions performed in the absence of PP as well as in the presence of PP. For a few studies, the nonspecific binding in the absence of PP was not measured, and in vitro fu was assumed to be 1. For one study (Bachmann et al., 2003), the in vitro fu in the presence of PP (in this case pure human serum) was not measured, so these in vitro fu values were sourced from independent studies (also obtained with pure human serum) for the five drugs examined in this study. All such cases are indicated in the footnotes of Supplemental Table 1.

The unbound $CL_{int\ in\ vitro}$ ($CL_{int,u\ in\ vitro}$) was also included and was obtained directly from the original papers or calculated by eq. 1:

$$CL_{int,u\ in\ vitro} = \frac{CL_{int,\ in\ vitro}}{in\ vitro\ fu} \quad (1)$$

When only the $CL_{int,u\ in\ vitro}$ was recorded by the authors, $CL_{int\ in\ vitro}$ could also be back-calculated based on eq. 1. When available, maximum uptake velocity (V_{max}), Michaelis constant (K_m), and $K_{m,u}$ values were also obtained directly as stated in the literature (which included both transporter and nontransporter substrates). Based on eqs. 2 and 3, these values were also used to calculate $CL_{int\ in\ vitro}$ or $CL_{int,u\ in\ vitro}$, respectively, as required (see footnotes of Supplemental Table 1 for specific details on how individual values were calculated). As with eq. 1, back-calculations of eqs. 2 and 3 were also performed as required.

$$CL_{int\ in\ vitro} = \frac{V_{max}}{K_m} \quad (2)$$

$$CL_{int,u\ in\ vitro} = \frac{V_{max}}{K_{m,u}} \quad (3)$$

To assess the impact of PP on all in vitro clearance terms (V_{max}, K_m, $CL_{int\ in\ vitro}$, $K_{m,u}$, and $CL_{int,u\ in\ vitro}$), the fold-change caused by the experimental addition of PP was calculated. The fold-change was calculated for each drug, in each study, comparing the relative change in the presence of PP to its experimentally matched no-PP controls [$CL_{int,u\ in\ vitro}$ (+PP)/$CL_{int,u\ in\ vitro}$ (no PP), with both values obtained under the same experimental conditions]. By using this approach to assess the impact of PP, comparisons across different species (e.g., rat and human) could be made despite clear species differences in the absolute $CL_{int\ in\ vitro}$ and $CL_{int,u\ in\ vitro}$ values. Because of the diverse nature of experimental conditions, the specific assay conditions (hepatocyte species, in vitro test system, cell source, type of albumin, cell density, plate format, shaking speed, drug concentration, and duration of experiments) were also recorded for comparison.

The physicochemical properties (molecular weight, water solubility, number of hydrogen donors and acceptors, polar surface area, log P, log $D_{7.4}$, acidic pK_a, basic pK_a, and ionization) of each drug obtained in the database were also collected (Supplemental Table 1). The ionization of each drug was defined based on their charge and percent ionization at physiologic pH (7.4) as follows: neutrals, <3% ionized; acids, >10% negatively charged; weak acids, >3 <10% negatively charged; bases, >10% positively charged; weak bases, >3 <10% positively charged; zwitterions, >10% positively and negatively charged. The extended clearance classification system (ECCS), permeability, and clearance mechanism as reported by Varma et al. (2015) were also noted. For drugs not included in the Varma et al. (2015) database, the ECCS group was manually assigned based on its ionization and molecular weight (see footnotes, Table 1).

Additional in vitro drug uptake parameters, passive permeability, uptake clearance, and active uptake (P_{diff}, CL_{uptake}, and CL_{active},

respectively) in the absence of PP were sourced for all drugs (mean values of multiple studies) when available from both rat and human hepatocyte assays. Finally, the fraction unbound in plasma and blood (fu_p and fu_b, respectively), unbound intrinsic CL in vivo ($CL_{int,u\ in\ vivo}$) and total hepatic CL (CL_H) values for rat and human were also collated, primarily based on the Wood et al. (2017) database, or independently sourced and mean values calculated. When necessary, some $CL_{int,u\ in\ vivo}$ values were calculated based on CL_H and fu_b; see footnotes of Table 1 for details.

IVIVE Analysis Part 1: PMU Database. Linear regression analysis was performed to quantify the identified relationship between log_{10}-transformed fu_p and log_{10}-transformed fold-change in $CL_{int,u\ in\ vitro}$ values caused by the addition of PP. No significant difference was observed between human and rat data sets, and thus a single equation was used to assess whether incorporation of predicted PMU could improve IVIVE for both species of this discrete set of drugs (see *Results* section for analysis). $CL_{int,u\ in\ vitro}$ (microliters per minute per 10^6 cells) obtained in the absence of PP and fu_p values from the PMU database was applied to eq. 4, predicting the fold-change in $CL_{int,u\ in\ vitro}$ caused by the addition of PP.

$$Log_{10}(Fold\text{-}change\ in\ CL_{int,u\ in\ vitro}) = -0.3774\left(Log_{10}(fu_p)\right) + 0.03253 \quad (4)$$

This fold-change was then applied to the absolute $CL_{int,u\ in\ vitro}$ values obtained in the absence of PP to predict the $CL_{int,u\ in\ vitro}$ values in the presence of PP (microliters per minute per 10^6 cells). These in vitro values ($CL_{int,u\ in\ vitro}$ in the absence of PP, $CL_{int,u\ in\ vitro}$ in the presence of PP, and predicted $CL_{int,u\ in\ vitro}$ based on the observed PMU relationship) were subsequently scaled up to in vivo values ($CL_{int,u\ in\ vivo}$, milliliters per minute per kilogram) after application of physiologically based scaling factors [hepatocellularity of 120×10^6 cells/g liver in both rat and human, and 40 g liver/kg bodyweight and 21.4 g liver/kg bodyweight in rat and human, respectively (Wood et al., 2017)] and compared with observed $CL_{int,u\ in\ vivo}$ values (Table 1). To assess accuracy and precision, the average fold error (AFE) and root-mean square error (RMSE) were calculated using eqs. 5 and 6, respectively:

$$AFE = 10^{\left(\left[\sum \log\left(\frac{predicted}{observed}\right)\right]/n\right)} \quad (5)$$

$$RMSE = \sqrt{\frac{1}{n}\sum(predicted - observed)^2} \quad (6)$$

where n represents the number of predictions. The percentage within 2-, 3-, >3-fold, was also calculated to evaluate accuracy of the data set. $CL_{int,u\ in\ vivo}$ values were then applied to the WSLM (eq. 7) to assess IVIVE of CL_H.

$$CL_H = \frac{Q_H \times fu_b \times CL_{int,u\ in\ vivo}}{Q_H + fu_b \times CL_{int,u\ in\ vivo}} \quad (7)$$

where Q_H represents hepatic blood flow [100 ml/min per kg for rat and 20.7 ml/min per kg for human, Wood et al. (2017)]. These predicted CL_H values were compared with observed CL_H values (Table 1), and accuracy and precision were assessed as above.

IVIVE Analysis Part 2: Wood et al. (2017) Database. Because of the relatively small number of drugs within the PMU database, IVIVE analysis was also performed using the previously published database by Wood et al. (2017). This database contains 148 compounds for rat and 117 for human, all of which are mean values reported from the literature, and this was deemed a reliable and comprehensive source for such IVIVE analysis. The fu_p and $CL_{int,u\ in\ vitro}$ values (milliliters per minute per kilogram) measured in the absence of PP from hepatocytes, from both rat and human were used to calculate the predicted fold-change in $CL_{int,u\ in\ vitro}$ values caused by the addition of PP. This was applied to the absolute $CL_{int,u\ in\ vitro}$ values, as above, to predict $CL_{int,u\ in\ vivo}$ values in the presence of PP. Considering the uncertainty regarding PMU effect in vivo, CL_H was also predicted from $CL_{int,u\ in\ vivo}$ values using the WSLM (eq. 7), thus avoiding the assumption of equivalent PMU effect in vivo. Full calculation of these predictions is shown in (Supplemental Table 2). IVIVE analysis (AFE, RMSE, and percent fold-within) was performed on $CL_{int,u\ in\ vivo}$ and CL_H values, as described previously. These predictions were repeated using alternative parallel tube and dispersion liver models (Ito and Houston, 2004) to verify the choice of WSLM (Supplemental Fig. 1).

Statistical Analysis. All data were analyzed using GraphPad Prism version 8.0. To assess the impact of PP on absolute $CL_{int,u\ in\ vitro}$ values, a paired two-tailed *t* test was performed (Supplemental Fig. 2). To assess the PMU phenomenon, log-log least-squares regression analysis with no weighting was performed on the fold-change in $CL_{int,u\ in\ vitro}$ and in vitro fu, with all data, and compared against a hypothetical slope of zero. This zero baseline would denote no effect of PP on $CL_{int,u\ in\ vitro}$ values as would be expected according to conventional normalization to unbound concentrations using fu. To identify whether in vitro assay conditions influenced the observed relationship between in vitro fu and fold-change in clearance parameters, log-log least-squares regression analysis with no weighting was performed, and an F-test was used to assess significant differences between the subsets ($\alpha = 0.05$). When statistical differences were observed (e.g., Supplemental Fig. 3), linear regression analysis was repeated on the log_{10}-transformed data, followed by an F-test to assess for significant differences between the subsets. To quantify the observed relationship between fu_p and the fold-change in $CL_{int,u\ in\ vitro}$ caused by the addition of physiologically equivalent concentrations of PP, linear least-squares regression analysis with no weighting was performed on the log_{10}-transformed fu_p and log_{10}-transformed fold-change in $CL_{int,u\ in\ vitro}$ values, followed by an F-test to assess whether there was a significant differences between the rat and human data sets ($\alpha = 0.05$).

Results

Scope of PMU Database. The PMU database consists of data from 11 studies on 26 different compounds with (cumulatively) 74 different reported values for the influence of PP on in vitro clearance parameters. Multiple studies on the same compound were considered independently (18 of 26 compounds contained multiple data points). These data were obtained from various experimental conditions, but all studies included direct comparisons to PP-free conditions, allowing for fold-change between the presence and absence of PP to be calculated (Supplemental Table 1). Although initially all cellular species were considered, only data from rat ($n = 36$) and human ($n = 38$) hepatocytes could be sourced and, thus, are evaluated here. The data set represents a broad range of compounds based on both their physicochemical properties and in vivo values, as summarized in Table 1. The majority of recent studies on the PMU phenomenon have focused on OATP transporter substrates (Miyauchi et al., 2018; Bowman et al., 2019; Li et al., 2020); however, this data set encompasses a wide range of drugs, including drugs cleared by passive hepatic uptake and metabolism, such as basic and neutral ECCS class 2 compounds (Fig. 1).

Impact of PMU on Clearance. Initial analysis examined trends at the in vitro level and potential discrepancies caused by experimental conditions. Absolute $CL_{int,u\ in\ vitro}$ values were significantly higher in both rat and human data sets in the presence of PP compared with the absence ($P = 0.0004$ and $P = 0.0025$, respectively, see Supplemental Fig. 2 for details). Trends between fold-change in clearance parameters measured in in vitro hepatocyte systems (namely, the $CL_{int\ in\ vitro}$,

TABLE 1

Overview of the physicochemical properties and in vivo values from rat and human of the compounds represented in the PMU database

References: [1] Varma et al. (2015), [2] Chung et al. (1990), [3] Miyauchi et al. (2018), [4] Avdeef, 2012, [5] Wood et al. (2017), [6] Li et al. (2020), [7] Yabe et al. (2011), [8] Brown et al. (2007), [9] Kim et al. (2019), [10] De Bruyn et al. (2018), [11] Watanabe et al. (2010), [12] Lave et al. (1997), [13] Blanchard et al. (2006), [14] Blanchard et al. (2004), [15] Brunton et al., 2011, [16] Bachmann et al. (2003).

Drug	Predicted Physicochemical Properties[a]					In Vivo Values							
						fu_p		fu_b		$CL_{int,u\ in\ vivo}$		CL_H	
	Molecular Weight	Ionization (A/B/Z/N)b	Log P	Log $D_{7.4}$	ECCS[1]	Human	Rat	Human	Rat	Human	Rat	Human	Rat
										ml/min per kilogram			
ANS[c]	299.3	A	2.45[d]	−2.18[d]	3a[e]		0.0043[2]		0.00796[3]				6.43[3]
Antipyrine	188.2	N	0.56[4]	0.26[4]	2	0.99[5]	1[5]	0.99[5]	1[5]	0.57[5]	5.4[5]	0.55[5]	5.1[5]
Asunaprevir	748.3	A	3.93[d]	3.72[d]	3b[e]		0.013[6]						38.4[6]
Atorvastatin	558.6	A	4.13[d]	1.3[7]	1b	0.02[5]	0.044[5]	0.036[5]	0.036[5]	2070[5]	1470[5]	16[5]	35[5]
Bosentan	551.6	A	1.15[d]	1.25[7]	1b	0.035[5]	0.016[5]	0.064[5]	0.015[5]	66[5]	2790[5]	3.5[5]	30[5]
(R-)Bufuralol	261.4	B	3.38[d]	1.22[d]	2[e]	0.19[8]				8.8[8]			
Carbamazepine	236.3	N	2.45[4]	2.45[4]	2[e]	0.26[5]		0.31[5]		5.4[5]		1.6[5]	
Cerivastatin	459.6	A	3.7[d]	1.9[7]	1b	0.00734[9]	0.029[5]	0.0127[9]	0.041[5]	908[9,10]f	1520[5]	5[9]	39[5]
Diclofenac	296.1	A	4.51[4]	1.3[4]	1a	0.005[5]	0.022[5]	0.0091[5]	0.041[5]	1340[5]	687[5]	7.7[5]	22[5]
Fluvastatin	411.5	A	4.17[4]	1.12[4]	1b	0.00398[9,11]	0.00986[11]	0.0069[9]		6270[9] *f*	3800[11]*f*	14[9]	20[6]
Glibenclamide	494.0	A	3.75[d]	2.23[d]	1b[e]	0.000787[9]	0.002[6]	0.0017[9]		1510[9]*f*		2.3[9]	6.8[6]
Mibefradil	495.6	B	6.29[d]	3.99[d]	2	0.01[a]				1060[12]*f*	78,300[12]*f*	4.88[13]	94[14]
Midazolam	325.8	WB	3.12[4]	3.1[4]	2	0.025[5]	0.051[5]	0.043[5]	0.062[5]	390[5]	1930[5]	9.2[5]	54[5]
Naloxone	327.4	B	1.74[4]	1.09[4]	2	0.62[5]	0.62[5]	0.51[5]	0.57[5]	333[5]	253[5]	18[5]	59[5]
Nateglinide	317.4	A	4.21[d]	1.22[7]	3a	0.00497[9]	0.015[6]	0.0099[9]		360[9] *f*		3.05[9]	58.1[6]
Oxazepam	286.7	N	2.37[4]	2.37[4]	2	0.048[5]		0.043[5]		30[5]		1.2[5]	26[14]
Phenytoin	252.3	A	2.24[4]	2.17[4]	2[e]	0.11[5]	0.23[5]	0.11[5]	0.23[5]	65[5]	97[5]	5.3[5]	18[5]
Pitavastatin	421.5	A	3.45[d]	1.2[7]	1b	0.00532[9,11]	0.0134[11]	0.0093[3]		1060[9,10]*f*	1850[11]*f*	9.64[9]	28[6]
Pravastatin	424.5	A	1.35[d]	−0.4[7]	3b	0.5585[9,11]	0.676[11]	1[9]		24.6[9,10] *f*	136[11] *f*	12.9[9]	59.7[6]
Procainamide	235.3	B	1.49[4]	−0.36[4]	2[e]	0.825[a]				0.9[15]		3.9[16]	
Quinidine	324.4	B	3.64[4]	2.41[4]	2	0.2[5]	0.31[5]	0.21[5]	0.2[5]	24[5]	193[5]	4.1[5]	28[5]
Repaglinide	452.6	A	4.69[d]	2.3[7]	1b	0.015[5]	0.015[5]	0.025[5]	0.025[5]	1390[5]	384[5]	13[5]	8.8[5]
Rosuvastatin	481.5	A	0.42[d]	−0.33[7]	3b	0.134[9]	0.064[5]	0.195[9]		121[9,10] *f*	1230[5]	12.1[9]	56.7[6]
RO-X[g]													55[14]
Theophylline	180.2	WA	0.00[4]	0.00[4]	2	0.59[5]		0.45[5]		1.1[5]	5.62[12] *f*	0.47[5]	
Valsartan	435.5	A	3.9[4]	−1.11[7]	3b	0.00165[9]	0.0029[6]	0.003[9]		214[9,10] *f*		0.678[9]	17.8[6]
RANGE (26 compounds)	180.2–748.3 Theophylline–Asunaprevir	A = 15, B = 5, N = 3, WA = 1, WB = 1, Unknown = 1 (RO-X)	0–6.29 Theophylline–Mibefradil	−2.18 to 3.99 ANS–Mibefradil	1a = 1, 1b = 7, 2 = 11, 3a = 2, 3b = 4, 4 = 0, Unknown = 1 (RO-X)	0.000787–0.99 Glibenclamide–Antipyrine	0.004–1 ANS–Antipyrine	0.0017–1 Glibenclamide–Pravastatin	0.00796–1 ANS–Antipyrine	0.57–6270 Antipyrine–Fluvastatin	5.4–78,300 Antipyrine–Mibefradil	0.47–18 Theophylline–Naloxone	5.1–94 Antipyrine–Mibefradil

A, acid; B, base; N, neutral; WA, weak acid; WB, weak base.

[a]Data obtained from Drugbank.

[b]Ionization class defined as in *Methods*.

[c]ANS, 1-anilino-8-naphthalene sulfonate.

[d]Predicted using ilabs: http://ilab.psds.ac.uk/.

[e]Manually assigned ECCS.

[f]Calculated using same methods as Wood et al. (2017) ($CL_{int,u\ in\ vivo} = (CL_H)/(fu_b \times [1-(CL_H/Q_H)])$ and $fu_b = fu_p/B : P$, B:P represents blood-to-plasma partitioning).

[g]In-house compounds from the literature.

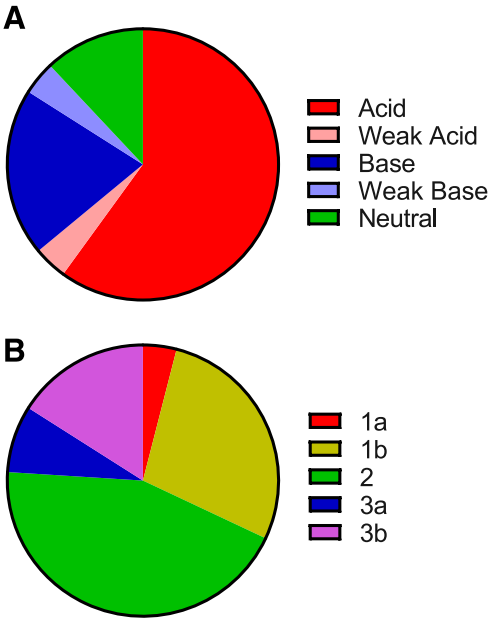

Fig. 1. Distribution of physicochemical properties of the 26 compounds represented in the PMU database. (A) Ionization and (B) ECCS group. Legend as indicated, *n* numbers given in Table 1.

$CL_{int,u\ in\ vitro}$, K_m, $K_{m,u}$, and V_{max}) and the in vitro fu were investigated. A clear positive relationship between the fold-change in $CL_{int\ in\ vitro}$ values and in vitro fu values was observed in both human and rat hepatocyte systems (Fig. 2A). This trend is unsurprising, as lower in vitro fu values conventionally correspond to lower drug availability in vitro and ultimately lead to lower $CL_{int,\ in\ vitro}$ values measured. However, when the $CL_{int\ in\ vitro}$ was normalized to the fraction of unbound drug available at equilibrium ($CL_{int,u\ in\ vitro}$), a clear negative trend was observed for both human and rat hepatocytes, with greater fold-change in the $CL_{int,u\ in\ vitro}$ observed for drugs that possess lower in vitro fu values (Fig. 2B). As expected for these data, this trend appears to contradict the assumption of the FDH; if only free drug could be cleared by hepatocytes, then $CL_{int,u\ in\ vitro}$ values should be unaffected by the presence of PP, and no fold-change in this parameter would be observed. This null hypothesis (in which $CL_{int,u\ in\ vitro}$ is unaffected by the presence of protein, and the slope would equal zero) was rejected with the presented (rat and human) data set [$F_{(1,72)} = 10.2$, $P = 0.0021$]. In addition to confirming the PMU phenomenon, this finding highlights that highly bound drugs may be more significantly affected by PMU than drugs with low binding. No significant difference between the rat and human data sets was observed for this trend [$F_{(2,70)} = 0.8858$, $P = 0.417$], demonstrating that the relationship between the fold-change in $CL_{int,u\ in\ vitro}$ and in vitro fu values is species-independent. However, higher variability in this trend was evident in human hepatocytes compared with rat and increased with lower in vitro fu values. This is likely to be due to inherent variability observed between human donors (Wood et al., 2017) in addition to sensitivity limitations in the quantification of low fu values.

When data were available, the fold-change in K_m ($n = 30$), $K_{m,u}$ ($n = 18$), and V_{max} ($n = 30$) was also investigated. No clear trends between the fold-change in the K_m were observed in relation to the in vitro fu; however, a clear positive trend between the in vitro fu value and fold-change in $K_{m,u}$ was observed (Fig. 2, C and D, respectively). This observation is based entirely on rat data, so this relationship cannot currently be confirmed for human hepatocytes. There was some evidence of a positive relationship between the fold-change in V_{max} and in vitro fu values in rat hepatocytes, but this trend was not observed within the human data set with a different subset of drugs (Supplemental Fig. 4).

Impact of Experimental Conditions Employed In Vitro. Because of the diverse nature of experimental conditions used within this database, it was investigated whether any of the in vitro conditions themselves could influence the fold-change observed and, thus, whether this would lead to any bias in the interpretation of the effect of PP. Firstly, the hepatocyte assay format (suspension, monolayer, or liver slice) was investigated (Fig. 3). The majority of data using human hepatocytes was obtained using the suspension assay format, so no statistical comparisons could be made within the human data set (Fig. 3A). In contrast, both suspension and monolayer assays were used throughout the rat data set, but no statistical differences were observed in either the fold-change in $CL_{int,u\ in\ vitro}$ or $K_{m,u}$ values (Fig. 3, B and C, respectively). This suggests that the observed trends between in vitro fu and fold-change in $CL_{int,u\ in\ vitro}$ and $K_{m,u}$ values are independent of assay format.

It has previously been suggested that the UWL adjacent to hepatocytes is a key limitation to the clearance of high-permeability compounds and that albumin may enhance clearance of high-permeability compounds by promoting drug diffusion through the UWL (Ichikawa et al., 1992; Wood et al., 2018). Therefore, it was subsequently investigated whether performing the suspension assay under static or shaken conditions would lead to differences in the fold-change observed in clearance parameters. The experimental details on the use of shaking (and shaking speed) were included in the PMU database (Supplemental Table 1). For a number of studies, the use of shaking during drug incubation was not documented. This might imply that these assays were performed under static conditions, but given the indeterminate conditions, these data should be interpreted with caution.

Comparison of the confirmed or unknown shaking conditions in suspension assay formats on fold-change in $CL_{int,u\ in\ vitro}$ values is shown in Fig. 4 (fold-change in $K_{m,u}$ values was not included due to insufficient data). No statistical differences between confirmed or unknown shaking conditions were observed in the rat or human data sets (Fig. 4, A and B). The higher variability in the human data set previously observed appears to be attributed to the unknown shaking conditions (possibly reflecting a mixture of shaking conditions). This high variability likely limits the power of such testing, as otherwise the unknown shaking conditions appear to be associated with generally lower PMU effect. Omission of this unknown shaking condition resulted in $CL_{int,u\ in\ vitro}$ fold-change that was highly similar across both species (Fig. 4C).

The final experimental variable investigated was the source of PP used in the in vitro studies. It is plausible that for drugs that bind to plasma proteins or lipoproteins other than albumin [e.g., α1-acid-glycoprotein 1 (AAG)], the specificity of protein used (e.g., whole plasma or isolated albumin) may lead to significant differences in the observed fold-change of clearance parameters. Furthermore, if albumin enhances the uptake of drugs via an albumin receptor mechanism (Weisiger et al., 1981) or albumin-specific interaction with the hepatocyte plasma membrane, it is possible that albumin from different species [human serum albumin (HSA) or bovine serum albumin (BSA), respectively] may also lead to differences in the fold-change observed. Within the database, five different types of PP were used—namely, BSA, HSA, human plasma, human serum, and rat serum. In human hepatocytes (Fig. 5A), no significant difference in the relationship of the fold-change in $CL_{int,u\ in\ vitro}$ values and in vitro fu values was observed between the various types of PP used in in vitro studies. It is noted, however, that this lack of significant difference is largely attributed to the high variability in the human data set. In rat hepatocytes, the type of

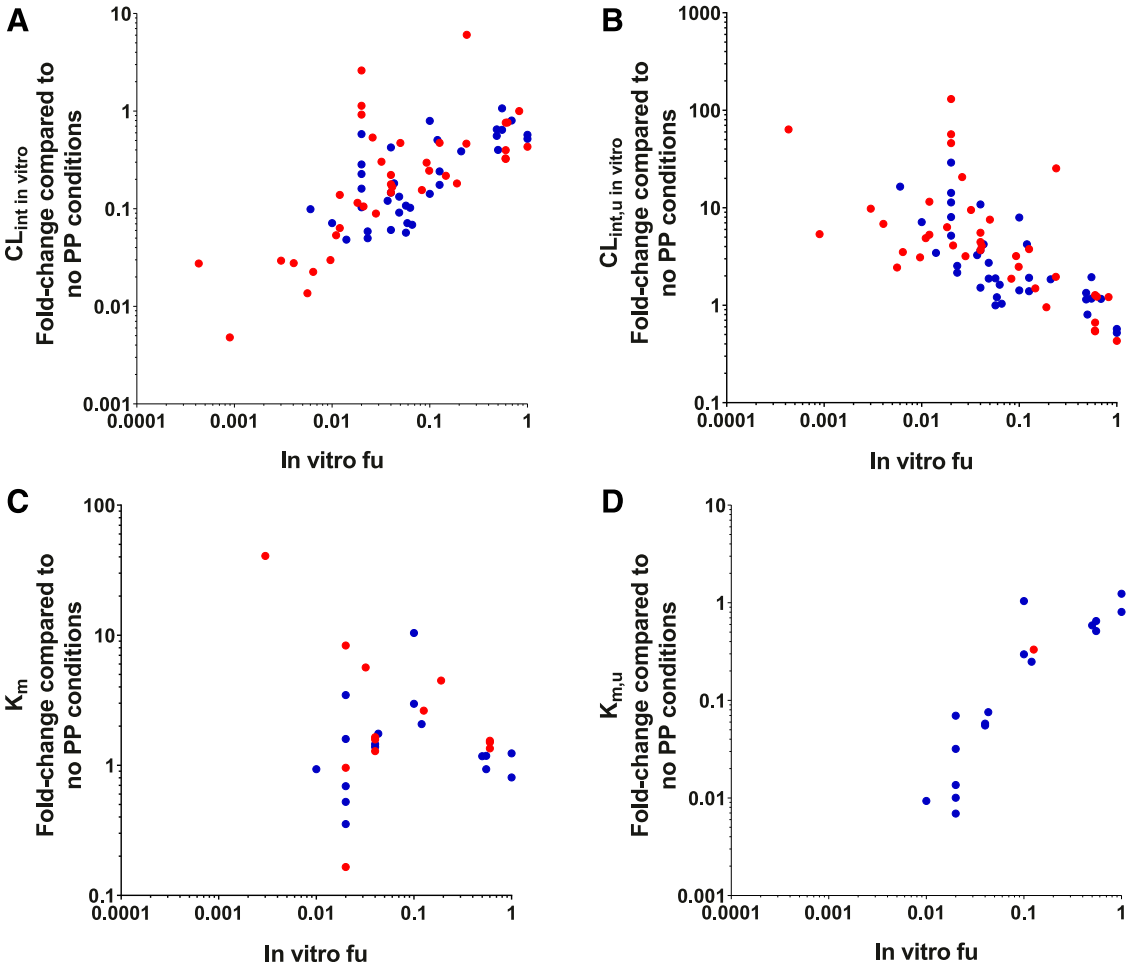

Fig. 2. General trends of the PMU database. Examining trends between in vitro fu values and (A) fold-change in $CL_{int\ in\ vitro}$, (B) fold-change in $CL_{int,u\ in\ vitro}$, (C) fold-change in K_m, and (D) fold-change in $K_{m,u}$. Red and blue indicate values obtained from human and rat hepatocytes, respectively.

albumin used did have a significant effect [$F_{(4,28)} = 6.957$, $P = 0.0005$] on the relationship between the fold-change in the $CL_{int,u\ in\ vitro}$ values and in vitro fu values observed (Fig. 5B; full statistical details are displayed in Supplemental Fig. 3). Studies performed with rat serum appeared to show the greatest increases in fold-change in $CL_{int,u\ in\ vitro}$ values, whereas studies using BSA appeared to show the smallest increases in fold-change in $CL_{int,u\ in\ vitro}$ values. This highlights that protein type may play in important role when studying PMU in vitro; however, it should be noted that each protein subset (BSA, human plasma, and rat serum) only contains data from one or two studies per subset (albeit with multiple drugs), so it is also possible that the differences observed here may be driven by interlaboratory variation. Further studies would be required to clarify whether this observation is truly a result of differences in protein type or simply interlaboratory variation. In contrast, no difference was observed between the use of human plasma and rat serum in rat hepatocyte experiments on the relationship between the fold-change in $K_{m,u}$ values and in vitro fu values (Fig. 5C).

Properties of Drugs Potentially Important in PMU. The in vitro fu value shows a clear correlation with the impact of PP on CL parameters measured in vitro. Although this strongly suggests that PP enhances unbound drug uptake beyond that determined using fu (when conventionally applying the FDH), it is important to understand the utility and implications of this in vivo. Therefore, the relationship between the fold-change in clearance parameters measured under physiologically relevant protein conditions in vitro and their fu_p and $CL_{int,u\ in\ vivo}$ values (Table 1) were examined. As this analysis focused on the implications at the in vivo level, only entries in the database that were performed under physiologically relevant albumin conditions were included [e.g., pitavastatin studies by Kim et al. (2019) that were conducted using 5% HSA were included; however, pitavastatin studies by Miyauchi et al. (2018) that were conducted at ≤1% HSA were excluded]. Such entries are annotated in Supplemental Table 1. Compounds for which no in vivo data were available were also excluded from this analysis.

The fold-change in $K_{m,u}$ and $CL_{int,u\ in\ vitro}$ relative to their fu_p were investigated and segregated by species, ECCS classification, and ionization (Fig. 6). Overall, trends between fold-change in $CL_{int,u\ in\ vitro}$ and $K_{m,u}$ values were observed with fu_p that were similar to those observed with in vitro fu for both human and rat data. Drugs with lower fu_p values showed the greatest decrease in $K_{m,u}$ values and the greatest increase in $CL_{int,u\ in\ vitro}$ values. No clear differences were observed in the fold-change in $CL_{int,u\ in\ vitro}$ values between the rat and human data sets, although fewer data are present in the rat data set (mainly as a result of a lack of rat fu_p values), and greater variability was observed in the human data set. No cross-species comparison could be made for the fold-change in $K_{m,u}$ as a result of the negligible number of human studies.

The observed relationship between the fold-change in $CL_{int,u\ in\ vitro}$ and fu_p appears to be independent of ECCS classification in both human and rat (Fig. 6, A and B, respectively). The ECCS class 2 compounds

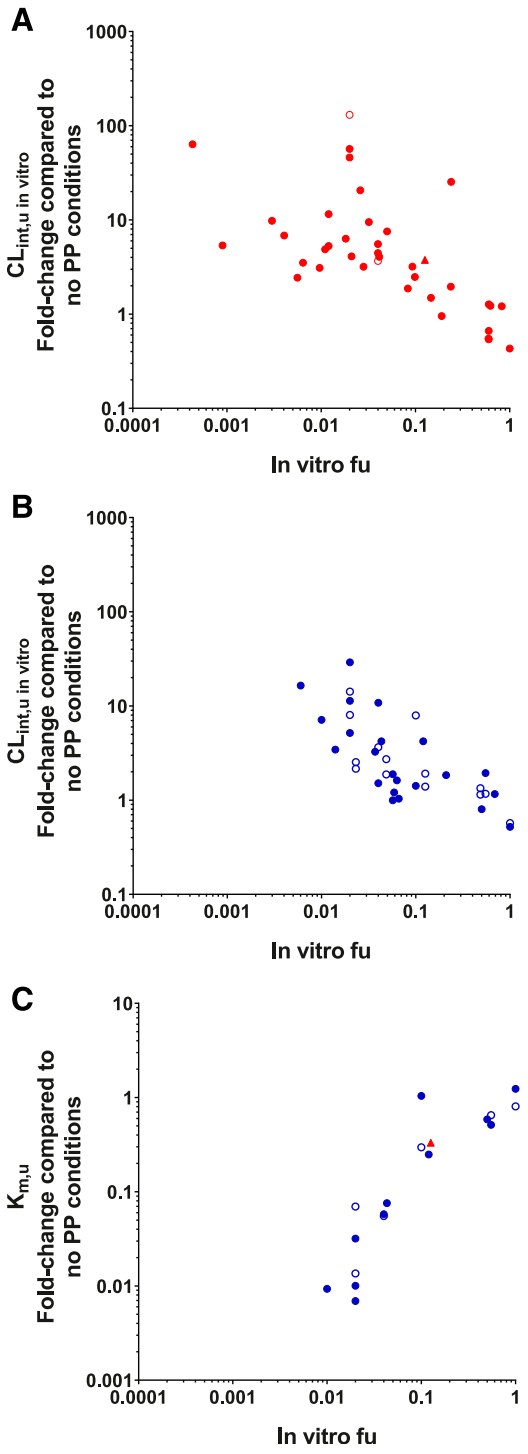

Fig. 3. Comparison of assay format on the $CL_{int,u\ in\ vitro}$ fold-change in (A) human (red) and (B) rat (blue) and (C) the $K_{m,u}$ fold-change in rat and human observed. Closed circles, suspension; open circles, monolayer; triangle, liver slice. (A) Human suspension, n = 34; human monolayer, n = 3; human liver slice, n = 1. (B) Rat suspension, n = 22; rat monolayer, n = 14. (C) Rat suspension, n = 11; rat monolayer, n = 6; human liver slice, n = 1.

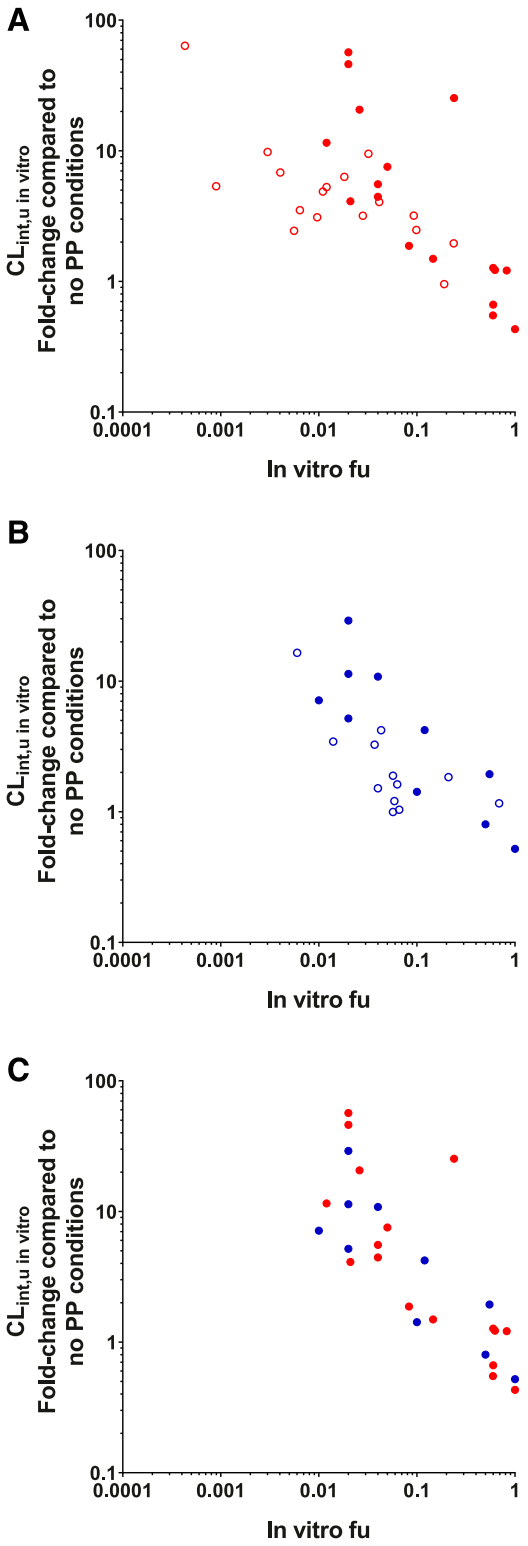

Fig.4. Comparison of shaking conditions in the suspension assay on the $CL_{int,u\ in\ vitro}$ fold-change observed. (A) Human (red), (B) rat (blue), and (C) rat and human data from only assays with confirmed shaking. Closed circles represent experiments performed with confirmed shaking conditions; open circles represent experiments performed under unknown/unconfirmed shaking conditions. Rat shaking, n = 10; rat unknown shaking, n = 12; human shaking, n = 17; human unknown shaking, n = 17.

(representing basic/neutral compounds with high permeability and predominantly cleared via metabolism), showed the clearest trend within the data, spanning fu_p values 0.01–1 (in human). All other ECCS classes appeared to conform to this trend, although fewer data were available for the other ECCS classes, and thus direct comparisons were difficult to assess. For high fu_p values (approaching 1), the fold-change in $CL_{int,u\ in\ vitro}$ ranged around 1, with the apparent negative effect in some cases probably reflecting experimental uncertainty (data within a 2-fold error margin). A few clear outliers of the ECCS class 1b were also noted

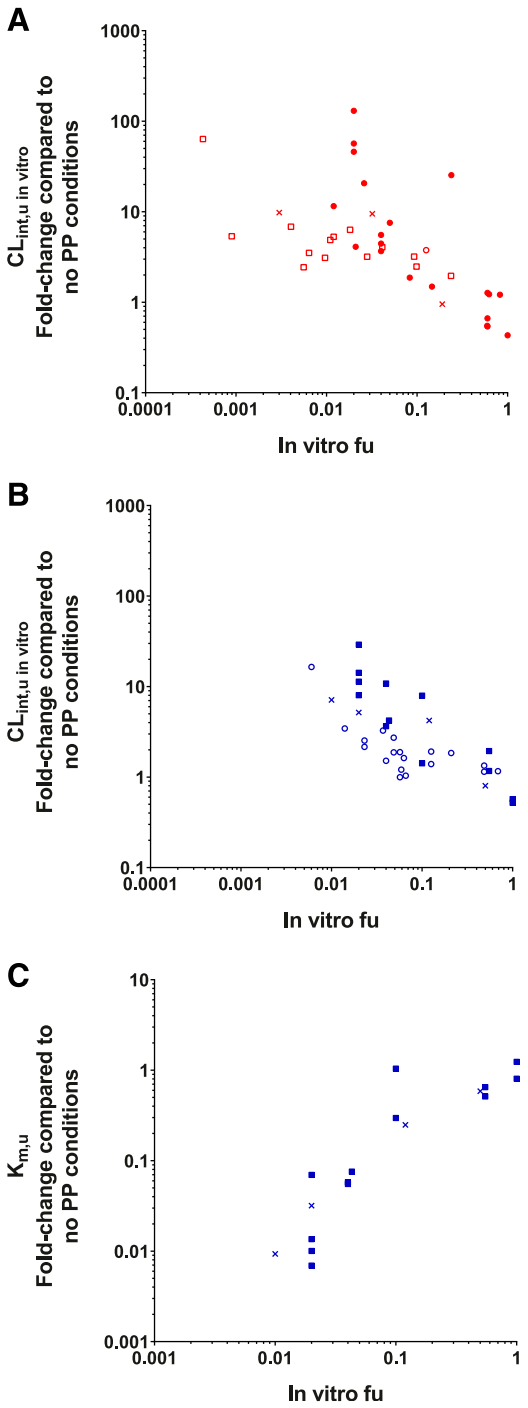

Fig. 5. Comparison of the different types of PP used in experimental conditions. Fold-change in $CL_{int,u\ in\ vitro}$ compared with in vitro fu in (A) human (red) and (B) rat (blue). (C) Fold-change in $K_{m,u}$ compared with in vitro fu in rat. Open circles, BSA; open squares, HSA; X, human plasma; closed circles, human serum; closed squares, rat serum. (A) BSA, $n = 1$; HSA, $n = 14$; human plasma, $n = 3$; human serum, $n = 20$. (B) BSA, $n = 19$; human plasma, $n = 4$; rat serum, $n = 13$. (C) Human plasma, $n = 4$; rat serum, $n = 13$.

in the human data set; in particular, the vertical spread of points at a fu_p of 0.035 represent different data for just one drug, bosentan, measured across multiple studies. On further investigation of these bosentan data, it was noted that the large variation in $CL_{int,u\ in\ vitro}$ fold-change (ranging from 5 to 130) could be accounted for by their differences in (absolute) $CL_{int,u\ in\ vitro}$ values measured without PP (ranging from 1.5 to 23.2 μl/min per 10^6 cells, Supplemental Table 1); thus, the >10-fold difference observed under the control conditions were reflected in the calculated fold-change here. In this particular case, it was difficult to ascertain whether the differences were due to interlaboratory or human donor variation, but it is nevertheless a reality for some drug cases in vitro and serves to illustrate the utility of database analysis in finding trends across multiple sources. For this reason, all bosentan (and other) data were used in the present database analysis without discrimination.

No clear differences based on ionization of the compounds were observed for either the fold-change in $CL_{int,u\ in\ vitro}$ or $K_{m,u}$ values in both rat and human (Fig. 6, D–F). Although it is clear that acidic and basic compounds are well represented in the human data set, the rat data set is marginally over-represented by acidic compounds (representing 60% of the data available), likely representing recent studies focused on the OATP transporter substrates. Within the human data set, the acidic drug bosentan is again a clear outlier due to its high variability.

Higher $CL_{int,u\ in\ vivo}$ compounds were shown to have the greatest fold-change in $CL_{int,u\ in\ vitro}$ values, implying that high metabolic turnover compounds may be more influenced by PMU. In rat, clear trends for both fold-change in $K_{m,u}$ (data not shown) and $CL_{int,u\ in\ vitro}$ values were observed in relation to their $CL_{int,u\ in\ vivo}$ values, both of which were independent of ECCS classification and ionization (Fig. 7, A and B). Specifically, the ECCS class 2 compounds showed this trend the clearest (across rat $CL_{int,u\ in\ vivo}$ values 5.4–78,300 ml/min per kg), and the ECCS class 3b agreed with this trend. The ECCS 1b compounds in this data set also appeared to agree with this trend, but because of their relatively narrow range of rat $CL_{int,u\ in\ vivo}$ values (1500–4000), this is stated with less certainty. This may insinuate that the PMU effect is associated with drug permeability, and thus correlations between drug-specific uptake parameters from PP-free studies (i.e., P_{diff}, CL_{uptake}, or CL_{active}) and fold-change in $CL_{int,u\ in\ vitro}$ values were also explored. No clear trends between any of the in vitro uptake parameters were observed (Supplemental Fig. 5), and thus the effect of permeability on PMU remains inconclusive.

Similar trends were observed within the human data set (Fig. 7, C and D), although much higher variability was noted with a few drugs (e.g., bosentan, naloxone, and carbamazepine), noticeable as outliers to this trend.

Application of PMU to Improve IVIVE 1: PMU Database. The current work has shown that the extent of PMU on $CL_{int,u\ in\ vitro}$ was correlated to the fu, both in vitro and in vivo (fu_p). This relationship appears to be independent of species, assay conditions, and drug properties, although human donor variability persists. It is important to note that this does not necessarily exclude these variables from influencing the PMU mechanism, but that the fu parameter itself may be capable of capturing, and thus accounting for, the majority of these potential effects.

Linear regression analysis was performed to quantify the identified relationship between $\log_{10}$-transformed fu_p and $\log_{10}$-transformed fold-change in $CL_{int,u\ in\ vitro}$ values caused by the addition of PP (Fig. 8). No significant difference was observed between human and rat data sets [$F_{(2,51)} = 2.996$, $P = 0.0589$], and thus a single equation (eq. 4) was used to assess whether incorporation of predicted PMU could improve IVIVE for both species of this discrete set of drugs. Because of the relatively weak correlation (r^2 for all data are 0.3), reanalysis without bosentan was performed, which yielded a stronger relationship while demonstrating no significant difference between rat and human data sets (r^2 −0.46, $P =$ 0.36, full details and statistical analysis are displayed in Supplemental Fig. 6). Therefore, despite the variability in the data, the relationship identified in Fig. 8 was used to assess whether accounting for the effect of PMU on $CL_{int,u\ in\ vitro}$ could improve IVIVE of hepatic CL. If the PMU phenomenon only occurs in vitro, it is still plausible that the incorporation of predicted PMU will improve prediction of CL by

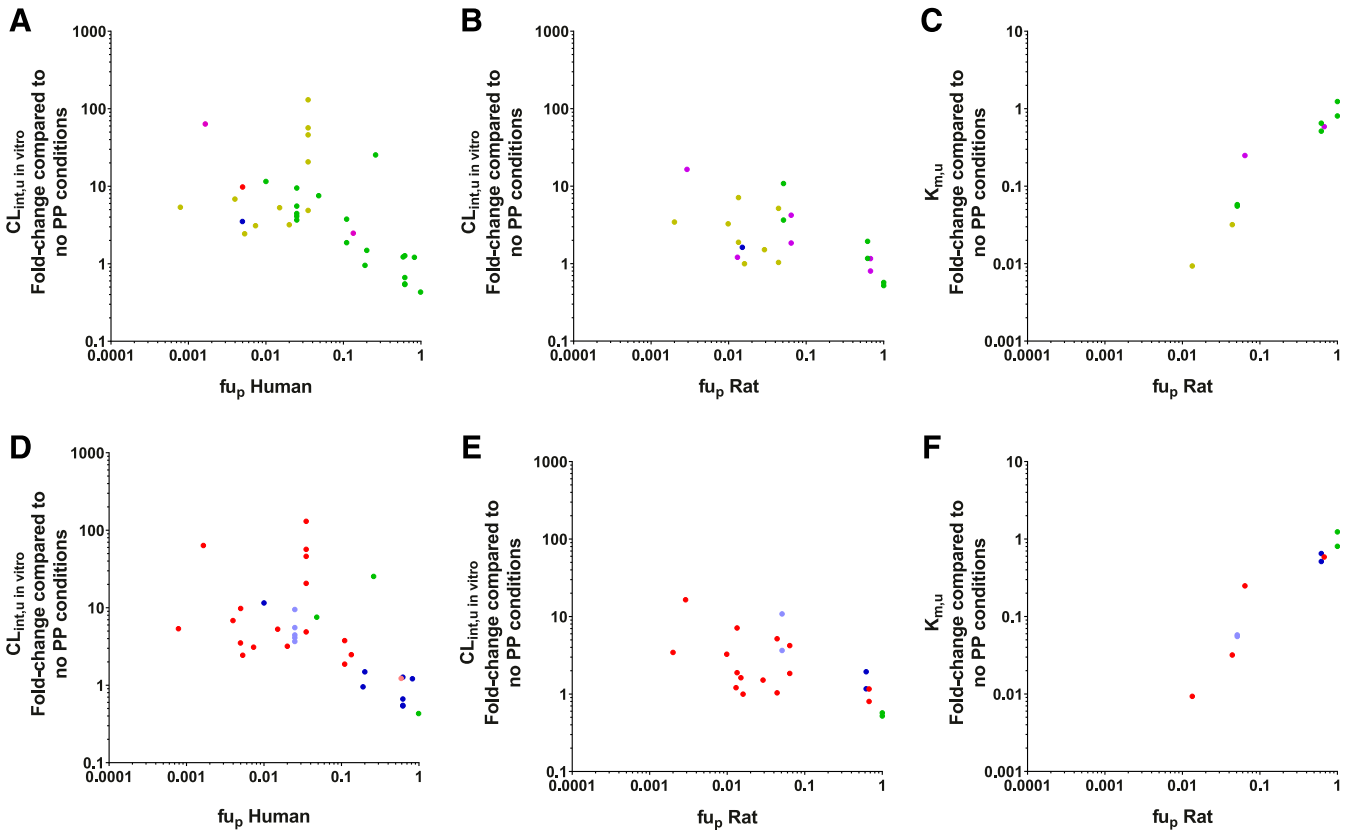

Fig. 6. Fold-change in in vitro clearance parameters in relation to their fu_p segregated according to their species and ECCS group [(A–C) 1a, red; 1b, yellow; 2, green; 3a, blue; 3b, purple) or ionization [(D–F) acid, red; weak acid, pink; neutral, green; base, blue; weak base, light blue). (A and D) Fold-change in $CL_{int,u\ in\ vitro}$ values from human data (ECCS: 1a = 1, 1b = 11, 2 = 19, 3a = 1, 3b = 2; ionization: acid = 17, weak acid = 1, neutral = 3, weak base = 5, base = 8). (B and E) Fold-change in $CL_{int,u\ in\ vitro}$ values from rat data (ECCS: 1b = 8, 2 = 10, 3a = 1, 3b = 6; ionization: acid = 15, neutral = 4, weak base = 2, base = 4). (C and F) Fold-change in $K_{m,u}$ values from rat data (ECCS: 1b = 2, 2 = 10, 3b = 2; ionization: acid = 4, neutral = 4, weak base = 2, base = 4).

optimization of the $CL_{int,u\ in\ vitro}$ value used. In contrast, if PMU represents a true physiologic process occurring in vivo, then improvements in IVIVE would be anticipated as a result of the complete incorporation of all key processes.

Firstly, the PMU database was used to assess the prediction of $CL_{int,u\ in\ vivo}$ and CL_H in both rat and human based on experimental values obtained in the absence of PP, experimental values obtained in the presence of PP, and the predicted values incorporating PMU (based on eq. 4). Overall, clear improvements for rat and human were observed for both $CL_{int,u\ in\ vivo}$ and CL_H values by either performing in vitro experiments with PP or by accounting for predicted PMU effect in comparison with data obtained in the absence of PP (Table 2). Graphical outputs of these results are shown in Supplemental Fig. 7. In the absence of PP, AFE for rat and human $CL_{int,u\ in\ vivo}$ were 3.02 and 3.55, respectively, and this reduced to <2 by either incorporation of predicted PMU enhancement or experimental addition of PP. For both rat and human $CL_{int,u\ in\ vivo}$ values, addition of PP showed no improvements to the precision of the in vivo predictions (compared with the absence of PP). However, use of the predicted PMU appeared to increase precision in rat (RMSE of 3200 compared with 25,000 in the absence of PP), although the high-CL drug mibefradil was not included in the rat PMU data set, as a rat fu_p could not be sourced, which may have skewed the analysis. The human CL_H predictions showed similar trends, with the predictions made in the experimental presence of PP or incorporation of predicted PMU enhancement showing improvements (by AFE values) compared with the predictions made in the absence of PP. The rat CL_H predictions were less conclusive, as reasonably accurate predictions were observed in the absence of PP (AFE = 1.39) for the small number of drugs analyzed within this data set (n = 13). Overall, predictions in the PMU database made with either addition of PP to experimental conditions or predicted PMU enhancement based on the identified trend in this work, showed equivalent improvements compared with predictions made in the absence of PP. This is despite the expected limitations in judging prediction based on a small data set comprising drugs with diverse CL routes [transport, metabolic, and potentially biliary (the latter, ECCS class 3b)].

Application of PMU to Improve IVIVE 2: Wood et al. (2017) Database. To further assess the utility of the PMU in IVIVE predictions, a broader data set, the Wood et al. (2017) database (which contains rat and human data, both $n \geq 100$), was used. This data set predominantly comprised metabolically cleared drugs (ECCS class 1a and 2). Incorporation of PMU effect in both rat and human data sets showed clear improvements in $CL_{int,u\ in\ vivo}$ predictions (Fig. 9). Predictions incorporating PMU effect were more accurate, as demonstrated by improved AFE values (from 4.67 to 1.21, and 4.20 to 1.56 in rat and human, respectively), and greater percentage of values within the 2- and 3-fold limits (Table 3). However, no improvements in precision (similar RMSE values) were observed.

Examining predictions for CL_H, it was again observed that incorporation of PMU improved the accuracy of IVIVE predictions (Fig. 10), reducing AFE values from 3.81 to 1.17 and from 2.73 to 1.17 in rat and human, respectively. Over 50% of compounds were predicted within 2-fold, and almost 75% were predicted within 3-fold of the observed values for both species after application of PMU enhancement

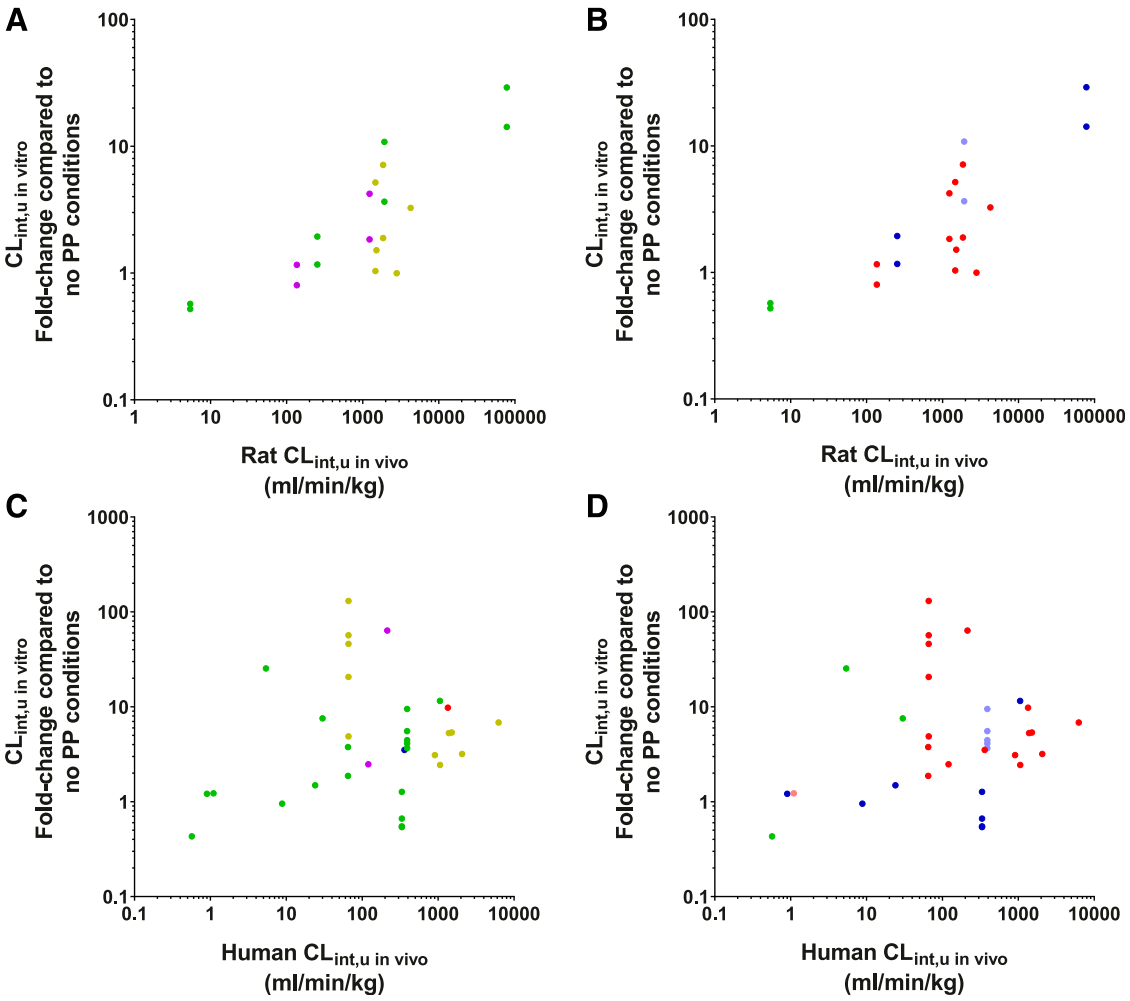

Fig. 7. Fold-change in $CL_{int,u\ in\ vitro}$ in comparison with their total $CL_{int,u\ in\ vivo}$, segregated by their species and ECCS group [(A and C) 1a, red; 1b, yellow; 2, green; 3a, blue; 3b, purple) or ionization [(B and D) acid, red; weak acid, pink; neutral, green; base, blue; weak base, light blue). Fold-change in $CL_{int,u\ in\ vitro}$ in rat [(A and B) ECCS: 1b = 8, 2 = 10, 3a = 1, 3b = 6; ionization: acid = 15, neutral = 4, weak base = 2, base = 4). Fold-change in $CL_{int,u\ in\ vitro}$ in human [(C and D) ECCS: 1a = 1, 1b = 11, 2 = 19, 3a = 1, 3b = 2; ionization: acid = 17, weak acid = 1, neutral = 3, weak base = 5, base = 8).

(Table 3). Without incorporation of PMU enhancement, <50% of CL_H values were predicted within 3-fold (both species). Precision is also improved within the rat data set (RMSE decreased from 42.3 to 24.1), but only a minor improvement in precision was observed for the human data set (6.65–5.51). Some overprediction of low-clearance compounds (<1 ml/min per kg) was observed.

Discussion

There is a vital need to address the shortcomings of existing IVIVE methodology for prediction of drug CL. Currently, a major yet unresolved issue is the role of PP in vitro and its apparent challenge to the conventional FDH. Although considerable compelling evidence of drug uptake into hepatocytes being dependent on bound rather than unbound drugs has accumulated, cases remain unresolved with mechanistic hypotheses and solutions that vary. The basis of the FDH is a rapidly maintained equilibrium of unbound drug in either side of a membrane in the absence of (asymmetric) energy-requiring transport processes. Although this may appear to be violated in the presence of PP (for which higher $CL_{int,u\ in\ vitro}$ than expected is reported), it is possible that the concentration of unbound drug at the hepatocyte surface is enhanced because of PMU, and thus the FDH would remain valid at a biochemical level while appearing violated as a result of discrepancy in fu between the hepatocyte surface and the bulk plasma. On this basis, a drug's hepatic disposition may be affected by PMU regardless of involvement of hepatic uptake transport.

In the present study, we have unified the reported quantitative effects of PP (or isolated albumin) in hepatocyte assays of CL (reported between 1997 and 2020) into a database to facilitate global trend analysis and an improved understanding of the impact of PP across the widest range of drugs (including drugs cleared predominantly by either transport or metabolism), potentially leading to a more generic prediction approach, was sought.

Initial analysis focused on the impact of PP at the in vitro level, with the impact of PP calculated as the fold-change in CL parameters caused by the addition of PP. A distinct, inverse linear trend (spanning several orders of magnitude) was observed between the fold-change in $CL_{int,u\ in\ vitro}$ and in vitro fu, demonstrating a clear effect of PMU beyond that expected from conventionally determined unbound drug concentrations. This is in agreement with previous studies that also indicated that the enhancement of $CL_{int,u\ in\ vitro}$ by PP might be dependent upon the extent of binding (Miyauchi et al., 2018; Bowman et al., 2019). Of extra significance, there was essentially no difference in this trend between human and rat hepatocytes, supporting potentially useful cross-species

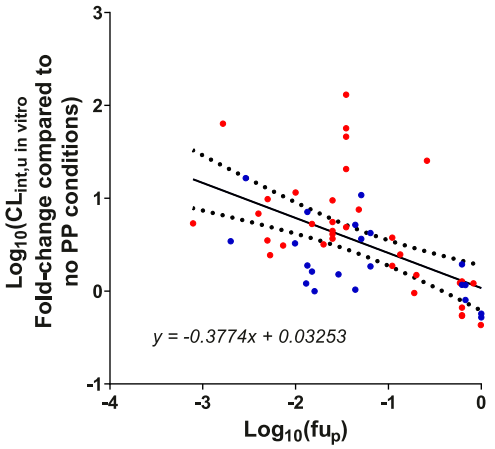

Fig. 8. Relationship between fu_p and the fold-change in $CL_{int,u\ in\ vitro}$ caused by the addition of physiologic relevant concentrations of PP compared with no-PP conditions. Linear regression analysis was performed on the log_{10}-transformed fu_p and fold-change in $CL_{int,u\ in\ vitro}$ data. All data (human and rat) were shown to have a significant slope [$F_{(1,53)} = 22.95$, $P < 0.0001$]. No significant difference was observed between the human (red) and rat (blue) data sets [$F_{(1,51)} = 2.996$, $P = 0.0589$], and thus the same equation (displayed) can be used for both species. The 95% confidence bands (dotted lines) are also displayed. r^2 values for rat, human, and total data for this line are 0.1099, 0.2782, and 0.3022, respectively.

equivalence. No clear trends were observed for the fold-change in K_m in relation to the in vitro fu; however, $K_{m,u}$ showed a clear positive relationship [in agreement with Bowman et al. (2019)], suggesting that this parameter may be underestimated during conventional adjustment for unbound drug (based on equilibrium fu values).

The impact of experimental conditions (assay format, shaking, and PP type) on the observed impact of PMU in relation to in vitro fu was also investigated to assess possible experimental bias and reveal potential mechanistic insight into PMU. No clear difference was observed between monolayer and suspension assays. However, for suspension assays with confirmed shaking, there appeared to be a marginally greater effect on fold-change in $CL_{int,u\ in\ vitro}$ compared with shaking assays performed under indeterminate shaking conditions. This suggests a potential (at least minor) role for the UWL barrier in PMU. The type of PP used was also investigated. To date, it has not been clarified whether PMU is specifically limited to albumin or if other PPs (i.e., AAG and lipoproteins) contribute, as only albumin has been tested repeatedly, in isolation. Although no distinction of effect between PP was observed in the human studies (confounded by high variability), a possible effect of PP type was observed in the rat data set; however, further studies are required to resolve this from potential interlaboratory variability.

The impact of PP on clearance parameters in vitro was also investigated at in vivo levels of PP binding, as well as whether drug properties (ionization and ECCS group) could affect these trends. Similar to the in vitro fu relationship, trends were observed between the fold-change in $CL_{int,u\ in\ vitro}$ and the fu_p, with the greatest increase in $CL_{int,u\ in\ vitro}$ values correlating with lower fu_p. This relationship is potentially useful considering the utility of readily obtained fu_p in prediction methodology. The fold-change also demonstrated a positive correlation with $CL_{int,u\ in\ vivo}$ values, indicating that highly bound ($fu_p < 0.1$) and higher-metabolic-turnover drugs tend to be more affected by PMU (particularly evident in rat). Again, no statistical difference between human and rat data sets was observed for either of these trends, further highlighting the usefulness of such cross-species comparison (Hallifax and Houston, 2019). The clear trends in the rat data helped provide confidence in the human data, despite the higher variability of the latter [due to multiple drug-dependent factors and human donor variability, Wood et al. (2017)]. Although the correlation between $CL_{int,u\ in\ vivo}$ and fu_p could be interpreted as a coincidental consequence of lipophilicity, it might reflect modulation of CL by plasma protein. For rapidly metabolized high-permeability drugs, the rate-limiting step in the CL could be drug diffusion through the UWL (Wood et al., 2018). If the presence of PP enhances drug diffusion through the UWL, as proposed by Ichikawa et al. (1992), then the extent of binding may be a critical rate determinant for such drugs, and the ability of PP to overcome such diffusional/permeation barriers may be reflected in the enhancement of $CL_{int,u\ in\ vitro}$.. Unfortunately, the trend of protein effect with absolute $CL_{int,u\ in\ vivo}$ could not be resolved further into uptake transport or metabolic CL because of the lack of specific data.

The relationship between fold-change in $CL_{int,u\ in\ vitro}$ and fu (in vitro and in vivo) appeared to be independent of ionization or ECCS group, suggesting that PMU involves a more general drug uptake process applicable across both passive and active uptake mechanisms. The majority of drugs studied were either ECCS class 1b or 2; the acidic class 1b drugs were generally more highly bound, and the basic or neutral class 2 drugs were less so, overlapping at about $fu_p = 0.2$ (in human). This continuum of PMU effect therefore clearly spanned drug type and, potentially, different responsible proteins. Basic drugs bind to albumin to a much lesser extent than acids, which, combined with their more avid binding to AAG, suggests that basic drugs would not share the same effect with acids, proportionally, if the mechanism relied on dissociation facilitated by an interaction of drug-protein complex with the hepatocyte plasma membrane, as has been explored with respect to albumin and acidic compounds (Stremmel et al., 1983; Miyauchi et al., 2018). This

TABLE 2

IVIVE Analysis of $CL_{int,u\ in\ vivo}$ and CL_H from the PMU database

	Rat $CL_{int,u\ in\ vivo}$			Human $CL_{int,u\ in\ vivo}$			Rat CL_H			Human CL_H		
	No PP	+PP	PMU	No PP	+PP	PMU	No PP	+PP	PMU	No PP	+PP	PMU
n^a	20	19	18	36	34	36	13	10	13	33	33	33
AFE	3.02	1.26	1.71	3.55	1.30	1.04	1.39	1.01	1.49	3.50	1.20	1.22
RMSE	24,770	24,940	3200	1200	1180	983	18.7	23.3	23.1	7.44	7.76	6.36
% < 2-fold	35	42	50	17	26	33	62	70	69	18	45	45
% < 3-fold	55	74	67	23	47	47	93	100	100	30	61	63
% > 3-fold	45	26	33	78	53	53	8	—	—	69	39	36

No PP, $CL_{int,u\ in\ vivo}$ predictions based on $CL_{int,u\ in\ vitro}$ values obtained from hepatocytes in the absence of PP; +PP, $CL_{int,u\ in\ vivo}$ predictions based on $CL_{int,u\ in\ vitro}$ values obtained from hepatocytes in the presence of PP; PMU, $CL_{int,u\ in\ vivo}$ predictions based on $CL_{int,u\ in\ vitro}$ values obtained from hepatocytes in the absence of PP and PMU enhancement predicted (and applied) based on fu_p (eq. 4).

[a] *n* number varies from previous analysis, between data sets, and between $CL_{int,u\ in\ vivo}$ and CL_H predictions due to the availability of in vivo data (fu_p, fu_b, and observed $CL_{int,u\ in\ vivo}$ and CL_H values) for the PMU database.

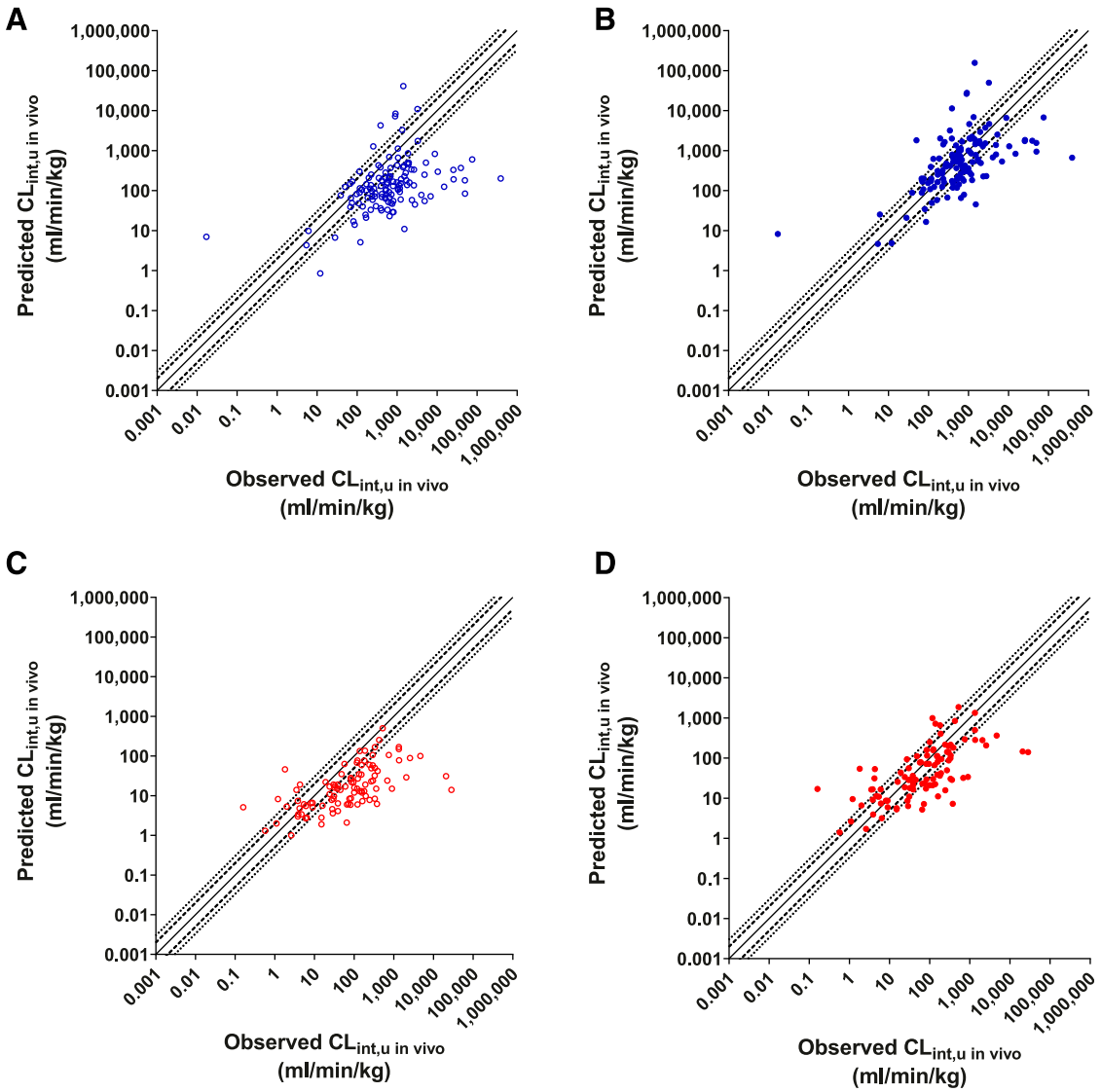

Fig. 9. IVIVE analysis of $CL_{int,u\ in\ vivo}$ for compounds obtained from the Wood et al. (2017) database. Observed vs. predicted values without PMU-enhanced prediction [open circles, (A and C)] or with PMU-enhanced prediction [closed circles, (B and D)] in rat [blue, (A and B)] and human [red, (C and D)]. Solid line, dashed line, and dotted line represent unity, 2-fold, and 3-fold error.

further highlights that future in vitro studies with various types of PP are required to improve our mechanistic understanding of PMU for acids and bases. Despite the mechanistic uncertainty, the fu_p parameter may adequately account for differences in the binding of acidic and basic drugs to PP in prospective prediction of PMU enhancement of CL.

Previous IVIVE assessment has suggested that the underprediction of CL is related to the extent of binding to PP (Ring et al., 2011; Bowman and Benet, 2016)—a possibility that might now be interpreted as a consequence of the PMU effect. To improve IVIVE, addition of PP into in vitro CL assays (Shibata et al., 2000; Blanchard et al., 2004, 2005, 2006; Li et al., 2020), determination of unbound drug Kp in hepatocytes in the presence of PP (Li et al., 2020; Riccardi et al., 2020), or semiempirically predicting the PMU effect based on an apparent shift in fu between plasma and interstitial fluid ($fu_{p\text{-adjusted}}$) has previously been

TABLE 3

IVIVE analysis of PMU effect in rat and human on $CL_{int,u\ in\ vivo}$ and CL_H values using the Wood et al. (2017) database

	Rat $CL_{int,u\ in\ vivo}$		Human $CL_{int,u\ in\ vivo}$		Rat CL_H		Human CL_H	
	No PMU	PMU	No PMU	PMU	No PMU	PMU	No PMU	PMU
n	128	128	100	100	128	128	100	100
AFE	4.67	1.21	4.20	1.56	3.81	1.17	2.73	1.17
RMSE	36,203	38,732	3566	3544	42.3	24.1	6.65	5.51
% < 2-fold	20	45	25	34	26	57	30	51
% < 3-fold	32	63	38	58	42	75	49	74
% > 3-fold	69	38	62	42	58	25	51	26

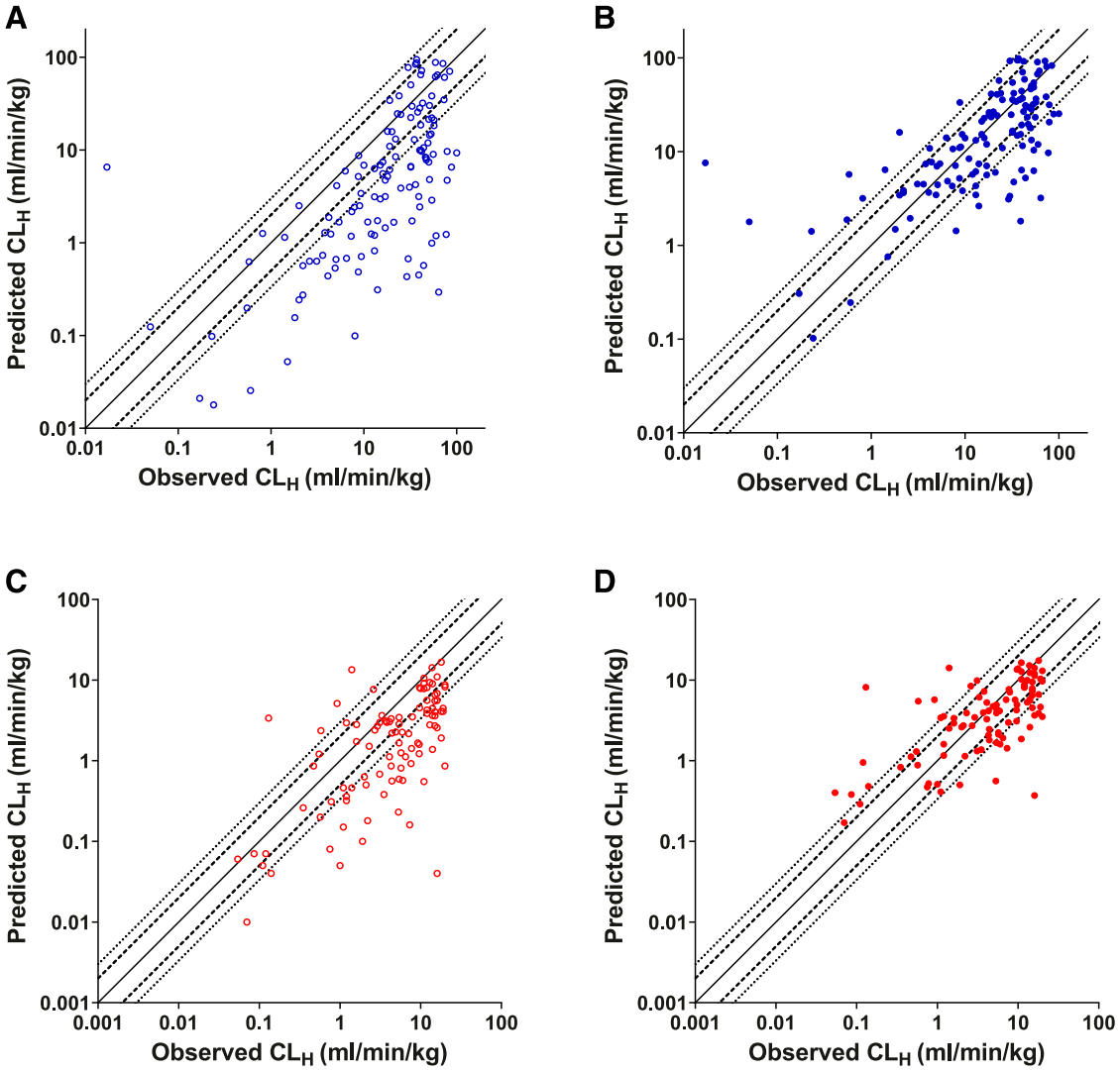

Fig. 10. IVIVE analysis of CL_H for compounds obtained from the Wood et al. (2017) database. Observed vs. predicted values without PMU-enhanced prediction [open circles, (A and C)] or with PMU-enhanced prediction [closed circles, (B and D)] in rat [blue, (A and B)] and human [red, (C and D)]. Solid line, dashed line, and dotted line represent unity, 2-fold, and 3-fold error.

suggested (Poulin and Haddad, 2015). Although all methods reported improved IVIVE, determination of unbound Kp in hepatocytes requires additional experimentation, incorporation of $fu_{p\text{-adjusted}}$ has presently only been justified for acidic compounds, and the addition of PP in vitro has the disadvantage of reducing the total $CL_{int\ in\ vitro}$ measured, making reliable quantification of highly bound and/or low-CL compounds challenging. The current work has shown that the PMU effect may be predicted using fu_p (independent of drug type), specific PP, and hepatocyte species; hence, $CL_{int,u\ in\ vitro}$ measured in the absence of PP can be converted to a PMU-corrected value by applying the formula in eq. 4. There is, however, considerable variability in the relationship between PMU effect and fu, which indicates that some procedural (e.g., protein type) or drug-specific factors are influential if as yet unresolved among available data. Nevertheless, the application of predicted PMU effect within the PMU database (n = 26) appears to improve IVIVE predictions to a similar extent to those predictions performed directly in the presence of PP, suggesting that the identified relationship accurately captures the observed PMU enhancement and that it is an appropriate tool to predict PMU for CL assays performed in the absence of PP. This proposition was subsequently tested with an unrelated data set [Wood et al. (2017), $n \geq 100$]. Clear improvements were observed in the IVIVE for both rat and human subsets (regardless of hepatic model used, Supplemental Fig. 1), achieving an AFE $<$1.2, and over 50% of compounds predicted within 2-fold of their observed values, demonstrating the utility of the relationship identified in this study. Although incorporation of this PMU prediction step effectively eliminates bias, there remains considerable imprecision in prediction, and further experimental effort to understand the variability between, for example, protein type or the impact of shaking in vitro is warranted. Beyond this, drug-specific factors such as rate-limiting elimination pathways may need more detailed assessment. Nevertheless, considering the lack of bias using this relationship for IVIVE and the occurrence of PMU in numerous IPL studies, PMU might be considered an in vivo as well as in vitro phenomenon.

In this study, we have demonstrated a generic relationship between fu and fold-change in $CL_{int,u\ in\ vitro}$ (for both uptake transport and metabolically cleared drugs) caused by the addition of PP, despite numerous potential underlying mechanisms. This offers a practical benefit for prospective prediction of CL across a broad range of drug uptake and clearance mechanisms. A simple empirical correction for

PMU based on independently determined equilibrium fu_p can be applied to a conventional hepatocyte assay (rat or human) without the need to add PP, thereby avoiding compromising CL assay sensitivity.

Acknowledgments

The authors would like to thank Leon Aarons for useful discussion on the data analysis.

Authorship Contributions

Participated in research design: Francis, Houston, Hallifax.

Performed data analysis: Francis, Hallifax.

Wrote or contributed to the writing of the manuscript: Francis, Houston, Hallifax.

References

Avdeef A (2012) Octanol water-partitioning, in *Absorption and Drug Development* pp 174–219, John Wiley & Sons, Inc., Hoboken, NJ.

Bachmann K, Byers J, and Ghosh R (2003) Prediction of in vivo hepatic clearance from in vitro data using cryopreserved human hepatocytes. *Xenobiotica* **33**:475–483.

Blanchard N, Alexandre E, Abadie C, Lavé T, Heyd B, Mantion G, Jaeck D, Richert L, and Coassolo P (2005) Comparison of clearance predictions using primary cultures and suspensions of human hepatocytes. *Xenobiotica* **35**:1–15.

Blanchard N, Hewitt NJ, Silber P, Jones H, Coassolo P, and Lavé T (2006) Prediction of hepatic clearance using cryopreserved human hepatocytes: a comparison of serum and serum-free incubations. *J Pharm Pharmacol* **58**:633–641.

Blanchard N, Richert L, Notter B, Delobel F, David P, Coassolo P, and Lavé T (2004) Impact of serum on clearance predictions obtained from suspensions and primary cultures of rat hepatocytes. *Eur J Pharm Sci* **23**:189–199.

Bowman CM and Benet LZ (2016) Hepatic clearance predictions from in vitro-in vivo extrapolation and the biopharmaceutics drug disposition classification system. *Drug Metab Dispos* **44**: 1731–1735.

Bowman CM, Okochi H, and Benet LZ (2019) The presence of a transporter-induced protein binding shift: a new explanation for protein-facilitated uptake and improvement for in vitro-in vivo extrapolation. *Drug Metab Dispos* **47**:358–363.

Brown HS, Griffin M, and Houston JB (2007) Evaluation of cryopreserved human hepatocytes as an alternative in vitro system to microsomes for the prediction of metabolic clearance. *Drug Metab Dispos* **35**:293–301.

Brunton L, Chabner BA, and Knollman B (2011) *Goodman and Gilman's the Pharmacological Basis of Therapeutics*, 2th ed, McGraw Hill Education, New York.

Chung YB, Miyauchi S, Sugiyama Y, Harashima H, Iga T, and Hanano M (1990) Effect of various organic anions on the plasma disappearance of 1-anilino-8-naphthalene sulfonate. *J Hepatol* **11**: 240–251.

De Bruyn T, Ufuk A, Cantrill C, Kosa RE, Bi YA, Niosi M, Modi S, Rodrigues AD, Tremaine LM, Varma MVS, et al. (2018) Predicting human clearance of organic anion transporting polypeptide substrates using cynomolgus monkey: in vitro-in vivo scaling of hepatic uptake clearance. *Drug Metab Dispos* **46**:989–1000.

Forker EL and Luxon BA (1981) Albumin helps mediate removal of taurocholate by rat liver. *J Clin Invest* **67**:1517–1522.

Forker EL and Luxon BA (1983) Albumin-mediated transport of rose bengal by perfused rat liver. Kinetics of the reaction at the cell surface. *J Clin Invest* **72**:1764–1771.

Fujino R, Hashizume K, Aoyama S, Maeda K, Ito K, Toshimoto K, Lee W, Ninomiya SI, and Sugiyama Y (2018) Strategies to improve the prediction accuracy of hepatic intrinsic clearance of three antidiabetic drugs: application of the extended clearance concept and consideration of the effect of albumin on CYP2C metabolism and OATP1B-mediated hepatic uptake. *Eur J Pharm Sci* **125**:181–192.

Hallifax D and Houston JB (2019) Use of segregated hepatocyte scaling factors and cross-species relationships to resolve clearance dependence in the prediction of human hepatic clearance. *Drug Metab Dispos* **47**:320–327.

Ichikawa M, Tsao SC, Lin TH, Miyauchi S, Sawada Y, Iga T, Hanano M, and Sugiyama Y (1992) 'Albumin-mediated transport phenomenon' observed for ligands with high membrane permeability. Effect of the unstirred water layer in the Disse's space of rat liver. *J Hepatol* **16**:38–49.

Ito K and Houston JB (2004) Comparison of the use of liver models for predicting drug clearance using in vitro kinetic data from hepatic microsomes and isolated hepatocytes. *Pharm Res* **21**: 785–792.

Kim SJ, Lee KR, Miyauchi S, and Sugiyama Y (2019) Extrapolation of in vivo hepatic clearance from in vitro uptake clearance by suspended human hepatocytes for anionic drugs with high binding to human albumin: improvement of in vitro-to-in vivo extrapolation by considering the "albumin-mediated" hepatic uptake mechanism on the basis of the "facilitated-dissociation model". *Drug Metab Dispos* **47**:94–103.

Lave T, Dupin S, Schmitt C, Chou RC, Jaeck D, and Coassolo P (1997) Integration of in vitro data into allometric scaling to predict hepatic metabolic clearance in man: application to 10 extensively metabolized drugs. *J Pharm Sci* **86**:584–590.

Li N, Badrinarayanan A, Li X, Roberts J, Hayashi M, Virk M, and Gupta A (2020) Comparison of in vitro to in vivo extrapolation approaches for predicting transporter-mediated hepatic uptake clearance using suspended rat hepatocytes. *Drug Metab Dispos* **48**:861–872.

Miyauchi S, Masuda M, Kim SJ, Tanaka Y, Lee KR, Iwakado S, Nemoto M, Sasaki S, Shimono K, Tanaka Y, et al. (2018) The phenomenon of albumin-mediated hepatic uptake of organic anion transport polypeptide substrates: prediction of the in vivo uptake clearance from the in vitro uptake by isolated hepatocytes using a facilitated-dissociation model. *Drug Metab Dispos* **46**:259–267.

Poulin P and Haddad S (2015) Albumin and uptake of drugs in cells: additional validation exercises of a recently published equation that quantifies the albumin-facilitated uptake mechanism(s) in physiologically based pharmacokinetic and pharmacodynamic modeling research. *J Pharm Sci* **104**:4448–4458.

Riccardi K, Ryu S, Tess D, Li R, Luo L, Johnson N, Jordan S, Patel R, and Di L (2020) Comparison of fraction unbound between liver homogenate and hepatocytes at 4°C. *AAPS J* **22**:91.

Ring BJ, Chien JY, Adkison KK, Jones HM, Rowland M, Jones RD, Yates JW, Ku MS, Gibson CR, He H, et al. (2011) PhRMA CPCDC initiative on predictive models of human pharmacokinetics, part 3: comparative assessement of prediction methods of human clearance. *J Pharm Sci* **100**:4090–4110.

Rowland A, Knights KM, Mackenzie PI, and Miners JO (2008) The "albumin effect" and drug glucuronidation: bovine serum albumin and fatty acid-free human serum albumin enhance the glucuronidation of UDP-glucuronosyltransferase (UGT) 1A9 substrates but not UGT1A1 and UGT1A6 activities. *Drug Metab Dispos* **36**:1056–1062.

Shibata Y, Takahashi H, and Ishii Y (2000) A convenient in vitro screening method for predicting in vivo drug metabolic clearance using isolated hepatocytes suspended in serum. *Drug Metab Dispos* **28**:1518–1523.

Stremmel W, Potter BJ, and Berk PD (1983) Studies of albumin binding to rat liver plasma membranes. Implications for the albumin receptor hypothesis. *Biochim Biophys Acta* **756**:20–27.

Tsao SC, Sugiyama Y, Sawada Y, Iga T, and Hanano M (1988) Kinetic analysis of albumin-mediated uptake of warfarin by perfused rat liver. *J Pharmacokinet Biopharm* **16**:165–181.

Varma MV, Steyn SJ, Allerton C, and El-Kattan AF (2015) Predicting clearance mechanism in drug discovery: Extended Clearance Classification System (ECCS). *Pharm Res* **32**:3785–3802.

Watanabe T, Kusuhara H, Maeda K, Kanamaru H, Saito Y, Hu Z, and Sugiyama Y (2010) Investigation of the rate-determining process in the hepatic elimination of HMG-CoA reductase inhibitors in rats and humans. *Drug Metab Dispos* **38**:215–222.

Weisiger R, Gollan J, and Ockner R (1981) Receptor for albumin on the liver cell surface may mediate uptake of fatty acids and other albumin-bound substances. *Science* **211**:1048–1051.

Weisiger RA and Ma WL (1987) Uptake of oleate from albumin solutions by rat liver. Failure to detect catalysis of the dissociation of oleate from albumin by an albumin receptor. *J Clin Invest* **79**:1070–1077.

Wood FL, Houston JB, and Hallifax D (2017) Clearance prediction methodology needs fundamental improvement: trends common to rat and human hepatocytes/microsomes and implications for experimental methodology. *Drug Metab Dispos* **45**:1178–1188.

Wood FL, Houston JB, and Hallifax D (2018) Importance of the unstirred water layer and hepatocyte membrane integrity in vitro for quantification of intrinsic metabolic clearance. *Drug Metab Dispos* **46**:268–278.

Yabe Y, Galetin A, and Houston JB (2011) Kinetic characterization of rat hepatic uptake of 16 actively transported drugs. *Drug Metab Dispos* **39**:1808–1814.

Address correspondence to: D. Hallifax, Centre for Applied Pharmacokinetic Research, Division of Pharmacy and Optometry, School of Health Sciences, Faculty of Biology, Medicine and Health, University of Manchester, Manchester Academic Health Science Centre, Manchester, M13 9PT, United Kingdom. E-mail: David.Hallifax@manchester.ac.uk

Supplemental Material for manuscript: DMD-AR-2020-000294

Title: Impact of plasma protein binding in drug clearance prediction: a database analysis of published studies and implications for in vitro in vivo extrapolation (IVIVE)

Authors: Francis LJ, Houston JB and Hallifax D

Journal: Drug Metabolism and Distribution

Supplemental Tables S1: PMU Database Tables

Table S1 A: In vitro values and fold-change in clearance parameters calculated with experimental details listed.

		In vitro values						Fold-Change compared to no PP conditions						Assay conditions						
Compound	**Protein conc.**	**In vitro fu**	**V_{max} [a]**	**K_m [b]**	**CL_{int} [c]**	**$K_{m,u}$ [b]**	**$CL_{int,u}$ [c]**	**V_{max}**	**$K_{m,u}$**	**K_m**	**$CL_{int,u}$**	**CL_{int}**	**Species**	**Assay format**	**PP type**	**Experimental Conditions**	**Shaking?**	**Drug concentration**	**Duration**	**REF**
ANS	0% [d]	1.00 [d]			60.30 [d, e]		60.30 [d]						Rat	Fresh hepatocytes, monolayer	BSA	6-well plate 0.33 X 10^6 cells/ml	NS	Unbound concentration fixed at 2.4μM	1-3 minutes	(Miyauchi et al., 2018)
	0.02% [d]	0.49 [d]			33.58 [d, e]		69.10 [d]				1.15 [d]	0.56 [d]	Rat	Fresh hepatocytes, monolayer	BSA	6-well plate 0.33 X 10^6 cells/ml	NS	Unbound concentration fixed at 2.4μM	1-3 minutes	(Miyauchi et al., 2018)
	0.09% [d]	0.13 [d]			10.58 [d, e]		84.00 [d]				1.39 [d]	0.18 [d]	Rat	Fresh hepatocytes, monolayer	BSA	6-well plate 0.33 X 10^6 cells/ml	NS	Unbound concentration fixed at 2.4μM	1-3 minutes	(Miyauchi et al., 2018)
	0.25% [d]	0.05 [d]			5.50 [d, e]		113 [d]				1.87 [d]	0.09 [d]	Rat	Fresh hepatocytes, monolayer	BSA	6-well plate 0.33 X 10^6 cells/ml	NS	Unbound concentration fixed at 2.4μM	1-3 minutes	(Miyauchi et al., 2018)
	0.51% [d]	0.02 [d]			3.00 [d, e]		130 [d]				2.16 [d]	0.05 [d]	Rat	Fresh hepatocytes, monolayer	BSA	6-well plate 0.33 X 10^6 cells/ml	NS	Unbound concentration fixed at 2.4μM	1-3 minutes	(Miyauchi et al., 2018)
	0% [d]	1.00 [d]			62.70 [d, e]		62.70 [d]						Rat	Fresh hepatocytes, monolayer	BSA	6-well plate 0.33 X 10^6 cells/ml	NS	20μM	1-3 minutes	(Miyauchi et al., 2018)
	0.02% [d]	0.49 [d]			40.78 [d, e]		83.90 [d]				1.34 [d]	0.65 [d]	Rat	Fresh hepatocytes, monolayer	BSA	6-well plate 0.33 X 10^6 cells/ml	NS	20μM	1-3 minutes	(Miyauchi et al., 2018)
	0.09% [d]	0.13 [d]			15.12 [d, e]		120 [d]				1.91 [d]	0.24 [d]	Rat	Fresh hepatocytes, monolayer	BSA	6-well plate 0.33 X 10^6 cells/ml	NS	20μM	1-3 minutes	(Miyauchi et al., 2018)
	0.25% [d]	0.05 [d]			8.33 [d, e]		171 [d]				2.73 [d]	0.13 [d]	Rat	Fresh hepatocytes, monolayer	BSA	6-well plate 0.33 X 10^6 cells/ml	NS	20μM	1-3 minutes	(Miyauchi et al., 2018)
	0.51% [d]	0.02 [d]			3.67 [d, e]		159 [d]				2.54 [d]	0.06 [d]	Rat	Fresh hepatocytes, monolayer	BSA	6-well plate 0.33 X 10^6 cells/ml	NS	20μM	1-3 minutes	(Miyauchi et al., 2018)
Antipyrine	0%	1.00	83.58 [f]	79.60 [g]	1.05	79.60 [g]	1.05						Rat	Fresh hepatocytes, monolayer	Rat Serum	24-well plate 1 X 10^6 cells/ml	NS	50, 100, 500μM	2-300 minutes	(Blanchard et al., 2004)
	Pure Serum	1.00	38.51 [f]	64.19 [g]	0.60	64.19 [g]	0.60	0.46	0.81	0.81	0.57	0.57	Rat	Fresh hepatocytes, monolayer	Rat Serum	24-well plate 1 X 10^6 cells/ml	NS	50, 100, 500μM	2-300 minutes	(Blanchard et al., 2004)
	0%	1.00	72.13 [f]	73.60 [g]	0.98	73.60 [g]	0.98						Rat	Fresh hepatocytes, suspension	Rat Serum	24-well plate 1 X 10^6 cells/ml	300rpm	50, 100, 500μM	2-300 minutes	(Blanchard et al., 2004)

	In vitro values							Fold-Change compared to no PP conditions					Assay conditions							
Compound	**Protein conc.**	**In vitro fu**	**V_{max} [a]**	**K_m [b]**	**CL_{int} [c]**	**$K_{m,u}$ [b]**	**$CL_{int,u}$ [c]**	**V_{max}**	**$K_{m,u}$**	**K_m**	**$CL_{int,u}$**	**CL_{int}**	**Species**	**Assay format**	**PP type**	**Experimental Conditions**	**Shaking?**	**Drug concentration**	**Duration**	**REF**
	Pure Serum	1.00	46.37 [f]	90.93 [g]	0.51	90.93 [g]	0.51	0.64	1.24	1.24	0.52	0.52	Rat	Fresh hepatocytes, suspension	Rat Serum	24-well plate 1 X 10^6 cells/ml	300rpm	50, 100, 500µM	2-300 minutes	(Blanchard et al., 2004)
	0%	1.00			0.54		0.54 [e]						Human	Cryopreserved hepatocytes, suspension	Human Serum	24-well plate 1.5 X 10^6 cells/ml	300rpm	100µM	Up to 300 minutes	(Blanchard et al., 2006)
	Pure Serum	1.00			0.23		0.23 [e]				0.43	0.43	Human	Cryopreserved hepatocytes, suspension	Human Serum	24-well plate 1.5 X 10^6 cells/ml	300rpm	100µM	Up to 300 minutes	(Blanchard et al., 2006)
Asunaprevir	0%	1.00			2,210 [e]		2,210						Rat	Cryopreserved hepatocytes, suspension	BSA	Centrifugal filtration 0.5 X 10^6 cells/ml	NS	1uM	20 seconds - 30 minutes	(Li et al., 2020)
	4%	0.06			157 [e]		2,668				1.21	0.07	Rat	Cryopreserved hepatocytes, suspension	BSA	Centrifugal filtration 0.5 X 10^6 cells/ml	NS	1uM	20 seconds - 30 minutes	(Li et al., 2020)
Atorvastatin	0%	1.00			24.20		24.20						Human	Cryopreserved hepatocytes, suspension	HSA	Centrifugal filtration 1 X 10^6 cells/ml	NS	3µM	0.25 and 1.25 minutes	(Kim et al., 2019)
	5%	0.03			2.16		77.00				3.18	0.09	Human	Cryopreserved hepatocytes, suspension	HSA	Centrifugal filtration 1 X 10^6 cells/ml	NS	3µM	0.25 and 1.25 minutes	(Kim et al., 2019)
	0%	1.00	1,650	3.60 [f]	458 [e]	3.61 [h]	458						Rat	Fresh hepatocytes, suspension	Human Plasma	24-well plate 0.5 X 10^6 cells/ml	Yes	1-100µM	2 minutes	(Bowman et al., 2019)
	Pure Plasma	0.02	272	5.74 [f]	47.40 [e]	0.12 [h]	2,370	0.16	0.03	1.59	5.17	0.10	Rat	Fresh hepatocytes, suspension	Human Plasma	24-well plate 0.5 X 10^6 cells/ml	Yes	1-100µM	2 minutes	(Bowman et al., 2019)
	0%	1.00			300 [e]		300						Rat	Cryopreserved hepatocytes, suspension	BSA	Centrifugal filtration 0.5 X 10^6 cells/ml	NS	1uM	20 seconds - 30 minutes	(Li et al., 2020)
	4%	0.07			20.53 [e]		311				1.04	0.07	Rat	Cryopreserved hepatocytes, suspension	BSA	Centrifugal filtration 0.5 X 10^6 cells/ml	NS	1uM	20 seconds - 30 minutes	(Li et al., 2020)
Bosentan	0%	1.00			23.20		23.20						Human	Cryopreserved hepatocytes, suspension	HSA	Centrifugal filtration 1 X 10^6 cells/ml	NS	3µM	0.25 and 1.25 minutes	(Kim et al., 2019)
	5%	0.01			1.24		113				4.87	0.05	Human	Cryopreserved hepatocytes, suspension	HSA	Centrifugal filtration 1 X 10^6 cells/ml	NS	3µM	0.25 and 1.25 minutes	(Kim et al., 2019)
	0%	1.00			1.76		1.76						Human	Cryopreserved hepatocytes, suspension	Human Serum	24-well plate 1.5 X 10^6 cells/ml	300rpm	5µM	Up to 300 minutes	(Blanchard et al., 2006)
	Pure Serum	0.03			0.94		36.27				20.64	0.54	Human	Cryopreserved hepatocytes, suspension	Human Serum	24-well plate 1.5 X 10^6 cells/ml	300rpm	5µM	Up to 300 minutes	(Blanchard et al., 2006)

		In vitro values						Fold-Change compared to no PP conditions					Assay conditions							
Compound	**Protein conc.**	**In vitro fu**	**V_{max} [a]**	**K_m [b]**	**CL_{int} [c]**	**$K_{m,u}$ [b]**	**$CL_{int,u}$ [c]**	**V_{max}**	**$K_{m,u}$**	**K_m**	**$CL_{int,u}$**	**CL_{int}**	**Species**	**Assay format**	**PP type**	**Experimental Conditions**	**Shaking?**	**Drug concentration**	**Duration**	**REF**
	0%	1.00	8.33	4.33 [g]	1.80		1.80 [e]						Human	Fresh hepatocytes, monolayer	Human Serum	24-well plate 0.6 X 10^6 cells/ml	NS	1, 10, 50µM	2-300 minutes	(Blanchard et al., 2005)
	Pure Serum	0.02	15.33	3.87 [g]	4.70		235 [e]	1.84		8.34	131	2.61	Human	Fresh hepatocytes, monolayer	Human Serum	24-well plate 0.6 X 10^6 cells/ml	NS	1, 10, 50µM	2-300 minutes	(Blanchard et al., 2005)
	0%	1.00	12.33	5.27 [g]	1.67		1.67 [e]						Human	Fresh hepatocytes, suspension	Human Serum	24-well plate 2 X 10^6 cells/ml	300rpm	1, 10, 50µM	2-300 minutes	(Blanchard et al., 2005)
	Pure Serum	0.02	7.67	5.54 [g]	1.53		76.67 [e]	0.62		0.17	46.00	0.92	Human	Fresh hepatocytes, suspension	Human Serum	24-well plate 2 X 10^6 cells/ml	300rpm	1, 10, 50µM	2-300 minutes	(Blanchard et al., 2005)
	0%	1.00	9.00	5.85 [g]	1.50		1.50 [e]						Human	Cryopreserved hepatocytes, suspension	Human Serum	24-well plate 2 X 10^6 cells/ml	300rpm	1, 10, 50µM	2-300 minutes	(Blanchard et al., 2005)
	Pure Serum	0.02	9.00	5.60 [g]	1.70		85.00 [e]	1.00		0.96	56.67	1.13	Human	Cryopreserved hepatocytes, suspension	Human Serum	24-well plate 2 X 10^6 cells/ml	300rpm	1, 10, 50µM	2-300 minutes	(Blanchard et al., 2005)
	0%	1.00			232 [e]		232						Rat	Cryopreserved hepatocytes, suspension	BSA	Centrifugal filtration 0.5 X 10^6 cells/ml	NS	1uM	20 seconds - 30 minutes	(Li et al., 2020)
	4%	0.06			13.17 [e]		231				1.00	0.06	Rat	Cryopreserved hepatocytes, suspension	BSA	Centrifugal filtration 0.5 X 10^6 cells/ml	NS	1uM	20 seconds - 30 minutes	(Li et al., 2020)
(R-)Bufuralol	0%	1.00	59.00	12.22 [i]	4.83 [f]		4.83 [e]						Human	Cryopreserved hepatocytes, suspension	Human Plasma	Unspecified 0.5 X 10^6 cells/ml	NS	2.25-288µM	25 mins	(Mao et al., 2012)
	Pure Plasma	0.19	48.00	54.83 [i]	0.88 [f]		4.61 [e]	0.81		4.49	0.95	0.18	Human	Cryopreserved hepatocytes, suspension	Human Plasma	Unspecified 0.5 X 10^6 cells/ml	NS	2.25-288µM	25 mins	(Mao et al., 2012)
Carbamazepine	0%	1.00 [j]			48.20		48.20 [e]						Human	Cryopreserved hepatocytes, suspension	Human Serum	Eppendorfs 2 X 10^6 cells/ml	96 oscilations/ min	"less than the reported Km"	0, 1, 2, 6 hours	(Bachmann et al., 2003)
	Pure Serum	0.24 [k]			292		1,221 [e]				25.33	6.05	Human	Cryopreserved hepatocytes, suspension	Human Serum	Eppendorfs 2 X 10^6 cells/ml	96 oscilations/ min	"less than the reported Km"	0, 1, 2, 6 hours	(Bachmann et al., 2003)
Cerivastatin	0%	1.00			77.50		77.50						Human	Cryopreserved hepatocytes, suspension	HSA	Centrifugal filtration 1 X 10^6 cells/ml	NS	3µM	0.25 and 1.25 minutes	(Kim et al., 2019)
	5%	0.01			2.31		240				3.10	0.03	Human	Cryopreserved hepatocytes, suspension	HSA	Centrifugal filtration 1 X 10^6 cells/ml	NS	3µM	0.25 and 1.25 minutes	(Kim et al., 2019)
	0% [d]	1.00 [d, j]	1,510 [d]	9.20 [d, l]	164 [d, f]	9.20 [d, l]	164 [d, e]						Rat	Fresh hepatocytes, suspension	Rat Serum	Eppendorfs 2 X 10^6 cells/ml	NS	0.3µM	0.5 and 2 minutes	(Shitara et al., 2004)

	In vitro values							Fold-Change compared to no PP conditions					Assay conditions							
Compound	**Protein conc.**	**In vitro fu**	**V_{max} [a]**	**K_m [b]**	**CL_{int} [c]**	**$K_{m,u}$ [b]**	**$CL_{int,u}$ [c]**	**V_{max}**	**$K_{m,u}$**	**K_m**	**$CL_{int,u}$**	**CL_{int}**	**Species**	**Assay format**	**PP type**	**Experimental Conditions**	**Shaking?**	**Drug concentration**	**Duration**	**REF**
	90% Serum [d]	0.04 [d]	481 [d]	16.10 [d, l]	29.88 [d, f]	0.70 [d, l]	692 [d, e]	0.32 [d]	0.08 [d]	1.75 [d]	4.21 [d]	0.18 [d]	Rat	Fresh hepatocytes, suspension	Rat Serum	Eppendorfs 2 X 10^6 cells/ml	NS	0.3µM	0.5 and 2 minutes	(Shitara et al., 2004)
	0%	1.00			527 [e]		527						Rat	Cryopreserved hepatocytes, suspension	BSA	Centrifugal filtration 0.5 X 10^6 cells/ml	NS	1uM	20 seconds - 30 minutes	(Li et al., 2020)
	4%	0.04			31.92 [e]		798				1.51	0.06	Rat	Cryopreserved hepatocytes, suspension	BSA	Centrifugal filtration 0.5 X 10^6 cells/ml	NS	1uM	20 seconds - 30 minutes	(Li et al., 2020)
Diclofenac	0%	1.00	410	34.58 [i]	11.86 [f]		11.86 [e]						Human	Cryopreserved hepatocytes, suspension	Human Plasma	Unspecified 0.5 X 10^6 cells/ml	NS	1.5-192µM	45 mins	(Mao et al., 2012)
	Pure Plasma	0.003	490	1,408 [i]	0.35 [f]		116 [e]	1.20		40.72	9.78	0.03	Human	Cryopreserved hepatocytes, suspension	Human Plasma	Unspecified 0.5 X 10^6 cells/ml	NS	75-9600µM	45 mins	(Mao et al., 2012)
Fluvastatin	0%	1.00			62.10		62.10						Human	Cryopreserved hepatocytes, suspension	HSA	Centrifugal filtration 1 X 10^6 cells/ml	NS	3µM	0.25 and 1.25 minutes	(Kim et al., 2019)
	5%	0.004			1.72		424				6.83	0.03	Human	Cryopreserved hepatocytes, suspension	HSA	Centrifugal filtration 1 X 10^6 cells/ml	NS	3µM	0.25 and 1.25 minutes	(Kim et al., 2019)
	0%	1.00			277 [e]		277						Rat	Cryopreserved hepatocytes, suspension	BSA	Centrifugal filtration 0.5 X 10^6 cells/ml	NS	1uM	20 seconds - 30 minutes	(Li et al., 2020)
	4%	0.04			33.41 [e]		903				3.26	0.12	Rat	Cryopreserved hepatocytes, suspension	BSA	Centrifugal filtration 0.5 X 10^6 cells/ml	NS	1uM	20 seconds - 30 minutes	(Li et al., 2020)
Glibenclamide	0%	1.00			32.30		32.30						Human	Cryopreserved hepatocytes, suspension	HSA	Centrifugal filtration 1 X 10^6 cells/ml	NS	3µM	0.25 and 1.25 minutes	(Kim et al., 2019)
	5%	0.0009			0.16		173				5.36	0.00	Human	Cryopreserved hepatocytes, suspension	HSA	Centrifugal filtration 1 X 10^6 cells/ml	NS	3µM	0.25 and 1.25 minutes	(Kim et al., 2019)
	0%	1.00			461 [e]		461						Rat	Cryopreserved hepatocytes, suspension	BSA	Centrifugal filtration 0.5 X 10^6 cells/ml	NS	1uM	20 seconds - 30 minutes	(Li et al., 2020)
	4%	0.01			22.22 [e]		1,587				3.44	0.05	Rat	Cryopreserved hepatocytes, suspension	BSA	Centrifugal filtration 0.5 X 10^6 cells/ml	NS	1uM	20 seconds - 30 minutes	(Li et al., 2020)
Mibefradil	0%	0.53	71.33 [f]	3.20 [g]	22.29	6.04 [g]	11.81						Rat	Fresh hepatocytes, monolayer	Rat Serum	24-well plate 1 X 10^6 cells/ml	NS	0.5, 2, 20µM	2-300 minutes	(Blanchard et al., 2004)

	In vitro values							Fold-Change compared to no PP conditions					Assay conditions							
Compound	**Protein conc.**	**In vitro fu**	**V_{max} [a]**	**K_m [b]**	**CL_{int} [c]**	**$K_{m,u}$ [b]**	**$CL_{int,u}$ [c]**	**V_{max}**	**$K_{m,u}$**	**K_m**	**$CL_{int,u}$**	**CL_{int}**	**Species**	**Assay format**	**PP type**	**Experimental Conditions**	**Shaking?**	**Drug concentration**	**Duration**	**REF**
	Pure Serum	0.02	70.26 [f]	11.10 [g]	6.33	0.42 [g]	168	0.99	0.07	3.47	14.20	0.28	Rat	Fresh hepatocytes, monolayer	Rat Serum	24-well plate 1 X 10^6 cells/ml	NS	0.5, 2, 20μM	2-300 minutes	(Blanchard et al., 2004)
	0%	0.53	369 [f]	9.20 [g]	40.13	17.36 [g]	21.27						Rat	Fresh hepatocytes, suspension	Rat Serum	24-well plate 1 X 10^6 cells/ml	300rpm	0.5, 2, 20μM	2-300 minutes	(Blanchard et al., 2004)
	Pure Serum	0.02	75.82 [f]	3.25 [g]	23.33	0.12 [g]	618	0.21	0.01	0.35	29.07	0.58	Rat	Fresh hepatocytes, suspension	Rat Serum	24-well plate 1 X 10^6 cells/ml	300rpm	0.5, 2, 20μM	2-300 minutes	(Blanchard et al., 2004)
	0%	1.00			12.72		12.72						Human	Cryopreserved hepatocytes, suspension	Human Serum	24-well plate, 1.5 X 10^6 cells/ml	300rpm	1μM	Up to 300 minutes	(Blanchard et al., 2006)
	Pure Serum	0.01			1.76		147				11.53	0.14	Human	Cryopreserved hepatocytes, suspension	Human Serum	24-well plate 1.5 X 10^6 cells/ml	300rpm	1μM	Up to 300 minutes	(Blanchard et al., 2006)
Midazolam	0%	0.98	530 [f]	8.16 [g]	64.92	8.33 [g]	63.62						Rat	Fresh hepatocytes, monolayer	Rat Serum	24-well plate 1 X 10^6 cells/ml	NS	1, 10, 50μM	2-300 minutes	(Blanchard et al., 2004)
	Pure Serum	0.04	107 [f]	11.30 [g]	9.48	0.46 [g]	232	0.20	0.06	1.38	3.65	0.15	Rat	Fresh hepatocytes, monolayer	Rat Serum	24-well plate 1 X 10^6 cells/ml	NS	1, 10, 50μM	2-300 minutes	(Blanchard et al., 2004)
	0%	0.98	865 [f]	7.80 [g]	111	7.96 [g]	109						Rat	Fresh hepatocytes, suspension	Rat Serum	24-well plate 1 X 10^6 cells/ml	300rpm	1, 10, 50μM	2-300 minutes	(Blanchard et al., 2004)
	Pure Serum	0.04	534 [f]	11.34 [g]	47.07	0.46 [g]	1,176	0.62	0.06	1.45	10.82	0.42	Rat	Fresh hepatocytes, suspension	Rat Serum	24-well plate 1 X 10^6 cells/ml	300rpm	1, 10, 50μM	2-300 minutes	(Blanchard et al., 2004)
	0%	0.82			19.56		23.95						Human	Cryopreserved hepatocytes, suspension	Human Serum	24-well plate 1.5 X 10^6 cells/ml	300rpm	5μM	Up to 300 minutes	(Blanchard et al., 2006)
	Pure Serum	0.02			2.06		98.27				4.10	0.11	Human	Cryopreserved hepatocytes, suspension	Human Serum	24-well plate 1.5 X 10^6 cells/ml	300rpm	5μM	Up to 300 minutes	(Blanchard et al., 2006)
	0%	1.00	53.33	4.20 [g]	18.87		18.87 [e]						Human	Fresh hepatocytes, monolayer	Human Serum	24-well plate 0.6 X 10^6 cells/ml	NS	1, 10, 50μM	2-300 minutes	(Blanchard et al., 2005)
	Pure Serum	0.04	13.33	6.63 [g]	2.77		69.17 [e]	0.25		1.58	3.67	0.15	Human	Fresh hepatocytes, monolayer	Human Serum	24-well plate 0.6 X 10^6 cells/ml	NS	1, 10, 50μM	2-300 minutes	(Blanchard et al., 2005)
	0%	1.00	60.00	7.50 [g]	11.27		11.27 [e]						Human	Fresh hepatocytes, suspension	Human Serum	24-well plate 2 X 10^6 cells/ml	300rpm	1, 10, 50μM	2-300 minutes	(Blanchard et al., 2005)
	Pure Serum	0.04	17.33	9.63 [g]	2.50		62.50 [e]	0.29		1.28	5.55	0.22	Human	Fresh hepatocytes, suspension	Human Serum	24-well plate 2 X 10^6 cells/ml	300rpm	1, 10, 50μM	2-300 minutes	(Blanchard et al., 2005)

	In vitro values							Fold-Change compared to no PP conditions					Assay conditions							
Compound	**Protein conc.**	**In vitro fu**	**V_{max} [a]**	**K_m [b]**	**CL_{int} [c]**	**$K_{m,u}$ [b]**	**$CL_{int,u}$ [c]**	**V_{max}**	**$K_{m,u}$**	**K_m**	**$CL_{int,u}$**	**CL_{int}**	**Species**	**Assay format**	**PP type**	**Experimental Conditions**	**Shaking?**	**Drug concentration**	**Duration**	**REF**
	0%	1.00	25.00	3.25 [g]	12.65		12.65 [e]						Human	Cryopreserved hepatocytes, suspension	Human Serum	24-well plate 2 X 10^6 cells/ml	300rpm	1, 10, 50µM	2-300 minutes	(Blanchard et al., 2005)
	Pure Serum	0.04	10.00	5.25 [g]	2.25		56.25 [e]	0.40		1.65	4.45	0.18	Human	Cryopreserved hepatocytes, suspension	Human Serum	24-well plate 2 X 10^6 cells/ml	300rpm	1, 10, 50µM	2-300 minutes	(Blanchard et al., 2005)
	0%	1.00	21.00	8.11 [i]	2.59 [f]		2.59 [e]						Human	Cryopreserved hepatocytes, suspension	Human Plasma	Unspecified 0.5 X 10^6 cells/ml	NS	1.25-160µM	35 mins	(Mao et al., 2012)
	Pure Plasma	0.03	36.00	45.83 [i]	0.79 [f]		24.55 [e]	1.71		5.65	9.48	0.30	Human	Cryopreserved hepatocytes, suspension	Human Plasma	Unspecified 0.5 X 10^6 cells/ml	NS	15-1920µM	35 mins	(Mao et al., 2012)
Naloxone	0%	1.00	1,688 [f]	11.00 [g]	153	11.00 [g]	153						Rat	Fresh hepatocytes, monolayer	Rat Serum	24-well plate 1 X 10^6 cells/ml	NS	1, 10, 50µM	2-300 minutes	(Blanchard et al., 2004)
	Pure Serum	0.55	1,281 [f]	13.00 [g]	98.52	7.15 [g]	179	0.76	0.65	1.18	1.17	0.64	Rat	Fresh hepatocytes, monolayer	Rat Serum	24-well plate 1 X 10^6 cells/ml	NS	1, 10, 50µM	2-300 minutes	(Blanchard et al., 2004)
	0%	1.00	5,360 [f]	15.00 [g]	357	15.00 [g]	357						Rat	Fresh hepatocytes, suspension	Rat Serum	24-well plate 1 X 10^6 cells/ml	300rpm	1, 10, 50µM	2-300 minutes	(Blanchard et al., 2004)
	Pure Serum	0.55	5,339 [f]	14.00 [g]	381	7.70 [g]	693	1.00	0.51	0.93	1.94	1.07	Rat	Fresh hepatocytes, suspension	Rat Serum	24-well plate 1 X 10^6 cells/ml	300rpm	1, 10, 50µM	2-300 minutes	(Blanchard et al., 2004)
	0%	1.00			27.02		27.02						Human	Cryopreserved hepatocytes, suspension	Human Serum	24-well plate 1.5 X 10^6 cells/ml	300rpm	1µM	Up to 300 minutes	(Blanchard et al., 2006)
	Pure Serum	0.60			8.84		14.83				0.55	0.33	Human	Cryopreserved hepatocytes, suspension	Human Serum	24-well plate 1.5 X 10^6 cells/ml	300rpm	1µM	Up to 300 minutes	(Blanchard et al., 2006)
	0%	1.00	290	5.30 [g]	71.00		71.00 [e]						Human	Fresh hepatocytes, monolayer	Human Serum	24-well plate 0.6 X 10^6 cells/ml	NS	1, 10, 50µM	2-300 minutes	(Blanchard et al., 2005)
	Pure Serum	0.60	177	7.97 [g]	23.00		38.33 [e]	0.61		1.50	0.54	0.32	Human	Fresh hepatocytes, monolayer	Human Serum	24-well plate 0.6 X 10^6 cells/ml	NS	1, 10, 50µM	2-300 minutes	(Blanchard et al., 2005)
	0%	1.00	447	4.80 [g]	118		118 [e]						Human	Fresh hepatocytes, suspension	Human Serum	24-well plate 2 X 10^6 cells/ml	300rpm	1, 10, 50µM	2-300 minutes	(Blanchard et al., 2005)
	Pure Serum	0.60	263	6.47 [g]	46.97		78.28 [e]	0.59		1.35	0.66	0.40	Human	Fresh hepatocytes, suspension	Human Serum	24-well plate 2 X 10^6 cells/ml	300rpm	1, 10, 50µM	2-300 minutes	(Blanchard et al., 2005)
	0%	1.00	220	2.75 [g]	79.50		79.50 [e]						Human	Cryopreserved hepatocytes, suspension	Human Serum	24-well plate 2 X 10^6 cells/ml	300rpm	1, 10, 50µM	2-300 minutes	(Blanchard et al., 2005)

	In vitro values							Fold-Change compared to no PP conditions					Assay conditions							
Compound	**Protein conc.**	**In vitro fu**	**V_{max} [a]**	**K_m [b]**	**CL_{int} [c]**	**$K_{m,u}$ [b]**	**$CL_{int,u}$ [c]**	**V_{max}**	**$K_{m,u}$**	**K_m**	**$CL_{int,u}$**	**CL_{int}**	**Species**	**Assay format**	**PP type**	**Experimental Conditions**	**Shaking?**	**Drug concentration**	**Duration**	**REF**
	Pure Serum	0.60	160	4.25 [g]	60.50		101 [e]	0.73		1.55	1.27	0.76	Human	Cryopreserved hepatocytes, suspension	Human Serum	24-well plate 2 X 10^6 cells/ml	300rpm	1, 10, 50µM	2-300 minutes	(Blanchard et al., 2005)
Nateglinide	0%	1.00			12.50		12.50						Human	Cryopreserved hepatocytes, suspension	HSA	Centrifugal filtration 1 X 10^6 cells/ml	NS	3µM	0.25 and 1.25 minutes	(Kim et al., 2019)
	5%	0.01			0.28		43.90				3.51	0.02	Human	Cryopreserved hepatocytes, suspension	HSA	Centrifugal filtration 1 X 10^6 cells/ml	NS	3µM	0.25 and 1.25 minutes	(Kim et al., 2019)
	0%	1.00			88.80 [e]		88.80						Rat	Cryopreserved hepatocytes, suspension	BSA	Centrifugal filtration 0.5 X 10^6 cells/ml	NS	1uM	20 seconds - 30 minutes	(Li et al., 2020)
	4%	0.06			9.07 [e]		144				1.62	0.10	Rat	Cryopreserved hepatocytes, suspension	BSA	Centrifugal filtration 0.5 X 10^6 cells/ml	NS	1uM	20 seconds - 30 minutes	(Li et al., 2020)
Oxazepam	0%	0.82	149 [f]	12.50 [g]	11.94	15.24 [g]	9.80						Rat	Fresh hepatocytes, monolayer	Rat Serum	24-well plate 1 X 10^6 cells/ml	NS	1, 10, 50µM	2-300 minutes	(Blanchard et al., 2004)
	Pure Serum	0.10	352 [f]	37.10 [g]	9.48	4.52 [g]	77.73	2.36	0.30	2.97	7.93	0.79	Rat	Fresh hepatocytes, monolayer	Rat Serum	24-well plate 1 X 10^6 cells/ml	NS	1, 10, 50µM	2-300 minutes	(Blanchard et al., 2004)
	0%	0.82	337 [f]	8.00 [g]	42.18	9.75 [g]	34.58						Rat	Fresh hepatocytes, suspension	Rat Serum	24-well plate 1 X 10^6 cells/ml	300rpm	1, 10, 50µM	2-300 minutes	(Blanchard et al., 2004)
	Pure Serum	0.10	499 [f]	83.25 [g]	5.99	10.15 [g]	49.11	1.48	1.04	10.41	1.42	0.14	Rat	Fresh hepatocytes, suspension	Rat Serum	24-well plate 1 X 10^6 cells/ml	300rpm	1, 10, 50µM	2-300 minutes	(Blanchard et al., 2004)
	0%	0.80			2.33		2.92						Human	Cryopreserved hepatocytes, suspension	Human Serum	24-well plate 1.5 X 10^6 cells/ml	300rpm	1µM	Up to 300 minutes	(Blanchard et al., 2006)
	Pure Serum	0.05			1.10		21.98				7.54	0.47	Human	Cryopreserved hepatocytes, suspension	Human Serum	24-well plate 1.5 X 10^6 cells/ml	300rpm	1µM	Up to 300 minutes	(Blanchard et al., 2006)
Phenytoin	0%	1.00	96.40	6.64 [f]	14.52 [e]	6.64 [m]	14.52 [f]						Human	Cryopreserved Liver Slice	BSA	24-well plate 2 Liver slices/well	Yes, placed on a rocker	0, 1-150µM	6 hours	(Ludden et al., 1997)
	4%	0.13	120	17.46 [f]	6.87 [e]	2.20 [m]	54.55 [f]	1.24	0.33	2.63	3.76	0.47	Human	Cryopreserved Liver Slice	BSA	24-well plate 2 Liver slices/well	Yes, placed on a rocker	0, 1-150µM	6 hours	(Ludden et al., 1997)
	0%	1.00 [j]			177		177 [e]						Human	Cryopreserved hepatocytes, suspension	Human Serum	Eppendorfs 2 X 10^6 cells/ml	96 oscilations/ min	"less than the reported Km"	0, 1, 2, 6 hours	(Bachmann et al., 2003)

	In vitro values							Fold-Change compared to no PP conditions					Assay conditions							
Compound	**Protein conc.**	**In vitro fu**	**V_{max}** [a]	**K_m** [b]	**CL_{int}** [c]	**$K_{m,u}$** [b]	**$CL_{int,u}$** [c]	**V_{max}**	**$K_{m,u}$**	**K_m**	**$CL_{int,u}$**	**CL_{int}**	**Species**	**Assay format**	**PP type**	**Experimental Conditions**	**Shaking?**	**Drug concentration**	**Duration**	**REF**
	Pure Serum	0.08 [k]			27.45		331 [e]				1.87	0.16	Human	Cryopreserved hepatocytes, suspension	Human Serum	Eppendorfs 2 X 10^6 cells/ml	96 oscilations/ min	"less than the reported Km"	0, 1, 2, 6 hours	(Bachmann et al., 2003)
Pitavastatin	0% [d]	1.00 [d]			26.90 [d, e]		26.90 [d]						Human	Cryopreserved hepatocytes, suspension	HSA	Centrifugal filtration 1 X 10^6 cells/ml	NS	5µM	0.25 and 1.25 minutes	(Miyauchi et al., 2018)
	0.13% [d]	0.24 [d]			12.47 [d, e]		52.60 [d]				1.96 [d]	0.46 [d]	Human	Cryopreserved hepatocytes, suspension	HSA	Centrifugal filtration 1 X 10^6 cells/ml	NS	5µM	0.25 and 1.25 minutes	(Miyauchi et al., 2018)
	0.25% [d]	0.09 [d]			7.97 [d, e]		85.80 [d]				3.19 [d]	0.30 [d]	Human	Cryopreserved hepatocytes, suspension	HSA	Centrifugal filtration 1 X 10^6 cells/ml	NS	5µM	0.25 and 1.25 minutes	(Miyauchi et al., 2018)
	0.50% [d]	0.04 [d]			4.50 [d, e]		109 [d]				4.05 [d]	0.17 [d]	Human	Cryopreserved hepatocytes, suspension	HSA	Centrifugal filtration 1 X 10^6 cells/ml	NS	5µM	0.25 and 1.25 minutes	(Miyauchi et al., 2018)
	1% [d]	0.02 [d]			3.09 [d, e]		170 [d]				6.32 [d]	0.12 [d]	Human	Cryopreserved hepatocytes, suspension	HSA	Centrifugal filtration 1 X 10^6 cells/ml	NS	5µM	0.25 and 1.25 minutes	(Miyauchi et al., 2018)
	0%	1.00			36.20		36.20						Human	Cryopreserved hepatocytes, suspension	HSA	Centrifugal filtration 1 X 10^6 cells/ml	NS	3µM	0.25 and 1.25 minutes	(Kim et al., 2019)
	5%	0.01			0.49		88.30				2.44	0.01	Human	Cryopreserved hepatocytes, suspension	HSA	Centrifugal filtration 1 X 10^6 cells/ml	NS	3µM	0.25 and 1.25 minutes	(Kim et al., 2019)
	0%	1.00	600	8.71 [f]	68.90 [e]	8.71 [h]	68.90						Rat	Fresh hepatocytes, suspension	Human Plasma	24-well plate 0.5 X 10^6 cells/ml	Yes	0.05-100µM	2 minutes	(Bowman et al., 2019)
	Pure Plasma	0.01	39.90	8.13 [f]	4.91 [e]	0.08 [h]	491	0.07	0.01	0.93	7.13	0.07	Rat	Fresh hepatocytes, suspension	Human Plasma	24-well plate 0.5 X 10^6 cells/ml	Yes	0.05-100µM	2 minutes	(Bowman et al., 2019)
	0%	1.00			249 [e]		249						Rat	Cryopreserved hepatocytes, suspension	BSA	Centrifugal filtration 0.5 X 10^6 cells/ml	NS	1uM	20 seconds - 30 minutes	(Li et al., 2020)
	4%	0.06			26.79 [e]		470				1.89	0.11	Rat	Cryopreserved hepatocytes, suspension	BSA	Centrifugal filtration 0.5 X 10^6 cells/ml	NS	1uM	20 seconds - 30 minutes	(Li et al., 2020)
Pravastatin	0%	1.00			3.55		3.55						Human	Cryopreserved hepatocytes, suspension	HSA	Centrifugal filtration 1 X 10^6 cells/ml	NS	3µM	0.25 and 1.25 minutes	(Kim et al., 2019)
	5%	0.50			NA		NA						Human	Cryopreserved hepatocytes, suspension	HSA	Centrifugal filtration 1 X 10^6 cells/ml	NS	3µM	0.25 and 1.25 minutes	(Kim et al., 2019)
	0%	1.00	208	16.51 [f]	12.60 [e]	16.50 [h]	12.60						Rat	Fresh hepatocytes, suspension	Human Plasma	24-well plate 0.5 X 10^6 cells/ml	Yes	0.1-300µM	2 minutes	(Bowman et al., 2019)

		In vitro values						Fold-Change compared to no PP conditions						Assay conditions						
Compound	**Protein conc.**	**In vitro fu**	**V_{max} [a]**	**K_m [b]**	**CL_{int} [c]**	**$K_{m,u}$ [b]**	**$CL_{int,u}$ [c]**	**V_{max}**	**$K_{m,u}$**	**K_m**	**$CL_{int,u}$**	**CL_{int}**	**Species**	**Assay format**	**PP type**	**Experimental Conditions**	**Shaking?**	**Drug concentration**	**Duration**	**REF**
	Pure Plasma	0.50	97.90	19.39 [f]	5.05 [e]	9.66 [h]	10.10	0.47	0.59	1.17	0.80	0.40	Rat	Fresh hepatocytes, suspension	Human Plasma	24-well plate 0.5 X 10^6 cells/ml	Yes	0.1-300µM	2 minutes	(Bowman et al., 2019)
	0%	1.00			8.87 [e]		8.87						Rat	Cryopreserved hepatocytes, suspension	BSA	Centrifugal filtration 0.5 X 10^6 cells/ml	NS	1uM	20 seconds - 30 minutes	(Li et al., 2020)
	4%	0.69			7.11 [e]		10.30				1.16	0.80	Rat	Cryopreserved hepatocytes, suspension	BSA	Centrifugal filtration 0.5 X 10^6 cells/ml	NS	1uM	20 seconds - 30 minutes	(Li et al., 2020)
Procainamide	0%	1.00 [j]			78.00		78.00 [e]						Human	Cryopreserved hepatocytes, suspension	Human Serum	Eppendorfs 2 X 10^6 cells/ml	96 oscilations/ min	"less than the reported Km"	0, 1, 2, 6 hours	(Bachmann et al., 2003)
	Pure Serum	0.83 [k]			78.00		94.55 [e]				1.21	1.00	Human	Cryopreserved hepatocytes, suspension	Human Serum	Eppendorfs 2 X 10^6 cells/ml	96 oscilations/ min	"less than the reported Km"	0, 1, 2, 6 hours	(Bachmann et al., 2003)
Quinidine	0%	1.00 [j]			330		330 [e]						Human	Cryopreserved hepatocytes, suspension	Human Serum	Eppendorfs 2 X 10^6 cells/ml	96 oscilations/ min	"less than the reported Km"	0, 1, 2, 6 hours	(Bachmann et al., 2003)
	Pure Serum	0.15 [k]			71.85		492 [e]				1.49	0.22	Human	Cryopreserved hepatocytes, suspension	Human Serum	Eppendorfs 2 X 10^6 cells/ml	96 oscilations/ min	"less than the reported Km"	0, 1, 2, 6 hours	(Bachmann et al., 2003)
Repaglinide	0%	1.00			39.20		39.20						Human	Cryopreserved hepatocytes, suspension	HSA	Centrifugal filtration 1 X 10^6 cells/ml	NS	3µM	0.25 and 1.25 minutes	(Kim et al., 2019)
	5%	0.01			2.48		207				5.28	0.06	Human	Cryopreserved hepatocytes, suspension	HSA	Centrifugal filtration 1 X 10^6 cells/ml	NS	3µM	0.25 and 1.25 minutes	(Kim et al., 2019)
Rosuvastatin	0%	1.00			4.01		4.01						Human	Cryopreserved hepatocytes, suspension	HSA	Centrifugal filtration 1 X 10^6 cells/ml	NS	3µM	0.25 and 1.25 minutes	(Kim et al., 2019)
	5%	0.10			0.98		9.94				2.48	0.25	Human	Cryopreserved hepatocytes, suspension	HSA	Centrifugal filtration 1 X 10^6 cells/ml	NS	3µM	0.25 and 1.25 minutes	(Kim et al., 2019)
	0%	1.00	323	4.00 [f]	80.80 [e]	4.00 [h]	80.80						Rat	Fresh hepatocytes, suspension	Human Plasma	24-well plate 0.5 X 10^6 cells/ml	Yes	0.05-100µM	2 minutes	(Bowman et al., 2019)
	Pure Plasma	0.12	339	8.28 [f]	40.92 [e]	1.00 [h]	341	1.05	0.25	2.07	4.22	0.51	Rat	Fresh hepatocytes, suspension	Human Plasma	24-well plate 0.5 X 10^6 cells/ml	Yes	0.05-100µM	2 minutes	(Bowman et al., 2019)
	0%	1.00			120 [e]		120						Rat	Cryopreserved hepatocytes, suspension	BSA	Centrifugal filtration 0.5 X 10^6 cells/ml	NS	1uM	20 seconds - 30 minutes	(Li et al., 2020)

		In vitro values						Fold-Change compared to no PP conditions						Assay conditions						
Compound	**Protein conc.**	**In vitro fu**	**V_{max}** [a]	**K_m** [b]	**CL_{int}** [c]	**$K_{m,u}$** [b]	**$CL_{int,u}$** [c]	**V_{max}**	**$K_{m,u}$**	**K_m**	**$CL_{int,u}$**	**CL_{int}**	**Species**	**Assay format**	**PP type**	**Experimental Conditions**	**Shaking?**	**Drug concentration**	**Duration**	**REF**
	4%	0.21			46.41 [e]		221				1.84	0.39	Rat	Cryopreserved hepatocytes, suspension	BSA	Centrifugal filtration 0.5 X 10^6 cells/ml	NS	1uM	20 seconds - 30 minutes	(Li et al., 2020)
RO-X	0%	0.89	151 [f]	23.60 [g]	6.41	26.51 [g]	5.71						Rat	Fresh hepatocytes, monolayer	Rat Serum	24-well plate 1 X 10^6 cells/ml	NS	1, 10, 50µM	2-300 minutes	(Blanchard et al., 2004)
	Pure Serum	0.02	16.79 [f]	16.30 [g]	1.03	0.36 [g]	45.83	0.11	0.01	0.69	8.03	0.16	Rat	Fresh hepatocytes, monolayer	Rat Serum	24-well plate 1 X 10^6 cells/ml	NS	1, 10, 50µM	2-300 minutes	(Blanchard et al., 2004)
	0%	0.89	138 [f]	15.10 [g]	9.17	16.90 [g]	8.16						Rat	Fresh hepatocytes, suspension	Rat Serum	24-well plate 1 X 10^6 cells/ml	300rpm	1, 10, 50µM	2-300 minutes	(Blanchard et al., 2004)
	Pure Serum	0.02	16.43 [f]	7.90 [g]	2.08	0.17 [g]	92.56	0.12	0.01	0.52	11.34	0.23	Rat	Fresh hepatocytes, suspension	Rat Serum	24-well plate 1 X 10^6 cells/ml	300rpm	1, 10, 50µM	2-300 minutes	(Blanchard et al., 2004)
Theophylline	0%	1.00 [j]			28.65		28.65 [e]						Human	Cryopreserved hepatocytes, suspension	Human Serum	Eppendorfs 2 X 10^6 cells/ml	96 oscilations/ min	"less than the reported Km"	0, 1, 2, 6 hours	(Bachmann et al., 2003)
	Pure Serum	0.63 [k]			21.90		35.04 [e]				1.22	0.76	Human	Cryopreserved hepatocytes, suspension	Human Serum	Eppendorfs 2 X 10^6 cells/ml	96 oscilations/ min	"less than the reported Km"	0, 1, 2, 6 hours	(Bachmann et al., 2003)
Valsartan	0%	1.00			1.87		1.87						Human	Cryopreserved hepatocytes, suspension	HSA	Centrifugal filtration 1 X 10^6 cells/ml	NS	3µM	0.25 and 1.25 minutes	(Kim et al., 2019)
	5%	0.0004			0.05		119				63.64	0.03	Human	Cryopreserved hepatocytes, suspension	HSA	Centrifugal filtration 1 X 10^6 cells/ml	NS	3µM	0.25 and 1.25 minutes	(Kim et al., 2019)
	0%	1.00			34.00 [e]		34.00						Rat	Cryopreserved hepatocytes, suspension	BSA	Centrifugal filtration 0.5 X 10^6 cells/ml	NS	1uM	20 seconds - 30 minutes	(Li et al., 2020)
	4%	0.006			3.36 [e]		560				16.47	0.10	Rat	Cryopreserved hepatocytes, suspension	BSA	Centrifugal filtration 0.5 X 10^6 cells/ml	NS	1uM	20 seconds - 30 minutes	(Li et al., 2020)

Abbreviations: ANS: 1-anilino-8-naphthalene sulfonate, BSA: Bovine Serum Albumin, HSA: Human Serum Albumin, NS: Not stated, PP: Plasma Protein, RO-X: in house compound.

a) Units represent pmol/min/10^6 cells

b) Units represent µM

c) Units represent µl/min/10^6 cells

d) Plasma protein in these experiments was used at concentrations lower than physiologically relevant (e.g., diluted plasma, diluted serum, or isolated albumin concentrations at less than 4%)

e) Calculated based on Eq 1

f) Calculated based on Eq 2 or Eq 3

g) K_m values were derived from simultaneously fitting depletion profiles of the parent compound obtained from total incubate (medium and cells) using 3 different drug concentrations (Blanchard et al., 2004; Blanchard et al., 2005). $K_{m,u}$ was calculated in Blanchard et al. (2004) by dividing K_m by the unbound fraction.

h) $K_{m,u}$ values were obtained by fitting uptake rates of parent compound from intracellular concentration obtained at multiple concentrations against the nominal concentration of drug applied multiplied by the fu as taken from the FDA product label (Bowman et al., 2019).

Compound	Protein conc.	In vitro fu	In vitro values					Fold-Change compared to no PP conditions					Species	Assay conditions						
			V_{max} [a]	K_m [b]	CL_{int} [c]	$K_{m,u}$ [b]	$CL_{int,u}$ [c]	V_{max}	$K_{m,u}$	K_m	$CL_{int,u}$	CL_{int}		Assay format	PP type	Experimental Conditions	Shaking?	Drug concentration	Duration	REF

i) K_m values were obtained by fitting the untransformed metabolite formation rates obtained at multiple concentrations based on total incubate (medium and cells) against nominally applied drug concentrations (no correction for binding) (Mao et al., 2012).

j) In vitro fu was not reported for no plasma protein conditions, and assumed to be 1

k) In vitro fu assumed based on independently sourced values using the exact same type (and concentration) of plasma protein. Carbamazepine: (Patsalos et al., 2017). Phenytoin: (Kodama et al., 1998). Procainamide: Drugbank (DB01035), (Wishart et al., 2018). Quinidine: (Shibata et al., 2002). Theophylline:(Brørs et al., 1983).

l) K_m values were obtained by fitting the initial uptake rate of parent compound from intracellular concentrations at one concentration against the nominally applied concentration (no correction for binding). $K_{m,u}$ values were calculated in Shitara et al. (2004) by dividing K_m by the unbound fraction.

m) $K_{m,u}$ values obtained by fitting metabolite formation rates obtained at multiple concentration from homogenised liver slices against the unbound concentration of drug applied (Ludden et al., 1997).

Table S1 B: Drug and physico-chemical properties, and where available, passive and active clearances for rat and human hepatocytes.

DRUG	Drug bank accension Number [a]	Molecular Weight [a]	Water Solubility (mg/ml) [a]	Hydrogen Acceptor Number [a]	Hydrogen Donor Number [a]	Polar Surface Area (Å²) [a]	LogP [b]	$LogD_{7.4}$ [b]	Strongest pKa, acid [c]	Strongest pKa, base [c]	Ionisation [d]	ECCS classification [b]	Permeability 10^{-6}cm/s [1]	Clearance Mechanism [1]	Human			Rat		
															P_{diff} (µl/min/10^6 cells)	CL_{uptake} (µl/min/10^6 cells)	CL_{active} (µl/min/10^6 cells)	P_{diff} (µl/min/10^6 cells)	CL_{uptake} (µl/min/10^6 cells)	CL_{active} (µl/min/10^6 cells)
ANS	DB04474	299.3	0.015	4	2	66.4	2.45	-2.18	0	0.9	A	3a								
Antipyrine	DB01435	188.2	47.400	2	0	23.55	0.56	0.26		1.8	N	2	31.7	Metabolism						
Asunaprevir	DB11586	748.3	0.003	9	3	182.33	3.93	3.72	7.6	1.3	A	3b								
Atorvastatin	DB01076	558.6	0.001	5	4	111.79	4.13	1.3	4.3	0	A	1b	5.5	Hepatic Uptake	6.88 [2, 3, 4]		53.86 [2, 3, 4, 5]	15.23 [6, 7]	856.68 [6, 7]	622.07 [6, 7, 8]
Bosentan	DB00559	551.6	0.009	9	2	145.65	1.15	1.25	4.9	2.6	A	1b	7.5	Hepatic Uptake	17.11 [4, 9, 10, 11]	81.00 [11]	27.10 [4, 5, 9, 10, 11]	12.13 [6, 12]	36.20 [6]	40.40 [6, 7, 8]
(R-)Bufuralol	DB06726	261.4	0.036	2	2	45.4	3.38	1.22	14	9.6	B	2								
Carbamazepine	DB00564	236.3	0.152	1	1	46.33	2.45	2.45	14	0.1	N	2								
Cerivastatin	DB00439	459.6	0.004	6	3	99.88	3.7	1.9	4.2	5.3	A	1b	10.3	Hepatic Uptake	112.00 [10, 11]	244.00 [11]	59.48 [5, 10, 11]	29.90 [6, 7, 13]	237.85 [6, 7]	210.50 [6, 7]
Diclofenac	DB00586	296.1	0.004	3	2	49.33	4.51	1.3	4.4		A	1a	18.5	Metabolism						
Fluvastatin	DB01095	411.5	0.004	4	3	82.69	4.17	1.12	4.3		A	1b	7.8	Hepatic Uptake	20.00 [10]		101.55 [5, 10]			
Glibenclamide	DB01016	494.0	0.002	5	3	113.6	3.75	2.23	5.2	0	A	1b			86.95 [4, 14]	222.00 [14]	134.02 [4, 5, 14]			
Mibefradil	DB01388	495.6	0.001	4	1	67.45	6.29	3.99	12.8	8.7	B	2	39.4	Metabolism						
Midazolam	DB00683	325.8	0.010	2	0	30.18	3.12	3.1		6.1	WB	2	26.3	Metabolism						
Naloxone	DB01183	327.4	5.640	5	2	70	1.74	1.09	9.6	7.9	B	2	24.6	Metabolism						
Nateglinide	DB00731	317.4	0.008	3	2	66.4	4.21	1.22	3.3		A	3a	4.2	Hepatic Uptake	14.70 [14, 15]	31.30 [14, 15]	18.95 [5, 14, 15]	16.60 [6]	195.60 [6]	179.00 [6]
Oxazepam	DB00842	286.7	0.088	3	2	61.69	2.37	2.37	11.5	1.8	N	2	33.5	Metabolism						
Phenytoin	DB00252	252.3	0.071	2	2	58.2	2.24	2.17	8.3		A	2								
Pitavastatin	DB08860	421.5	0.004	5	3	90.65	3.45	1.2	4.2	5.3	A	1b	5.7	Hepatic Uptake	42.07 [4, 9, 11]	172.00 [11]	118.18 [4, 5, 9, 11]	17.37 [6, 7, 12]	182.90 [6, 7]	139.13 [6, 7, 12]
Pravastatin	DB00175	424.5	0.242	6	4	124.29	1.35	-0.4	4.3		A	3b	0.4	Hepatic Uptake	0.55 [4, 9, 11]	1.00 [11]	3.46 [3, 4, 5, 9, 10, 11, 16]	1.21 [6, 12, 16]	33.37 [6]	21.59 [6, 12, 16]
Procainamide	DB01035	235.3	3.020	3	2	58.36	1.49	-0.36	14	9.3	B	2								

DRUG	Drug bank accension Number [a]	Molecular Weight [a]	Water Solubility (mg/ml) [a]	Hydrogen Acceptor Number [a]	Hydrogen Donor Number [a]	Polar Surface Area (Å²) [a]	LogP [b]	LogD$_{7.4}$ [b]	Strongest pKa, acid [c]	Strongest pKa, base [c]	Ionisation [d]	ECCS classification [b]	Permeability 10^{-6}cm/s [1]	Clearance Mechanism [1]	Human			Rat		
															P_{diff} (µl/min/10^6 cells)	CL_{uptake} (µl/min/10^6 cells)	CL_{active} (µl/min/10^6 cells)	P_{diff} (µl/min/10^6 cells)	CL_{uptake} (µl/min/10^6 cells)	CL_{active} (µl/min/10^6 cells)
Quinidine	DB00908	324.4	0.334	4	1	45.59	3.64	2.41	11.8	8.6	B	2	10.3	Metabolism						
Repaglinide	DB00912	452.6	0.003	5	2	78.87	4.69	2.3	3.6	6	A	1b	16.2	Hepatic Uptake	47.12 [9, 10, 11, 14, 17]	86.00 [11, 14]	41.00 [9, 10, 11, 14, 17]	33.13 [6, 7, 12]	226.50 [6, 7]	135.67 [6, 7, 12]
Rosuvastatin	DB01098	481.5	0.089	8	3	140.92	0.42	-0.33	4.3	1.5	A	3b	0.9	Hepatic Uptake	1.66 [2, 4, 9, 10, 11, 18, 19]	24.27 [11, 19]	17.74 [2, 4, 5, 9, 10, 11]	18.15 [6, 7, 12]	316.04 [6, 7]	177.70 [6, 7, 8, 12]
RO-X																				
Theophylline	DB00277	180.2	22.900	3	1	69.3	0	0	8.7		WA	2	21.7	Metabolism						
Valsartan	DB00177	435.5	0.023	6	2	112.07	3.9	-1.11	3.1		A	3b	0.4	Hepatic Uptake	0.40 [4, 9, 10, 11, 20]	15.90 [11]	7.51 [4, 5, 9, 10, 11]	2.13 [6, 7, 12, 20]	27.66 [6, 7]	24.87 [6, 7, 12]

Abbreviations: ANS: 1-anilino-8-naphthalene sulfonate, ECCS: Extended Clearance Classification System, RO-X: in house compound.

a) Data obtained from drugbank (Wishart et al., 2018)

b) See Table 1 for References

c) Obtained from ilabs (http://ilab.psds.ac.uk/)

d) The ionisation of each drug was defined based on their charge and percentage ionisation at physiological pH (7.4) as follows: Neutrals, <3% ionised. Acids, >10% negatively charged. Weak acids, >3<10% negatively charged. Bases, >10% positively charged. Weak bases, >3<10% positively charged. Zwitterions, >10% positively and negatively charged.

References: [1] (Varma et al., 2015) [2] (Liao et al., 2019) [3] (Li et al., 2013) [4] (Nordell et al., 2013) [5] (Izumi et al., 2018) [6] (Yabe et al., 2011) [7] (Harrison et al., 2018) [8] (Lave et al., 1997) [9] (Menochet et al., 2012) [10] (Jones et al., 2012) [11] (De Bruyn et al., 2018) [12] (Ménochet et al., 2012) [13] (Shitara et al., 2004) [14] (Fujino et al., 2018) [15] (Kimoto et al., 2018) [16] (Watanabe et al., 2009) [17] (Varma et al., 2013) [18] (Shen et al., 2013) [19] (Schaefer et al., 2018) [20] (Poirier et al., 2009).

Supplemental Tables S2: IVIVE analysis of Wood et al. (2017) database (WSLM)

Table S2 A: Rat

Compound	Observed CL_H (ml/min/kg) [a]	Predicted CL_H (no PMU) (ml/min/kg) [a]	fu_b [a]	fu_p [a]	$CL_{int,u\ in\ vitro}$ in the absence of albumin (ml/min/kg) [a]	Calculated fold-change caused by PMU-effect	Predicted $CL_{int,u\ in\ vivo}$ in the presence of albumin (ml/min/kg)	Predicted CL_H (PMU-adjusted) (ml/min/kg)
Acetaminophen	24	38.39	0.82	0.82	76	1.16	88.28	41.99
Alfentanil	45		0.24	0.16		2.15		
Alprazolam	19	34.28	0.35	0.56	149	1.34	199.87	41.16
Antipyrine	5.1	4.12	1	1	4.3	1.08	4.63	4.43
Atorvastatin	35	12.94	0.036	0.044	413	3.50	1,446.91	34.25
Bosentan	30	0.67	0.015	0.016	45	5.13	230.94	3.35
Caffeine	0.017	6.54	1	0.8	7	1.17	8.21	7.58
Cerivastatin	39	0.45	0.041	0.029	11	4.10	45.10	1.82
Chlordiazepoxide	10	6.85	0.15	0.15	49	2.21	108.06	13.95
Chlorpromazine	61		0.068	0.067		2.99		
Clobazam	32	22.34	0.21	0.21	137	1.94	266.10	35.85
Clonazepam	20	15.75	0.21	0.21	89	1.94	172.87	26.63
Dextromethorphan	62	64.41	0.26	0.45	696	1.46	1,013.95	72.50
Diazepam	51	30.17	0.1	0.13	432	2.33	1,005.57	50.14
Diclofenac	22	13.14	0.041	0.022	369	4.55	1,679.29	40.78
Diltiazem	71	85.50	0.18	0.17	3277	2.10	6,893.42	92.54
Domperidone	67		0.07	0.092		2.65		
Erythromycin	32	50.35	0.6	0.78	169	1.18	200.05	54.55
Ethoxycoumarin	54	38.29	0.22	0.22	282	1.91	538.21	54.21
Felodipine	3.8		0.07	0.1		2.57		
Fexofenadine	38	25.56	0.34	0.34	101	1.62	163.56	35.74
FK079	2.6	0.63	0.095	0.06	6.7	3.12	20.88	1.95

Compound	Observed CL_H (ml/min/kg) [a]	Predicted CL_H (no PMU) (ml/min/kg) [a]	fu_b [a]	fu_p [a]	$CL_{int,u\ in\ vitro}$ in the absence of albumin (ml/min/kg) [a]	Calculated fold-change caused by PMU-effect	Predicted $_{CLint,u\ in\ vivo}$ in the presence of albumin (ml/min/kg)	Predicted CL_H (PMU-adjusted) (ml/min/kg)
Galantamine	32		0.76	0.76		1.20		
Granisetron	41	64.82	0.61	0.61	302	1.30	392.24	70.52
Ibuprofen	4.9		0.038	0.023		4.48		
Indinavir	51		0.65	0.4		1.52		
Indomethacin	0.6	0.03	0.005	0.003	5.1	9.65	49.23	0.25
Ketanserin	5.9		0.018	0.012		5.72		
Lorcainide	86		0.22	0.26		1.79		
Lubeluzole	33		0.01	0.008		6.67		
Mazapertine	62		0.047	0.03		4.05		
Metoprolol	73	34.87	0.53	0.81	101	1.17	117.87	38.45
Midazolam	54	22.19	0.062	0.051	460	3.31	1,524.23	48.59
Naloxone	59	87.89	0.57	0.62	1273	1.29	1,643.27	90.35
Nebivolol	41		0.013	0.015		5.26		
Nelfinavir	37	94.39	0.041	0.035	41070	3.82	156,864.05	98.47
Norcisapride	27		0.43	0.65		1.27		
Oxodipine	18		1	1		1.08		
Phenytoin	18	15.87	0.23	0.23	82	1.88	153.90	26.14
Pindolol	59	61.63	0.64	0.64	251	1.28	320.15	67.20
Prazosin	49	11.92	0.33	0.33	41	1.64	67.15	18.14
Propafenone	42	71.63	0.023	0.022	10977	4.55	49,955.50	91.99
Propranolol	74	60.58	0.088	0.091	1746	2.66	4,649.78	80.36
Quinidine	28		0.2	0.31		1.68		
Quinotolast	54	2.87	0.051	0.033	58	3.91	226.50	10.36
Repaglinide	8.8	8.72	0.025	0.015	382	5.26	2,008.80	33.43
Risperidone	76		0.14	0.12		2.40		

Compound	Observed CL_H (ml/min/kg) [a]	Predicted CL_H (no PMU) (ml/min/kg) [a]	fu_b [a]	fu_p [a]	$CL_{int,u\ in\ vitro}$ in the absence of albumin (ml/min/kg) [a]	Calculated fold-change caused by PMU-effect	Predicted $_{CLint,u\ in\ vivo}$ in the presence of albumin (ml/min/kg)	Predicted CL_H (PMU-adjusted) (ml/min/kg)
Ritonavir	30	77.62	0.048	0.04	7225	3.63	26,239.19	92.64
Rosuvastatin	51	4.80	0.084	0.064	60	3.04	182.49	13.29
Sabeluzole	43		0.019	0.016		5.13		
Saquinavir	36	83.94	0.062	0.051	8428	3.31	27,926.57	94.54
Tolbutamide	0.81	1.26	0.13	0.1	9.8	2.57	25.19	3.17
Triazolam	84	70.51	0.28	0.19	854	2.02	1,722.61	82.83
Troglitazone	37	87.25	0.16	0.092	4277	2.65	11,343.20	94.78
Verapamil	43	32.04	0.071	0.063	664	3.06	2,031.55	59.06
S-Warfarin	0.24	0.02	0.021	0.012	0.85	5.72	4.86	0.10
Zidovudine	41	9.96	0.79	0.79	14	1.18	16.49	11.53
AZ1	11	1.67	0.025	0.014	68	5.40	367.02	8.40
AZ2	16	7.43	0.071	0.039	113	3.67	414.32	22.73
AZ3	12	1.24	0.035	0.019	36	4.81	173.15	5.71
AZ4	36	4.23	0.032	0.032	138	3.95	545.21	14.86
AZ5	57	21.09	0.16	0.16	167	2.15	359.43	36.51
AZ6	9.3	3.40	0.016	0.016	220	5.13	1,129.06	15.30
AZ7	13	1.20	0.038	0.038	32	3.70	118.49	4.31
AZ8	57	18.30	0.14	0.14	160	2.26	362.16	33.64
AZ9	46	8.34	0.05	0.05	182	3.34	607.59	23.30
AZ10	23	24.62	0.029	0.029	1126	4.10	4,616.99	57.25
AZ11	40	2.43	0.086	0.086	29	2.72	78.89	6.35
AZ12	50	7.41	0.086	0.086	93	2.72	253.01	17.87
AZ13	33	1.72	0.076	0.076	23	2.85	65.56	4.75
AZ14	21	1.66	0.036	0.036	47	3.78	177.61	6.01
AZ15	32	6.65	0.089	0.089	80	2.69	214.84	16.05

Compound	Observed CL_H (ml/min/kg) [a]	Predicted CL_H (no PMU) (ml/min/kg) [a]	fu_b [a]	fu_p [a]	$CL_{int,u\ in\ vitro}$ in the absence of albumin (ml/min/kg) [a]	Calculated fold-change caused by PMU-effect	Predicted $_{CLint,u\ in\ vivo}$ in the presence of albumin (ml/min/kg)	Predicted CL_H (PMU-adjusted) (ml/min/kg)
AZ16	17	1.45	0.03	0.03	49	4.05	198.36	5.62
AZ17	13	3.13	0.19	0.19	17	2.02	34.29	6.12
AZ18	47	8.19	0.085	0.085	105	2.73	286.92	19.61
AZ19	53	14.86	0.09	0.09	194	2.67	518.80	31.83
AZ20	39	3.15	0.013	0.013	250	5.55	1,387.61	15.28
AZ21	41	18.57	0.1	0.1	228	2.57	585.96	36.95
AZ22	18	5.18	0.011	0.011	497	5.91	2,938.09	24.43
AZ23	8.7	0.48	0.0036	0.002	135	11.25	1,518.64	5.18
AZ24	7.9	2.42	0.062	0.062	40	3.08	123.12	7.09
AZ25	17	3.15	0.13	0.13	25	2.33	58.19	7.03
AZ26	7.3	1.17	0.036	0.036	33	3.78	124.71	4.30
AZ27	19	6.14	0.017	0.017	385	5.02	1,931.16	24.72
AZ28	17	4.72	0.084	0.084	59	2.74	161.94	11.97
AZ29	22	8.45	0.045	0.045	205	3.47	712.13	24.27
AZ30	50	21.39	0.056	0.056	486	3.20	1,554.53	46.54
AZ31	56	8.97	0.062	0.062	159	3.08	489.42	23.28
AZ32	25	3.88	0.064	0.064	63	3.04	191.61	10.92
AZ33	51	14.46	0.13	0.13	130	2.33	302.60	28.23
AZ34	32	6.54	0.076	0.076	92	2.85	262.24	16.62
AZ35	1.5	0.05	0.0018	0.001	29	14.61	423.77	0.76
AZ36	16	5.57	0.083	0.083	71	2.76	195.76	13.98
AZ37	2	0.24	0.0018	0.001	135	14.61	1,972.71	3.43
AZ38	40	28.23	0.19	0.19	207	2.02	417.54	44.24
AZ39	42	9.68	0.047	0.047	228	3.42	779.14	26.80
AZ40	13	6.30	0.14	0.14	48	2.26	108.65	13.20

Compound	Observed CL_H (ml/min/kg) [a]	Predicted CL_H (no PMU) (ml/min/kg) [a]	fu_b [a]	fu_p [a]	$CL_{int,u\ in\ vitro}$ in the absence of albumin (ml/min/kg) [a]	Calculated fold-change caused by PMU-effect	Predicted $_{CLint,u\ in\ vivo}$ in the presence of albumin (ml/min/kg)	Predicted CL_H (PMU-adjusted) (ml/min/kg)
AZ41	8.7	5.18	0.14	0.14	39	2.26	88.28	11.00
AZ42	40	9.94	0.16	0.16	69	2.15	148.51	19.20
AZ43	14	1.73	0.022	0.022	80	4.55	364.07	7.42
AZ44	19	10.97	0.11	0.11	112	2.48	277.67	23.40
AZ45	25	24.20	0.28	0.28	114	1.74	198.64	35.74
AZ46	2.2	0.27	0.0018	0.001	152	14.61	2,221.13	3.84
AZ47	3.6	0.73	0.009	0.009	82	6.38	522.89	4.49
AZ48	33	29.60	0.29	0.29	145	1.72	249.34	41.96
AZ49	4.4	1.24	0.008	0.008	157	6.67	1,046.65	7.73
AZ50	15	2.97	0.011	0.011	278	5.91	1,643.44	15.31
H1	44	10.58	0.035	0.035	338	3.82	1,290.97	31.12
H2	4.9		0.042	0.042		3.57		
H3	0.05	0.12	0.001	0.001	124	14.61	1,811.97	1.78
H4	0.17	0.02	0.001	0.001	21	14.61	306.87	0.31
H5	1.4	1.14	0.011	0.011	105	5.91	620.72	6.39
H6	0.55	0.20	0.003	0.003	66	9.65	637.10	1.88
H7	0.58	0.62	0.003	0.003	209	9.65	2,017.49	5.71
H8	3.8	1.28	0.01	0.01	130	6.13	796.66	7.38
H9	4.2	1.87	0.009	0.009	212	6.38	1,351.87	10.85
H10	0.23	0.10	0.001	0.001	98	14.61	1,432.04	1.41
H11	15	6.87	0.041	0.041	180	3.60	647.65	20.98
H12	5.4	1.67	0.02	0.02	85	4.72	401.00	7.42
H13	100	9.30	0.051	0.051	201	3.31	666.02	25.35
H14	5	0.66	0.002	0.002	333	11.25	3,745.98	6.97
H15	2	2.51	0.006	0.006	429	7.43	3,187.96	16.06

Compound	Observed CL_H (ml/min/kg) [a]	Predicted CL_H (no PMU) (ml/min/kg) [a]	fu_b [a]	fu_p [a]	$CL_{int,u\ in\ vitro}$ in the absence of albumin (ml/min/kg) [a]	Calculated fold-change caused by PMU-effect	Predicted $_{CLint,u\ in\ vivo}$ in the presence of albumin (ml/min/kg)	Predicted CL_H (PMU-adjusted) (ml/min/kg)
H16	0.72		0.002	0.002		11.25		
H17	3.1	0.63	0.006	0.006	106	7.43	787.70	4.51
H18	4.9	0.53	0.008	0.008	67	6.67	446.66	3.45
H19	6.5	0.68	0.006	0.006	114	7.43	847.15	4.84
H20	31	3.98	0.005	0.005	828	7.96	6,591.27	24.79
H22	9	2.51	0.018	0.018	143	4.91	701.98	11.22
H23	0.25		0.001	0.001		14.61		
H24	44	0.57	0.003	0.003	191	9.65	1,843.73	5.24
H25	14	0.31	0.004	0.004	78	8.66	675.47	2.63
H26	2.2	0.56	0.008	0.008	71	6.67	473.33	3.65
H27	7.4	2.16	0.014	0.014	158	5.40	852.78	10.67
H28	4.1	0.44	0.004	0.004	110	8.66	952.59	3.67
H29	13	0.82	0.025	0.025	33	4.34	143.11	3.45
H30	6.3	5.93	0.097	0.097	65	2.60	168.98	14.08
H31	9.4	0.71	0.013	0.013	55	5.55	305.27	3.82
H32	1.8	0.16	0.003	0.003	52	9.65	501.96	1.48
H33	88	6.54	0.019	0.019	368	4.81	1,770.01	25.17
H34	29	0.43	0.006	0.006	72	7.43	535.04	3.11
H35	47	7.82	0.017	0.017	499	5.02	2,502.99	29.85
H37	60	1.19	0.002	0.002	602	11.25	6,772.01	11.93
H39	79	4.72	0.015	0.015	330	5.26	1,735.35	20.65
H40	54	0.99	0.008	0.008	125	6.67	833.32	6.25
H2a	79	9.63	0.036	0.025	296	4.34	1,283.63	31.61
H12a	77	1.23	0.0069	0.004	180	8.66	1,558.78	9.71
H13a	8	0.10	0.0018	0.001	55	14.61	803.70	1.43

Compound	Observed CL_H (ml/min/kg) [a]	Predicted CL_H (no PMU) (ml/min/kg) [a]	fu_b [a]	fu_p [a]	$CL_{int,u\ in\ vitro}$ in the absence of albumin (ml/min/kg) [a]	Calculated fold-change caused by PMU-effect	Predicted $_{CLint,u\ in\ vivo}$ in the presence of albumin (ml/min/kg)	Predicted CL_H (PMU-adjusted) (ml/min/kg)
H15a	64	0.29	0.0035	0.002	84	11.25	944.93	3.20

a, data obtained from Wood et al. (2017).

Table S2 B: Human

Compound	Observed CL_H (ml/min/kg) [a]	Predicted CL_H (no PMU) (ml/min/kg) [a]	fu_b [a]	fu_p [a]	$CL_{int,u\ in\ vitro}$ in the absence of albumin (ml/min/kg) [a]	Calculated fold-change caused by PMU-effect	Predicted $CLint,u\ in\ vivo$ in the presence of albumin (ml/min/kg)	Predicted CL_H (PMU-adjusted) (ml/min/kg)
Acebutolol	5.4	3.44	0.81	0.81	5.1	1.17	5.95	3.91
Acetaminophen	4.4	2.20	0.88	0.88	2.8	1.13	3.17	2.46
Alfentanil	6.9		0.16	0.096		2.61		
Alprazolam	0.78	0.31	0.31	0.29	1	1.72	1.72	0.52
Alprenolol	14	9.00	0.27	0.22	59	1.91	112.60	12.32
Amitriptyline	9.6	1.59	0.054	0.061	32	3.10	99.11	4.25
Amobarbital	0.37		0.26	0.39		1.54		
Antipyrine	0.55	1.21	0.99	0.99	1.3	1.08	1.41	1.30
Atenolol	0.13	3.37	0.79	0.05	5.1	3.34	17.03	8.15
Atorvastatin	16		0.036	0.02		4.72		
Betaxolol	2.9	2.68	0.56	0.56	5.5	1.34	7.38	3.44
Bosentan	3.5	0.38	0.064	0.035	6	3.82	22.92	1.37
Bupivacaine	7.1	2.16	0.071	0.053	34	3.27	111.04	5.71
Buprenorphine	15	2.71	0.04	0.04	78	3.63	283.27	7.32
Caffeine	1.2	2.95	0.65	0.68	5.3	1.25	6.61	3.56
Carbamazepine	1.6	1.73	0.31	0.26	6.1	1.79	10.93	2.91
Carvedilol	10	7.85	0.05	0.05	253	3.34	844.62	13.89
Chlorpheniramine	1.6	2.81	0.44	0.7	7.4	1.23	9.12	3.36
Chlorpromazine	11	10.56	0.043	0.037	501	3.74	1,873.82	16.47
Cimetidine	2.6	7.67	0.87	0.81	14	1.17	16.34	8.43
Clozapine	4.1	1.12	0.054	0.053	22	3.27	71.85	3.27
Codeine	13.8	14.27	0.73	0.7	63	1.23	77.68	15.16
Cyclosporine A	5.4	0.59	0.047	0.068	13	2.97	38.64	1.67
Desipramine	11	9.08	0.21	0.18	77	2.06	158.52	12.76

Compound	Observed CL_H (ml/min/kg) [a]	Predicted CL_H (no PMU) (ml/min/kg) [a]	fu_b [a]	fu_p [a]	$CL_{int,u\ in\ vitro}$ in the absence of albumin (ml/min/kg) [a]	Calculated fold-change caused by PMU-effect	Predicted $CL_{int,u\ in\ vivo}$ in the presence of albumin (ml/min/kg)	Predicted CL_H (PMU-adjusted) (ml/min/kg)
Dexamethasone	5.7	1.25	0.29	0.23	4.6	1.88	8.63	2.23
Diazepam	0.57	0.20	0.036	0.022	5.6	4.55	25.49	0.88
Diclofenac	7.7	1.42	0.0091	0.005	168	7.96	1,337.36	7.66
Diflusinal	0.14	0.04	0.0053	0.0017	7.8	11.96	93.29	0.48
Diltiazem	12	5.61	0.22	0.22	35	1.91	66.80	8.59
Diphenhydramine	18	4.09	0.34	0.22	15	1.91	28.63	6.62
Domperidone	12	3.87	0.097	0.072	49	2.91	142.55	8.29
Felodipine	16		0.0057	0.004		8.66		
Fenoprofen	7. 3	0.16	0.0055	0.003	29	9.65	279.94	1.43
Flumazenil	15	6.56	0.6	0.58	16	1.32	21.18	7.87
Flunitrazepam	3.1	0.68	0.25	0.19	2.8	2.02	5.65	1.32
Fluphenazine	0.58	2.36	0.14	0.08	19	2.80	53.12	5.47
Furosemide	1.2		0.02	0.013		5.55		
Gemfibrozil	3.1	2.98	0.026	0.014	134	5.40	723.25	9.85
Glimepiride	1	0.05	0.0055	0.003	9.8	9.65	94.60	0.51
Glipizide	0.75	0.08	0.02	0.011	4.1	5.91	24.24	0.47
Glyburide	2	0.63	0.038	0.021	17	4.63	78.74	2.61
Granisetron	11	7.83	0.7	0.35	18	1.60	28.83	10.22
Haloperidol	9.6	1.22	0.1	0.08	13	2.80	36.35	3.09
Hexobarbital	3.6		0.53	0.53		1.37		
Hydrocortisone	3.3	3.63	0.2	0.2	22	1.98	43.53	6.13
Ibuprofen	1.4	0.46	0.018	0.01	26	6.13	159.33	2.52
Indomethacin	2.1	0.50	0.019	0.01	27	6.13	165.46	2.73
Irbesartan	3.8	2.99	0.1	0.057	35	3.18	111.21	7.23
Ketanserin	9.7	8.06	0.097	0.068	136	2.97	404.28	13.55

Compound	Observed CL_H (ml/min/kg) [a]	Predicted CL_H (no PMU) (ml/min/kg) [a]	fu_b [a]	fu_p [a]	$CL_{int,u\ in\ vitro}$ in the absence of albumin (ml/min/kg) [a]	Calculated fold-change caused by PMU-effect	Predicted $CLint,u\ in\ vivo$ in the presence of albumin (ml/min/kg)	Predicted CL_H (PMU-adjusted) (ml/min/kg)
Ketoprofen	2.2	0.18	0.015	0.0078	12	6.73	80.77	1.14
Labetalol	14	4.47	0.38	0.5	15	1.40	21.00	5.76
Levoprotiline	14	1.38	0.19	0.19	7.8	2.02	15.73	2.61
Lidocaine	14	3.64	0.34	0.29	13	1.72	22.35	5.56
Lorazepam	1.1	0.15	0.08	0.082	1.9	2.77	5.26	0.41
Lorcainide	20	8.74	0.17	0.13	89	2.33	207.17	13.04
Lovastatin	15		0.082	0.047		3.42		
Methadone	1.7		0.21	0.16		2.15		
Methohexital	16		0.39	0.27		1.77		
Methoxsalen	18		0.13	0.09		2.67		
Methylprednisolone	5.9	2.25	0.18	0.18	14	2.06	28.82	4.15
Metoclopramide	4.3	3.32	0.6	0.6	6.6	1.31	8.63	4.14
Metoprolol	12	8.09	0.83	0.89	16	1.13	18.02	8.68
Mianserin	18	1.91	0.14	0.14	15	2.26	33.95	3.87
Midazolam	9.2	1.66	0.043	0.025	42	4.34	182.14	5.68
Montelukast	1.1	0.46	0.0062	0.004	76	8.66	658.15	3.41
Nadolol	0.92	5.12	0.83	0.83	8.2	1.16	9.48	5.70
Naloxone	18	16.65	0.51	0.62	167	1.29	215.57	17.42
Naltrexone	1.4	13.42	0.83	0.79	46	1.18	54.19	14.18
Naproxen	0.12	0.07	0.001	0.001	68	14.61	993.66	0.95
Nifedipine	5.4	1.66	0.03	0.041	60	3.60	215.88	4.93
Nisoldipine	12		0.003	0.003		9.65		
Nitrendipine	20	0.86	0.029	0.02	31	4.72	146.25	3.52
Omeprazole	11	0.55	0.067	0.04	8.4	3.63	30.51	1.86
Ondansetron	6.5	1.12	0.33	0.27	3.6	1.77	6.36	1.91

Compound	Observed CL_H (ml/min/kg) [a]	Predicted CL_H (no PMU) (ml/min/kg) [a]	fu_b [a]	fu_p [a]	$CL_{int,u\ in\ vitro}$ in the absence of albumin (ml/min/kg) [a]	Calculated fold-change caused by PMU-effect	Predicted $CL_{int,u\ in\ vivo}$ in the presence of albumin (ml/min/kg)	Predicted CL_H (PMU-adjusted) (ml/min/kg)
Oxaprozin	0.07	0.01	0.0007	0.00039	12	20.85	250.17	0.17
Oxazepam	1.2	0.36	0.043	0.048	8.4	3.39	28.48	1.16
Oxprenolol	5.4	2.85	0.3	0.3	11	1.70	18.67	4.41
Phenacetin	20	8.24	0.57	0.57	24	1.33	31.98	9.69
Phenytoin	5.3	0.23	0.11	0.11	2.1	2.48	5.21	0.56
Pindolol	3.7	3.10	0.56	0.56	6.5	1.34	8.72	3.95
Prazosin	4.4	0.56	0.067	0.047	8.6	3.42	29.39	1.80
Prednisolone	4.9	2.27	0.17	0.12	15	2.40	35.99	4.72
Prednisone	4.9		0.3	0.25		1.82		
Prochlorperazine	16	0.04	0.0027	0.0027	14	10.04	140.62	0.37
Promazine	12	4.24	0.092	0.11	58	2.48	143.79	8.07
Promethazine	16	10.97	0.22	0.22	106	1.91	202.30	14.13
Propafenone	19	4.47	0.057	0.04	100	3.63	363.17	10.35
Propranolol	15	5.51	0.15	0.13	50	2.33	116.39	9.47
(-)-Propranolol	13	2.79	0.17	0.15	19	2.21	41.90	5.30
(+)-Propranolol	15	3.61	0.19	0.16	23	2.15	49.50	6.47
Quinidine	4.1	3.04	0.21	0.2	17	1.98	33.63	5.27
Ranitidine	2.7	2.40	0.8	0.84	3.4	1.15	3.91	2.72
Repaglinide	13		0.025	0.015		5.26		
Rifabutin	4.1		0.48	0.29		1.72		
Risperidone	7.9	3.49	0.15	0.1	28	2.57	71.96	7.09
Ritonavir	1.2	0.32	0.015	0.015	22	5.26	115.69	1.60
Salbutamol	3		0.93	0.93		1.11		
Saquinavir	18		0.038	0.028		4.16		
Scopolamine	13	9.36	0.9	0.9	19	1.12	21.31	9.95

Compound	Observed CL_H (ml/min/kg) [a]	Predicted CL_H (no PMU) (ml/min/kg) [a]	fu_b [a]	fu_p [a]	$CL_{int,u\ in\ vitro}$ in the absence of albumin (ml/min/kg) [a]	Calculated fold-change caused by PMU-effect	Predicted $CLint,u\ in\ vivo$ in the presence of albumin (ml/min/kg)	Predicted CL_H (PMU-adjusted) (ml/min/kg)
Sildenafil	7.6	0.92	0.04	0.04	24	3.63	87.16	2.98
Sumatriptan	15	4.04	0.81	0.83	6.2	1.16	7.17	4.53
Tacrolimus	0.71		0.004	0.2		1.98		
Temazepam	1.9	0.10	0.017	0.017	6	5.02	30.10	0.50
Tenoxicam	0.054	0.06	0.013	0.0085	4.8	6.52	31.28	0.40
Theophylline	0.47	0.86	0.45	0.59	2	1.32	2.63	1.12
Timolol	9.7	4.52	0.59	0.9	9.8	1.12	10.99	4.94
Tolbutamide	0.35	0.26	0.076	0.05	3.4	3.34	11.35	0.83
Trazodone	2.3	1.51	0.086	0.07	19	2.94	55.87	3.90
Triazolam	4.3	0.86	0.14	0.1	6.4	2.57	16.45	2.07
Trimipramine	16	5.59	0.051	0.051	150	3.31	497.03	11.39
Verapamil	16	6.82	0.096	0.081	106	2.78	294.97	11.96
Warfarin	0.086	0.07	0.023	0.013	3	5.55	16.65	0.38
Wafarin (S-)	0.11	0.05	0.018	0.01	2.7	6.13	16.55	0.29
Zaleplon	16	2.56	0.4	0.4	7.3	1.52	11.12	3.66
Zidovudine	19	4.08	0.82	0.8	6.2	1.17	7.27	4.63
Zileuton	6	0.57	0.1	0.07	5.9	2.94	17.35	1.60
Zolpidem	5.7	0.81	0.1	0.079	8.4	2.81	23.60	2.12

a, data obtained from Wood et al. (2017).

Supplemental Figures S1: IVIVE predictions for CL_H from the Wood et al. (2017) database using various liver models

Rat

The WSLM (blue circles), dispersion (purple squares), and parallel tube (green triangles) liver models were used to predict CL_H in the absence (open symbols) and presence (closed symbols) of predicted PMU. AFE, RMSE, and the % of compounds within 2-fold are displayed. Solid line represents line of unity, dashed line represents 2-fold error and dotted line represents 3-fold error.

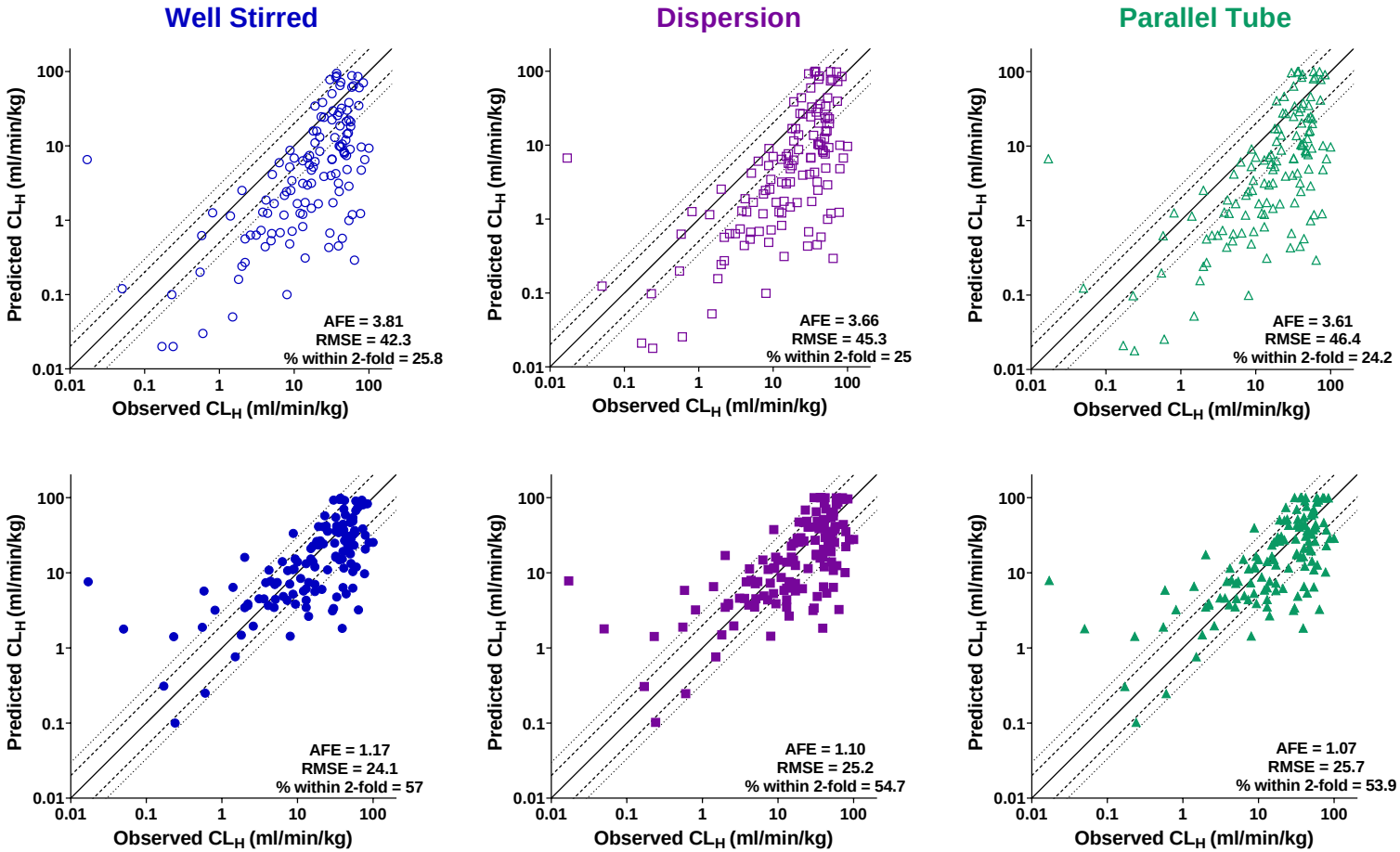

Human

The WSLM (red circles), dispersion (brown squares), and parallel tube (yellow triangles) liver model were used to predict CL_H in the absence (open symbols) and presence (closed symbols) of predicted PMU. AFE, RMSE, and the % of compounds within 2-fold are displayed. Solid line represents line of unity, dashed line represents 2-fold error and dotted line represents 3-fold error.

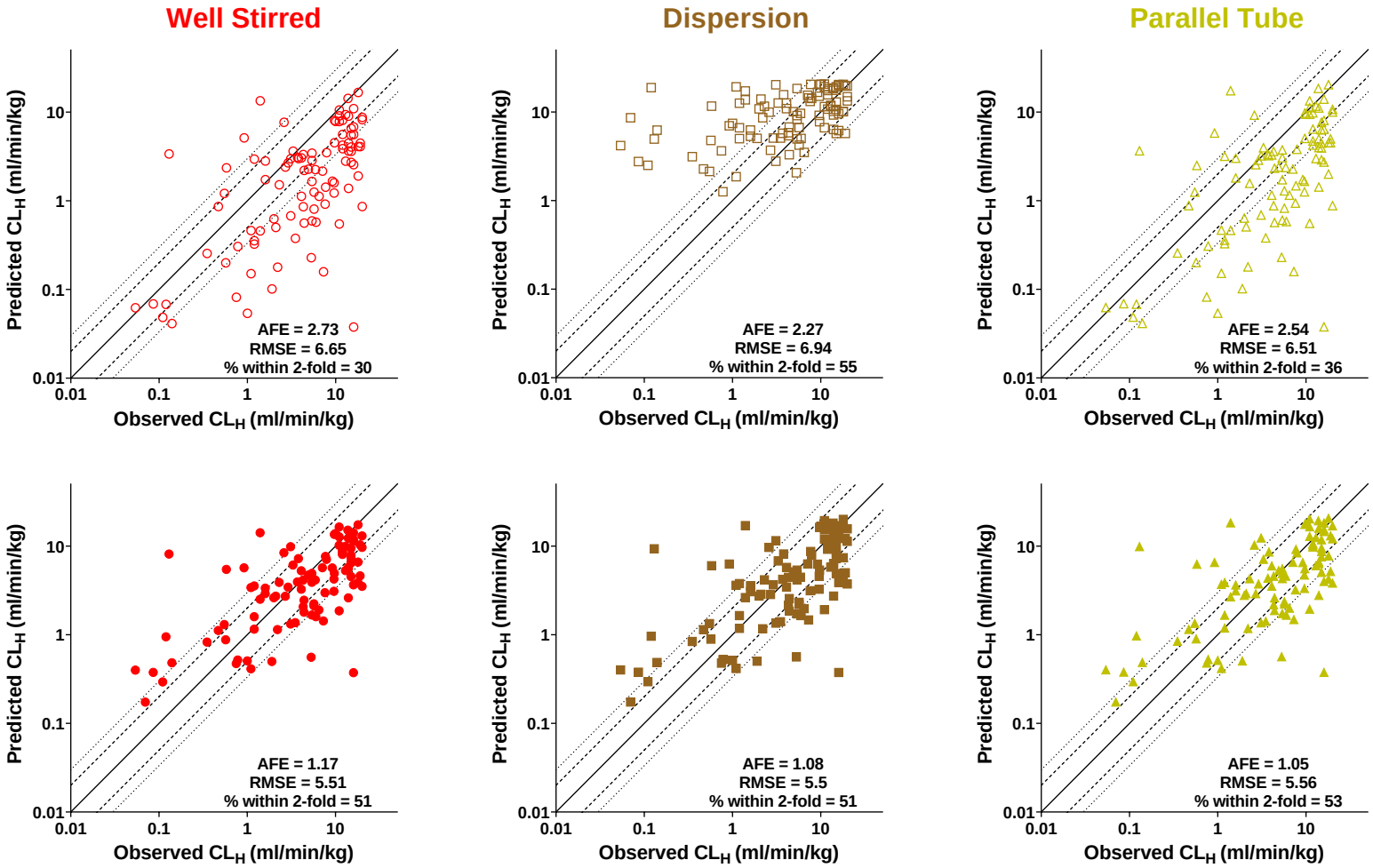

Well stirred Liver model: Eq 7. Q_H = 100ml/min/kg for rat and 20.7ml/min/kg for human (Wood et al., 2017).

Dispersion Liver model:

$$CL_H = Q_H[1 - \frac{4a}{(1+a)^2 \exp\left[\frac{a-1}{2Dn}\right] - (1-a)^2 \exp\left[\frac{a+1}{2Dn}\right]}$$

Where Dn = 0.17 (for rat, (Ito and Houston, 2004) and human (Kim et al., 2019)), $a = \sqrt{1+4RnDn}$ and $Rn = \frac{fu_b \times CL_{int,u\ in\ vivo}}{Q_H}$

Parallel Tube Liver Model:

$$CL_H = Q_H\left[1 - \exp\left(-\frac{fu_b \times CL_{int,u\ in\ vivo}}{Q_H}\right)\right]$$

Supplemental Figure S2: Impact of PP on absolute $CL_{int,u\ in\ vitro}$ values

$CL_{int,u\ in\ vitro}$ values were found to be significantly higher in the presence of PP in both rat and human datasets (a two-tailed paired t-test, $T_{(35)} = 3.942$, $p = 0.0004$, and $T_{(37)} = 3.251$, $p = 0.0025$, respectively). All data sourced contained no PP controls to calculate PMU effect (see Methods), thus paired samples represent the exact same drug, from the same study, under the exact same experimental conditions (+/- PP).

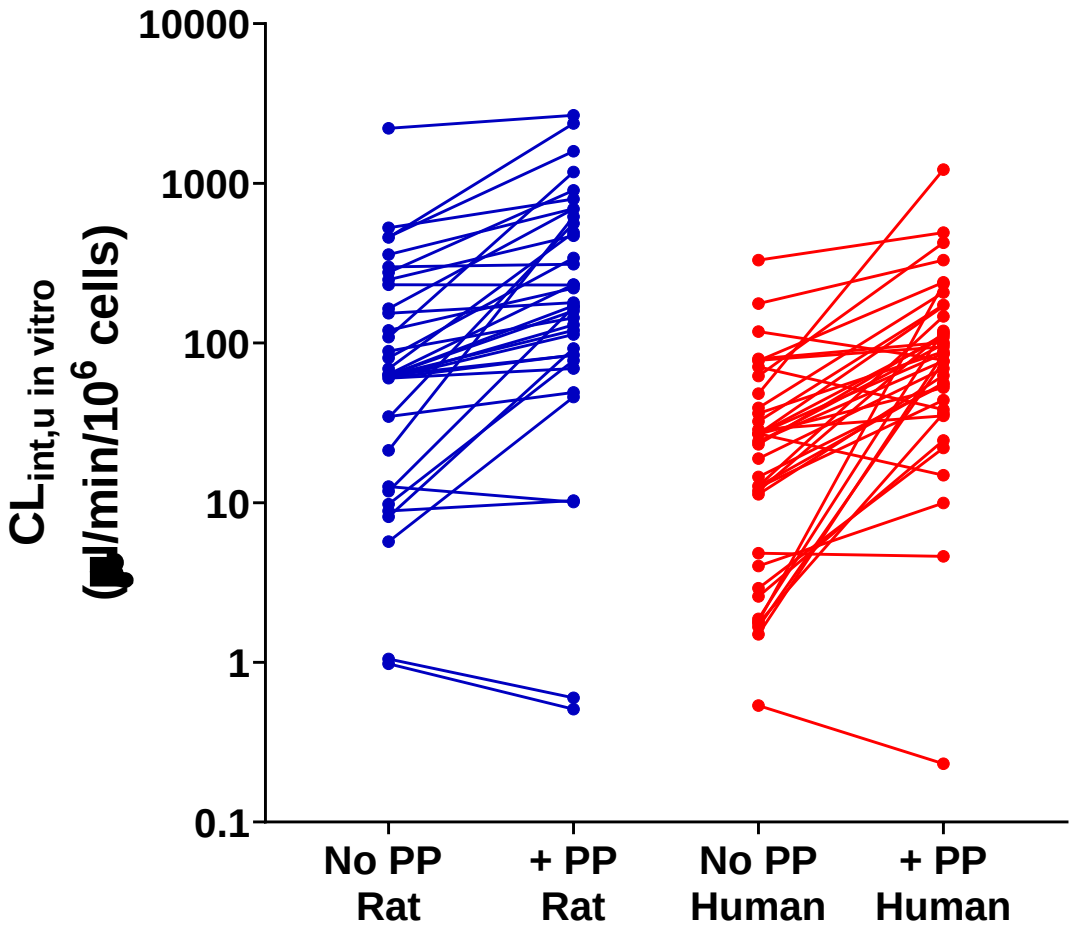

Supplemental Figure S3: Influence of PP on relationship between fold-change in $CL_{int,u\ in\ vitro}$ and in vitro fu in rat hepatocytes

Linear regression analysis on the Log_{10} transformed data revealed statistical differences ($F_{(4,28)}$ = 6.957, p = 0.0005) between the types of PP used in the PMU database in rat hepatocytes, brown: BSA, red: human plasma, blue: rat serum. The equations for each of these PP subsets and references are displayed in the table below.

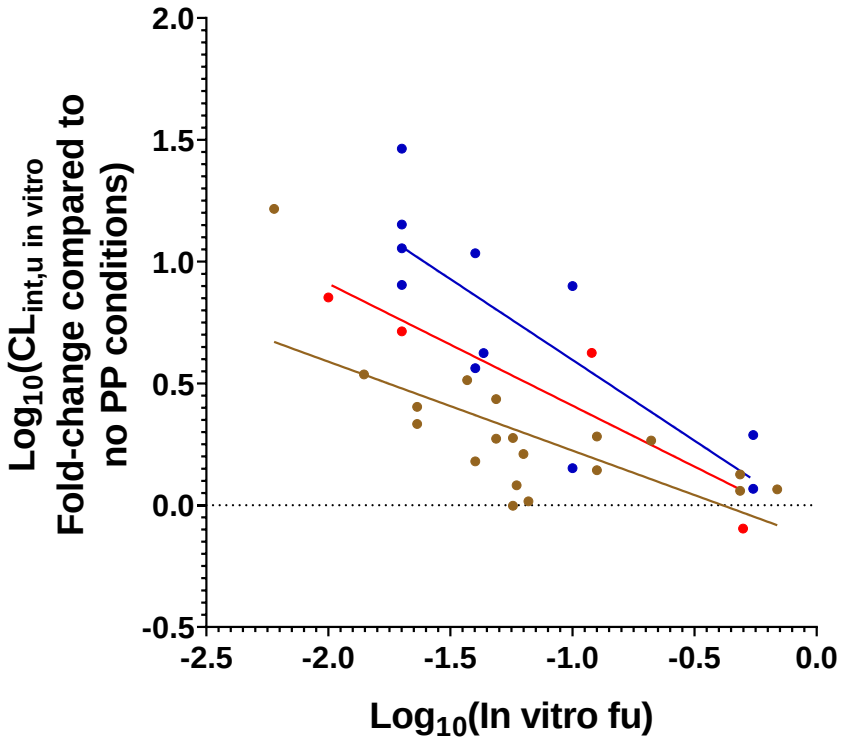

	BSA	Human Plasma	Rat Serum
Equation	y = -0.1408x – 0.3651	y = -0.09196x – 0.5007	y = -0.06677x – 0.6632
r^2	0.4883	0.8240	0.6544
Number of drugs	19	4	11
Studies	Miyauchi et al. (2018)	Bowman et al. (2019)	Blanchard et al. (2004)
	Li et al. (2020)		Shitara et al. (2004)

Supplemental Figure S4: Trends between in vitro fu values and fold-change in V_{max}. Red and blue indicate values obtained from human and rat hepatocytes, respectively.

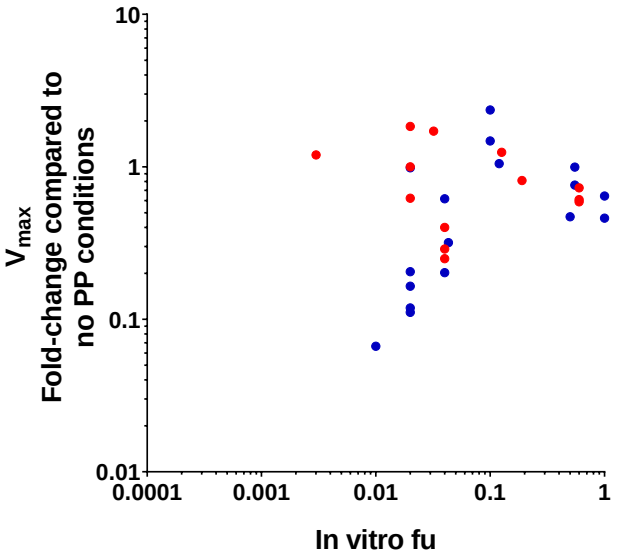

Supplemental Figure S5: Relationship between the fold-change in $CL_{int,u\ in\ vitro}$ and absolute CL parameters from in vitro hepatocyte assays in the absence of PP.

The fold-change in $CL_{int,u\ in\ vitro}$ was compared where possible to the passive, active and total uptake clearance from in vitro rat (blue) and human (red) hepatocyte assays as labelled. No clear trends were observed.

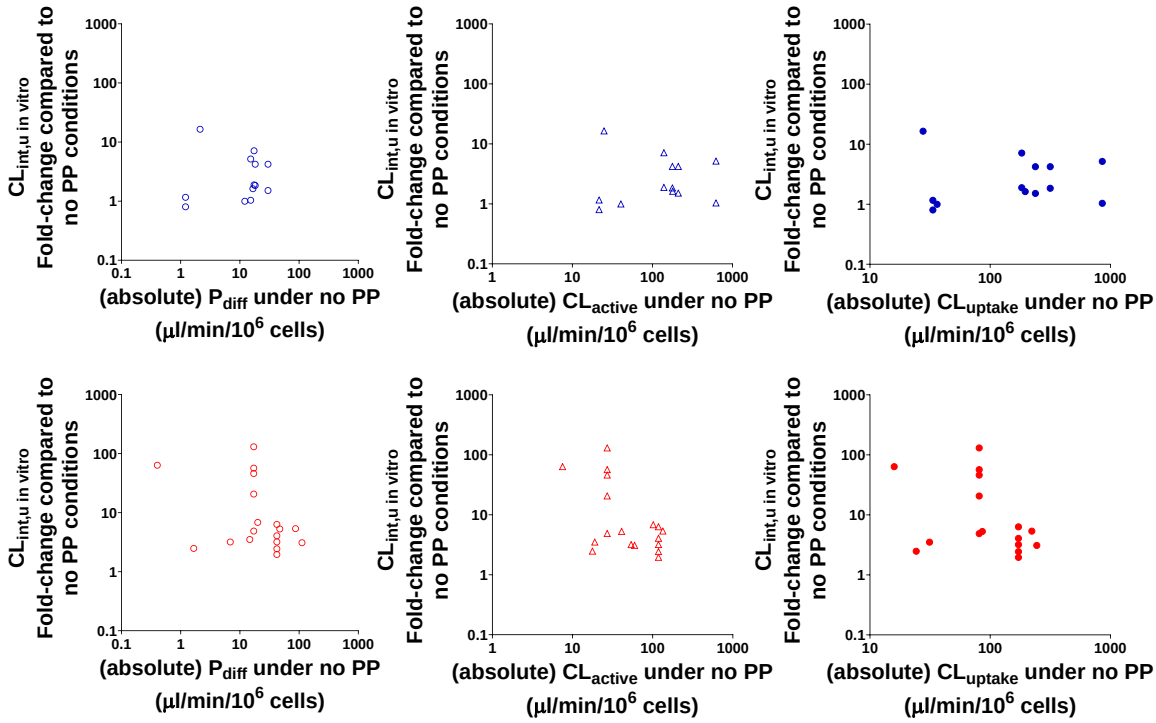

Supplemental Figure S6: Relationship between fu_p and $CL_{int,u\ in\ vitro}$ fold-change, without bosentan

Linear regression analysis between the log transformed fu_p and fold-change in $CL_{int,u\ in\ vitro}$, omitting bosentan, was performed. No significant difference between the human (red) and rat (blue) datasets were observed ($F_{(2,45)}$ = 1.038, p= 0.3626), and a higher r^2 value is achieved. 95% confidence bands (dotted lines) are also displayed. r^2 values for rat, human, and total data for this line are 0.3608, 0.4772, and 0.4566, respectively.

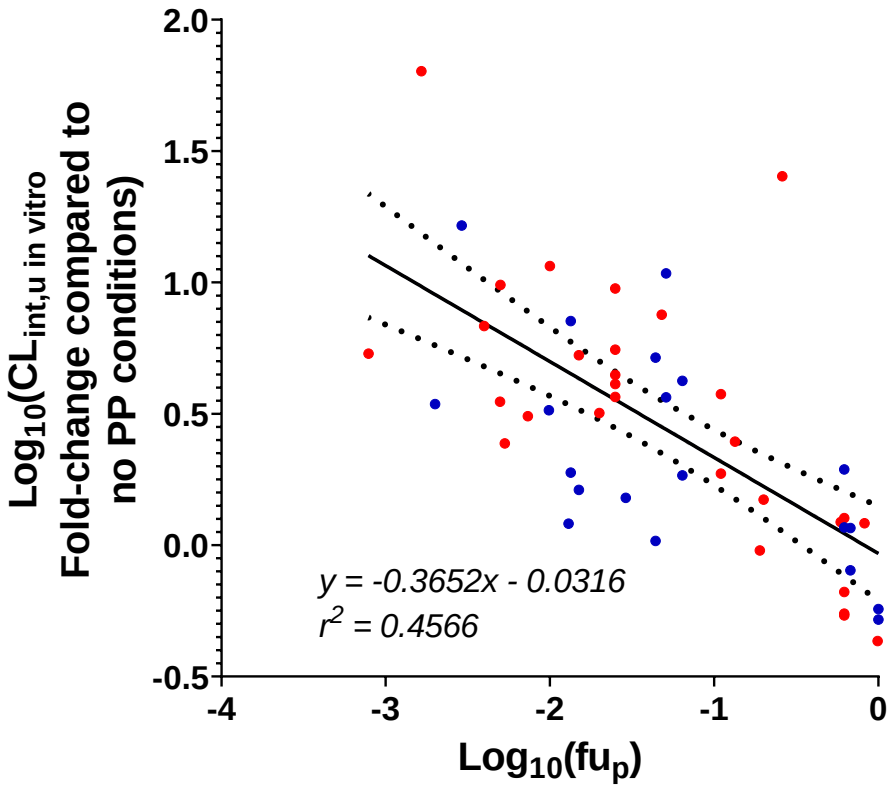

Supplemental Figure S7: IVIVE of the 26 compounds in the PMU database

$CL_{int,u\ in\ vivo}$

Graphical outputs for the IVIVE analysis, rat (blue) and human (red). Open circles represent IVIVE predictions in the absence of PP (A and D), closed squares represent IVIVE predictions in the presence of PP (B and E), and closed circles represent IVIVE predictions based on predicted PMU-enhancement (C and F).

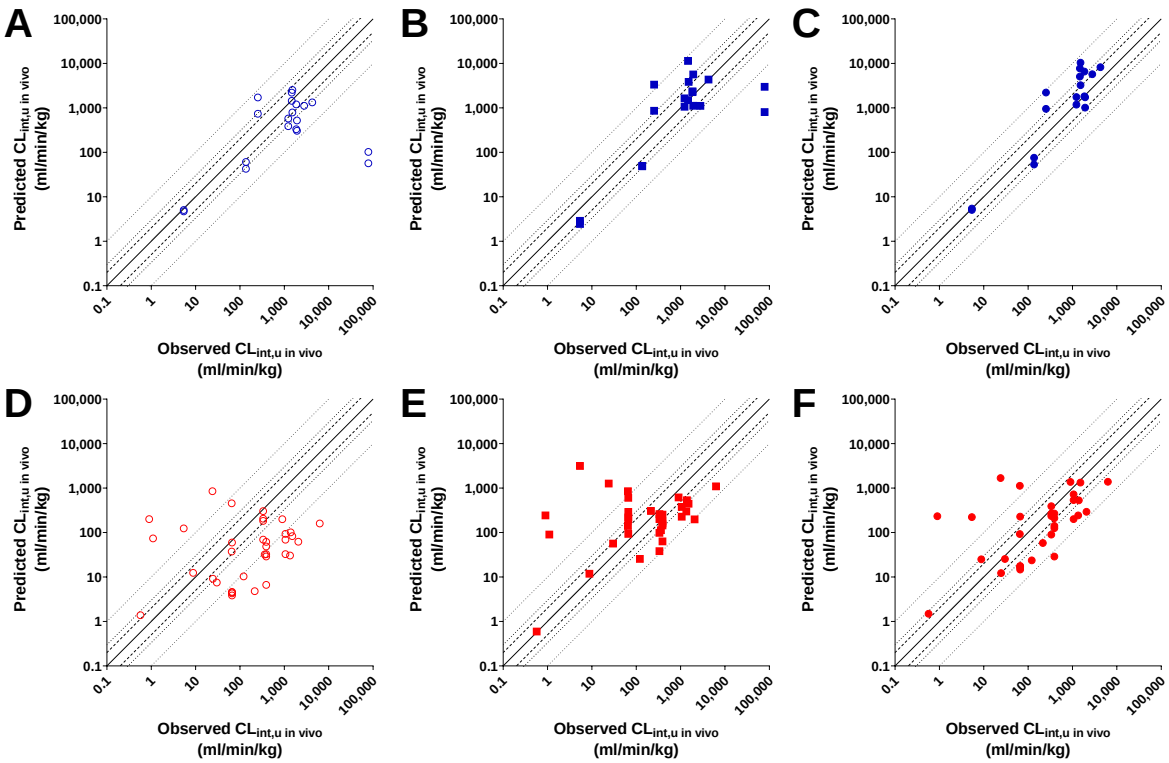

CL_H

Graphical outputs for the IVIVE analysis, rat (blue) and human (red). Open circles represent IVIVE predictions in the absence of PP (A and D), closed squares represent IVIVE predictions in the presence of PP (B and E), and closed circles represent IVIVE predictions based on predicted PMU-enhancement (C and F).

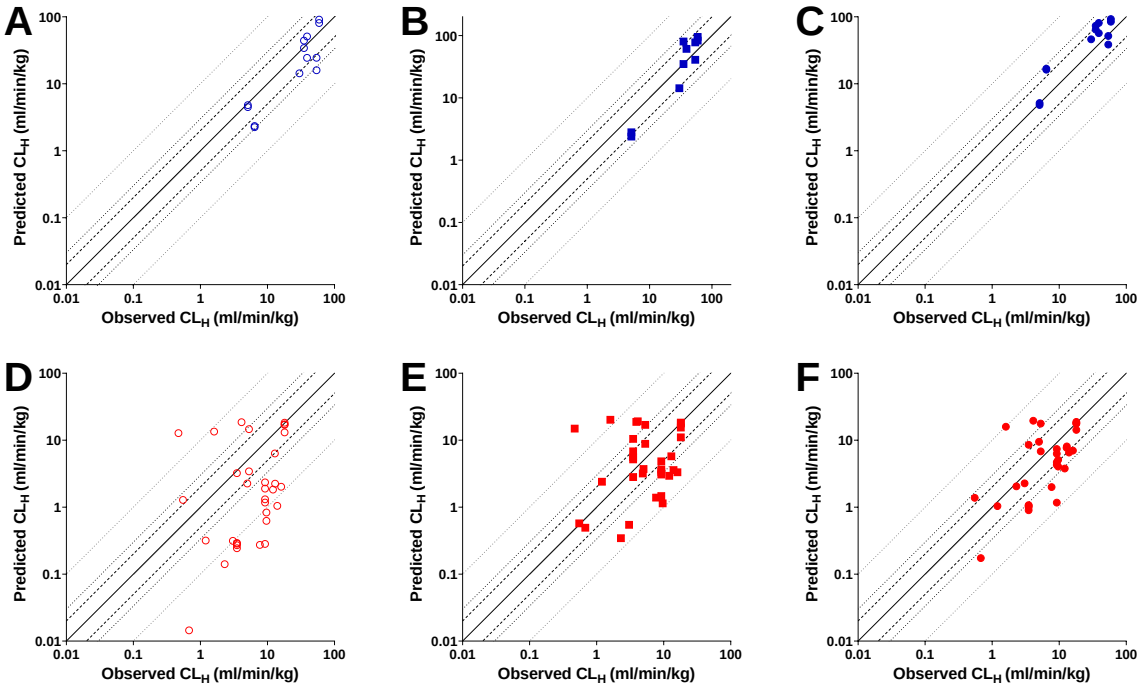

Supplementary References (n = 37)

Bachmann K, Byers J, and Ghosh R (2003) Prediction of in vivo hepatic clearance from in vitro data using cryopreserved human hepatocytes. *Xenobiotica* **33:**475-483.

Blanchard N, Alexandre E, Abadie C, Lavé T, Heyd B, Mantion G, Jaeck D, Richert L, and Coassolo P (2005) Comparison of clearance predictions using primary cultures and suspensions of human hepatocytes. *Xenobiotica* **35:**1-15.

Blanchard N, Hewitt NJ, Silber P, Jones H, Coassolo P, and Lavé T (2006) Prediction of hepatic clearance using cryopreserved human hepatocytes: a comparison of serum and serum-free incubations. *J Pharm Pharmacol* **58:**633-641.

Blanchard N, Richert L, Notter B, Delobel F, David P, Coassolo P, and Lavé T (2004) Impact of serum on clearance predictions obtained from suspensions and primary cultures of rat hepatocytes. *Eur J Pharm Sci* **23:**189-199.

Bowman CM, Okochi H, and Benet LZ (2019) The Presence of a Transporter-Induced Protein Binding Shift: A New Explanation for Protein-Facilitated Uptake and Improvement for In Vitro-In Vivo Extrapolation. *Drug Metab Dispos* **47:**358-363.

Brørs O, Sager G, Sandnes D, and Jacobsen S (1983) Binding of theophylline in human serum determined by ultrafiltration and equilibrium dialysis. *Br J Clin Pharmacol* **15:**393-397.

De Bruyn T, Ufuk A, Cantrill C, Kosa RE, Bi YA, Niosi M, Modi S, Rodrigues AD, Tremaine LM, Varma MVS, Galetin A, and Houston JB (2018) Predicting Human Clearance of Organic Anion Transporting Polypeptide Substrates Using Cynomolgus Monkey: In Vitro-In Vivo Scaling of Hepatic Uptake Clearance. *Drug Metab Dispos* **46:**989-1000.

Fujino R, Hashizume K, Aoyama S, Maeda K, Ito K, Toshimoto K, Lee W, Ninomiya SI, and Sugiyama Y (2018) Strategies to improve the prediction accuracy of hepatic intrinsic clearance of three antidiabetic drugs: Application of the extended clearance concept and consideration of the effect of albumin on CYP2C metabolism and OATP1B-mediated hepatic uptake. *Eur J Pharm Sci* **125:**181-192.

Harrison J, De Bruyn T, Darwich AS, and Houston JB (2018) Simultaneous Assessment In Vitro of Transporter and Metabolic Processes in Hepatic Drug Clearance: Use of a Media Loss Approach. *Drug Metab Dispos* **46:**405-414.

Ito K and Houston JB (2004) Comparison of the use of liver models for predicting drug clearance using in vitro kinetic data from hepatic microsomes and isolated hepatocytes. *Pharm Res* **21:**785-792.

Izumi S, Nozaki Y, Kusuhara H, Hotta K, Mochizuki T, Komori T, Maeda K, and Sugiyama Y (2018) Relative Activity Factor (RAF)-Based Scaling of Uptake Clearance Mediated by Organic Anion Transporting Polypeptide (OATP) 1B1 and OATP1B3 in Human Hepatocytes. *Mol Pharm* **15:**2277-2288.

Jones HM, Barton HA, Lai Y, Bi YA, Kimoto E, Kempshall S, Tate SC, El-Kattan A, Houston JB, Galetin A, and Fenner KS (2012) Mechanistic pharmacokinetic modeling for the prediction of transporter-mediated disposition in humans from sandwich culture human hepatocyte data. *Drug Metab Dispos* **40:**1007-1017.

Kim SJ, Lee KR, Miyauchi S, and Sugiyama Y (2019) Extrapolation of In Vivo Hepatic Clearance from In Vitro Uptake Clearance by Suspended Human Hepatocytes for Anionic Drugs with High Binding to Human Albumin: Improvement of In Vitro-to-In Vivo Extrapolation by Considering the "Albumin-Mediated" Hepatic Uptake Mechanism on the Basis of the "Facilitated-Dissociation Model". *Drug Metab Dispos* **47:**94-103.

Kimoto E, Mathialagan S, Tylaska L, Niosi M, Lin J, Carlo AA, Tess DA, and Varma MVS (2018) Organic Anion Transporter 2-Mediated Hepatic Uptake Contributes to the Clearance of High-Permeability-Low-Molecular-Weight Acid and Zwitterion Drugs: Evaluation Using 25 Drugs. *J Pharmacol Exp Ther* **367:**322-334.

Kodama H, Kodama Y, Shinozawa S, Kanemaru R, Todaka K, and Mitsuyama Y (1998) Serum protein binding kinetics of phenytoin in monotherapy patients. *Journal of clinical pharmacy and therapeutics* **23:**361-365.

Lave T, Dupin S, Schmitt C, Chou RC, Jaeck D, and Coassolo P (1997) Integration of in vitro data into allometric scaling to predict hepatic metabolic clearance in man: application to 10 extensively metabolized drugs. *J Pharm Sci* **86:**584-590.

Li L, Nouraldeen A, and Wilson AG (2013) Evaluation of transporter-mediated hepatic uptake in a non-radioactive high-throughput assay: a study of kinetics, species difference and plasma protein effect. *Xenobiotica* **43:**253-262.

Li N, Badrinarayanan A, Li X, Roberts J, Hayashi M, Virk M, and Gupta A (2020) Comparison of In Vitro to In Vivo Extrapolation Approaches for Predicting Transporter-Mediated Hepatic Uptake Clearance Using Suspended Rat Hepatocytes. *Drug Metab Dispos*.

Liao M, Zhu Q, Zhu A, Gemski C, Ma B, Guan E, Li AP, Xiao G, and Xia CQ (2019) Comparison of uptake transporter functions in hepatocytes in different species to determine the optimal model for evaluating drug transporter activities in humans. *Xenobiotica* **49:**852-862.

Ludden LK, Ludden TM, Collins JM, Pentikis HS, and Strong JM (1997) Effect of albumin on the estimation, in vitro, of phenytoin Vmax and Km values: implications for clinical correlation. *J Pharmacol Exp Ther* **282:**391-396.

Mao J, Mohutsky MA, Harrelson JP, Wrighton SA, and Hall SD (2012) Predictions of cytochrome P450-mediated drug-drug interactions using cryopreserved human hepatocytes: comparison of plasma and protein-free media incubation conditions. *Drug Metab Dispos* **40:**706-716.

Menochet K, Kenworthy KE, Houston JB, and Galetin A (2012) Use of mechanistic modeling to assess interindividual variability and interspecies differences in active uptake in human and rat hepatocytes. *Drug Metab Dispos* **40:**1744-1756.

Ménochet K, Kenworthy KE, Houston JB, and Galetin A (2012) Simultaneous assessment of uptake and metabolism in rat hepatocytes: a comprehensive mechanistic model. *J Pharmacol Exp Ther* **341:**2-15.

Miyauchi S, Masuda M, Kim SJ, Tanaka Y, Lee KR, Iwakado S, Nemoto M, Sasaki S, Shimono K, Tanaka Y, and Sugiyama Y (2018) The Phenomenon of Albumin-Mediated Hepatic Uptake of Organic Anion Transport Polypeptide Substrates: Prediction of the In Vivo Uptake Clearance from the In Vitro Uptake by Isolated Hepatocytes Using a Facilitated-Dissociation Model. *Drug Metab Dispos* **46:**259-267.

Nordell P, Winiwarter S, and Hilgendorf C (2013) Resolving the distribution-metabolism interplay of eight OATP substrates in the standard clearance assay with suspended human cryopreserved hepatocytes. *Mol Pharm* **10:**4443-4451.

Patsalos PN, Zugman M, Lake C, James A, Ratnaraj N, and Sander JW (2017) Serum protein binding of 25 antiepileptic drugs in a routine clinical setting: A comparison of free non-protein-bound concentrations. *Epilepsia* **58:**1234-1243.

Poirier A, Cascais AC, Funk C, and Lavé T (2009) Prediction of pharmacokinetic profile of valsartan in human based on in vitro uptake transport data. *J Pharmacokinet Pharmacodyn* **36:**585-611.

Schaefer M, Morinaga G, Matsui A, Schänzle G, Bischoff D, and Süssmuth RD (2018) Quantitative Expression of Hepatobiliary Transporters and Functional Uptake of Substrates in Hepatic Two-Dimensional Sandwich Cultures: A Comparative Evaluation of Upcyte and Primary Human Hepatocytes. *Drug Metab Dispos* **46:**166-177.

Shen H, Yang Z, Mintier G, Han YH, Chen C, Balimane P, Jemal M, Zhao W, Zhang R, Kallipatti S, Selvam S, Sukrutharaj S, Krishnamurthy P, Marathe P, and Rodrigues AD (2013) Cynomolgus monkey as a potential model to assess drug interactions involving hepatic organic anion transporting polypeptides: in vitro, in vivo, and in vitro-to-in vivo extrapolation. *J Pharmacol Exp Ther* **344:**673-685.

Shibata Y, Takahashi H, Chiba M, and Ishii Y (2002) Prediction of hepatic clearance and availability by cryopreserved human hepatocytes: an application of serum incubation method. *Drug Metab Dispos* **30:**892-896.

Shitara Y, Hirano M, Adachi Y, Itoh T, Sato H, and Sugiyama Y (2004) In vitro and in vivo correlation of the inhibitory effect of cyclosporin A on the transporter-mediated hepatic uptake of cerivastatin in rats. *Drug Metab Dispos* **32:**1468-1475.

Varma MV, Lai Y, Kimoto E, Goosen TC, El-Kattan AF, and Kumar V (2013) Mechanistic modeling to predict the transporter- and enzyme-mediated drug-drug interactions of repaglinide. *Pharm Res* **30:**1188-1199.

Varma MV, Steyn SJ, Allerton C, and El-Kattan AF (2015) Predicting Clearance Mechanism in Drug Discovery: Extended Clearance Classification System (ECCS). *Pharm Res* **32:**3785-3802.

Watanabe T, Kusuhara H, Maeda K, Shitara Y, and Sugiyama Y (2009) Physiologically based pharmacokinetic modeling to predict transporter-mediated clearance and distribution of pravastatin in humans. *J Pharmacol Exp Ther* **328:**652-662.

Wishart DS, Feunang YD, Guo AC, Lo EJ, Marcu A, Grant JR, Sajed T, Johnson D, Li C, Sayeeda Z, Assempour N, Iynkkaran I, Liu Y, Maciejewski A, Gale N, Wilson A, Chin L, Cummings R, Le D, Pon A, Knox C, and Wilson M (2018) DrugBank 5.0: a major update to the DrugBank database for 2018. *Nucleic Acids Res* **46:**D1074-D1082.

Wood FL, Houston JB, and Hallifax D (2017) Clearance Prediction Methodology Needs Fundamental Improvement: Trends Common to Rat and Human Hepatocytes/Microsomes and Implications for Experimental Methodology. *Drug Metab Dispos* **45:**1178-1188.

Yabe Y, Galetin A, and Houston JB (2011) Kinetic characterization of rat hepatic uptake of 16 actively transported drugs. *Drug Metab Dispos* **39:**1808-1814.